Spatially Controlled Organic/Inorganic Hybrids Designed to Enhance Cellular Response

by

Linh Ngoc Luong

A dissertation submitted in partial fulfillment
of the requirements for the degree of
Doctor of Philosophy
(Biomedical Engineering)
in The University of Michigan
2011

Doctoral Committee:

Professor David H. Kohn, Chair
Professor William V. Giannobile
Professor Steven P. Schwendeman
Associate Professor Shuichi Takayama

To my family, especially my parents,
for their love, endless support, and encouragement

Acknowledgements

I would like to take the opportunity to express my gratitude and appreciation to all the people who have contributed so much during my time in graduate school.

First, I would like to thank my advisor David Kohn for allowing me the opportunity to learn with his guidance and encouragement. I am grateful for the opportunity he gave me in pursuing my research interests, while guiding and challenging me to think beyond the obvious. I have learned to become a better researcher and a more critical reviewer. I would also like to thank the members of my committee, William Giannobile, Shuichi Takayama, and Steven Schwendeman, for their invaluable insight and suggestions.

I would like to thank the past and present members of our lab: Rupak Rajachar, Joey Wallace, Sharon Miller, Nadder Sahar, Kyungsup Shin, Ricky Rossello, Sun Ig Hong, Erin McNerny, Janani Ramaswamy, Harsha Ramaraju, Michael Friedman, Hojun Song, Champa Jayasuriya, Laura Darjatmoko, and Elena Leonova. I value the time that I have had with each and every person. It has been a pleasure to be a part of such a helpful and diverse lab.

I would like to thank and acknowledge the co-authors on my publications: Sun Ig Hong, Rusha Patel, Mark Outslay, Kristen McFalls, Sharon Miller, and David Kohn. Additionally, I appreciate the hard work of the other undergraduate students that have worked with me through the years: Jeff Borgeson, Viral Patel, and Sid Bhandari. Much

appreciation also goes to Liz Rodriguiz and Maria Steele for making our departments run efficiently and taking care of everything behind the scenes.

I would also like to acknowledge that this research was made possible by funding from NIH DE 015411, DE 13380, Tissue Engineering and Regeneration Grant T32 DE 07057, and the NSF Graduate Research Fellowship.

To Erin McNerny and Janani Ramaswamy, not only are they great labmates, they have become dear friends. Thanks for all the fun times we've had outside of lab. Thanks to Dan McNerny for our hockey rivalry and our friendship. Thanks to Hima Nandivada, Shelley Brown, Laura Smith, Sylva Krizan, Borhan Chueh, and Connie Soves for all of our conversations, lunches, and coffee breaks. I appreciate the mutual support, the cheerleading, commiserating, and the successes that we have shared. I will cherish all the memories and hope that we will share more in the future.

Thanks to my friends from undergrad, Kristin Rorick, Perry Lin, and Jennifer Jeon for their continued friendship and visits. I also am grateful to Sarah Yon, and Shelly Leung for their encouraging words and unfailing support.

And finally, I would like to thank my family for their neverending love, support, and encouragement, especially in the recent years. A special thanks to my parents for coming to this country and enduring so much hardship to provide a good life for me and my brother. I appreciate all the hard work and time that was sacrificed to provide the best life possible. With my family's love, dedication, and hard work, I have been able to make this journey and become the person I am today.

Table of Contents

List of Figures

Chapter 2

Chapter 3

Chapter 4

Chapter 5

List of Tables

List of Appendices

Abstract

Bone is a complex organ that serves many functions. However, in cases of trauma, congenital malformations, and skeletal disorders, impaired healing occurs. Bone tissue engineering is an alternative to conventional therapies such as bone grafting. The work presented in this dissertation involves the development of a bone engineering approach whereby coprecipitation, a biomimetic strategy to precipitate bone-like apatite onto a biomaterial, is used to incorporate biomolecules in a spatially-controlled manner.

The global hypothesis was that the coprecipitation of biomolecules with apatite can enhance cell response compared to adsorption, specifically: 1) enhancing transfection efficiency by coprecipitating DNA-lipoplexes with apatite and 2) enhancing osteogenic differentiation by coprecipitating multiple growth factors in a spatially controlled manner within apatite. Coprecipitation spatially localized protein within apatite and allowed for higher protein retention compared to adsorption. Applying these advantages towards gene delivery, the coprecipitation of DNA-Lipoplexes transfected cells with a higher efficiency compared to adsorption and polymer incorporation methods.

To provide the design criteria for a multiple growth factor delivery system to better mimic *in vivo* conditions, BMP-2 and FGF-2 were chosen due to their roles in osteogenesis. The concentrations and sequence of BMP-2 and FGF-2 had significant effects on osteogenic differentiation of BMSCs cultured on TCPS, with low concentrations of FGF-2 enhancing DNA content, and high concentrations of BMP-2

enhancing osteogenesis. Delivery of FGF-2 followed by BMP-2 or delivery of BMP-2 followed by BMP-2 and FGF-2 enhanced osteogenic differentiation compared to simultaneous delivery. For the hybrid delivery system, the individual release profiles of BMP-2 and FGF-2 were significantly affected by the concentration used during coprecipitation. Utilizing coprecipitation to control BMP-2 and FGF-2 localization within apatite to mimic the sequential exposure required by BMSCs, minimal effects on DNA and osteogenic differentiation were demonstrated. The presence of mineral may have delayed or inhibited osteogenic response with a possible compensation upon sequential delivery.

These organic/inorganic delivery systems have the potential of delivering multiple biomolecules to better mimic spatiotemporal gradients in the *in vivo* environment. Utilizing this novel approach to better simulate the cellular environment by manipulating interfaces can facilitate the development of multiple tissue systems.

Chapter 1

Introduction to Biomimetic Materials

1.1 Bone Biology and Clinical Motivation

Bone is a complex organ that serves many functions, including providing motility and mechanical support for the body while maintaining a supply of essential minerals. Bone is typically composed of one-third organic matrix that provides structure and flexibility, while the remaining two-thirds are composed of minerals that provide the strength and load-bearing capabilities [1]. Bone undergoes a continual process of formation and resorption which is dependent on a regulatory system that responds to both internal and external stimuli. In the cases of trauma, congenital malformations, and progressively deforming skeletal disorders, the regulatory system may not function properly, leading to delayed or impaired healing.

In the United States, approximately 5.6 million fractures occur annually, and approximately 5-10% exhibit delayed or impaired healing. Thus, there is a clinical need for treatments that augment and/or accelerate healing [2]. Current medical solutions to augment or accelerate healing include bone grafting and direct administration of growth factors. However, direct administration of growth factors is not always effective due to rapid diffusion of the factor away from the defect site, and loss of biological activity [3], while bone grafting is not optimal due to limited supply, the possibility of graft resorption, and the potential transfer of pathogens [4]. Additionally, metal implants are

also widely used; however, when the metal-alloy undergoes corrosion, the products can lead to a negative biological response [5]. Metal implants also require a second surgery if they fail, and in medical situations, are difficult to image clinically. A growing alternative to these current therapies that could potentially overcome these limitations is bone tissue engineering, which involves the regeneration of bone through the use of engineering design to control the biological response of a system.

1.2 Bone Tissue Engineering

Bone tissue engineering uses engineering design to combine the following biological components essential in regeneration: cells, an extracellular matrix (ECM) analogue, and/or signaling molecules [3]. Three approaches that incorporate these important biological elements respectively are cell transplantation, conduction, and induction. Cell transplantation approaches require the implantation of donor cells. Conductive approaches include the implantation of synthetic materials, which serve as an ECM analogue allowing the body to heal itself via selective activation of host cells while simultaneously preventing unwanted cells from entering the defect site. Inductive techniques include the delivery of growth factors or plasmid DNA as signaling molecules that promote tissue regeneration. An ideal bone tissue engineering approach would incorporate osteoconductivity, osteoinductivity, and the ability to support cell transplantation, as well as, biocompatibility, degradability, and mechanical integrity.

Strategies for regenerating bone via inductive and/or cell transplantation approaches have focused on the use of biodegradable materials. PLGA (poly-lactic-co-glycolic acid) is an FDA approved synthetic polymer currently used for sutures and in

drug delivery systems [6]. The degradation of PLGA results in the production of lactic and glycolic acid, which are present in normal metabolic pathways in the body [2]. Inorganic materials used for conductive, inductive, and transplantation approaches include hydroxyapatite and tricalcium phosphate, which resorb slowly and have a high affinity for osteogenic factors [7]. By synthesizing a composite biomaterial that assimilates the characteristics of ceramics and polymers, a substrate can be developed that is biodegradable, osteoconductive, and a source of mechanical support.

1.3 Biomineralization and Osteoconductivity

Inorganic biomineralization has been used to synthesize conductive materials for use in bone tissue engineering. The observation that direct bonding between implants and host bone occurs if a layer of bone-like mineral forms on the surface of the implant [8] has led to the utilization of biomimetic strategies to precipitate bone-like mineral onto a variety of substrates to induce bone formation. Bone-like mineral is heterogeneously precipitated onto the surface of a substrate by utilizing a simulated body fluid (SBF), leading to the nucleation of a calcium phosphate coating. For example, titanium implants coated with a uniform apatite layer exhibited significantly higher failure loads and more direct bone formation compared to uncoated implants [9]. The creation of a biomimetic apatite layer may therefore also enhance the function of transplanted cells. Cells prefer an electropositive substrate for interactions and attachment [2, 10], therefore the formation of the biomimetic layer would enhance cell adhesion.

Formation of biomimetically precipitated bone-like mineral requires the utilization of a supersaturated ionic solution, also known as simulated body fluid (SBF),

with ionic concentrations similar to those found in blood plasma (Table 1.1) [11]. Bone-like mineral properties can be tailored by changing the ion concentrations, pH, and temperature of the SBF. For example, mineral thickness, mineral morphology, and mineral dissolution kinetics can be controlled via increasing or decreasing the ion concentrations/ratios and/or mineralization time. Additionally, depositing a layer of mineral via biomineralization techniques can be achieved at physiological temperatures, pressures, and pH, which is preferred over techniques such as sintering, which requires high temperatures and pressures. Physiological conditions allow for the retention of biological activity when biomolecules are incorporated into the apatite.

1.4 Biomolecules and Osteoinductivity

Osteoinductive properties can be integrated into a material by immobilizing proteins such as growth factors to surfaces using physical adsorption (affinity, electrostatic), physical entrapment (hydrogels, dispersed matrices), and covalent attachment [12]. Delivery systems for inductive molecules have been developed using different configurations ranging from microspheres to scaffolds and materials ranging from natural materials to synthetic polymers. Protein immobilization to surfaces via different techniques (e.g. adsorption, entrapment, covalent attachment) can result in different loading efficiencies and levels of retention. However, these methods can result in denaturation, irreversible binding of the proteins, and binding receptor changes [13]. The ideal immobilization method should result in high retention of biomolecules after immobilization and a high fraction retaining their bioactivity over the appropriate time period for the clinical application of interest [12].

Methods of adsorption onto bioceramics include dispersing a growth factor over the surface of porous hydroxyapatite [14, 15], adsorbing antibiotic to each new layer of mineral deposited [16], and binding ceramic pellets together with gel with the growth factor adsorbed to the surface of the pellets [17]. The release profile of a surface adsorbed growth factor is rapid release, followed by a slower release based on the chemical and/or physical attraction between the material and the growth factor adsorbed [18, 19]. However, for some growth factors, a more sustained release is required to maximize physiological effects. Sustained release can be achieved by encapsulating biomolecules, such as BMP-2 (bone morphogenetic protein-2) and TGF-β (transforming growth factor-β), in polymer microspheres [20, 21]. Coupling the microparticles to a scaffold provides structural support [22], but adverse effects include the possibility of protein denaturation depending on the processing procedures. Proteins have been incorporated into hydroxyapatite crystals, and while this method resulted in a sustained release, limitations include protein/drug stability, dosing requirements (ease of injection) and low mechanical properties [23].

Polymeric systems capable of incorporating biomolecules provide inductivity [24, 25], but many lack osteoconductivity. Incorporation of growth factors in hydrogels is only appropriate for certain situations due to the inability of hydrogels to sustain a controlled release over a long period of time [26] and low load bearing ability. Larger proteins are also hard to incorporate in hydrogels due to stability and proteins can diffuse out before cells can respond to them [27]. Another option is the use of injectable carriers, but challenges include the narrow range of acceptable temperatures, the need for rapid polymerization, and the need for protein stability [26].

A method combining osteoconductivity and osteoinductivity was achieved by encapsulating rhBMP-2 within PLGA microparticles added to calcium phosphate cement powder [28]. While this method resulted in slow release, the total quantity released was low, and the compressive strength of the composite scaffold was much lower compared to an unloaded scaffold. Biomolecules have also been incorporated into the polymer component of composite scaffolds and can be actively released in a timed fashion [29].

Inductive techniques do not meet all of the criteria of an ideal bone tissue engineering approach. Many approaches meet a single criterion such as osteoconductivity or osteoinductivity, but rarely both. Developing a bone tissue engineering approach that meets all of the criteria is the motivation for utilizing coprecipitation to incorporate biomolecules within the biomimetically prepared bone-like mineral onto degradable polymer substrates.

1.5 Coprecipitation

A promising alternative to other methods of incorporation is the coprecipitation of biological factors and calcium phosphate. Many techniques for depositing ceramics onto a substrate involve high temperatures and organic solvents, which may alter the conformation of a biomolecule and/or its biological efficacy [30]. An important advantage to coprecipitation is the ability to produce calcium phosphate coatings at a physiological temperature [31, 32], therefore minimizing conditions that would alter the biological activity of the factors.

The process of coprecipitation has been used to incorporate a range of molecules within a layer of apatite including laminin, cytochrome C, and antibiotics [33-37].

Coprecipitation has been utilized for incorporating BMP-2 into the biomimetic coatings prepared on titanium substrates with retention of biological activity [38]. The presence of the bone-like mineral layer will serve as an osteoconductive surface and as a source of mechanical support, design parameters not provided by a polymer system capable of temporal delivery. Integrating bone-like apatite with inductive factors in the development of a delivery system via coprecipitation allows for the efficient utilization of the apatite interface.

1.6 Growth Factor Induced Osteogenic Differentiation

The most common biological factors that are incorporated and released from biomaterials are growth factors. Growth factors are proteins that regulate cellular signals in a concentration dependent manner and can stimulate or inhibit cellular migration, adhesion, proliferation, and differentiation. Many cell types can produce the same growth factor and subsequently that single growth factor can act on other cells with similar or different effects. Growth factors can also influence the activation of other growth factors in a synergistic or antagonistic manner.

Typically, when a biomaterial carrier system is developed, only a single factor is delivered. While the use of one growth factor can elicit cellular proliferation and/or differentiation [6, 39, 40], the biological environment is not limited to the activation of a single growth factor. To better simulate the microenvironment that cells are subjected to *in vivo*, exposure to multiple biological agents with a spatial and temporal gradient would be ideal. While there are carrier systems that deliver multiple factors, the means of varying the release can be limited in regards to localization of the factors of interest. The

major obstacle in designing a delivery system that can deliver multiple types of biomolecules is the ability to control the spatial and therefore the temporal exposure of each biomolecule to the cells. Because osteogenic differentiation is dependent on the gradients of multiple growth factors, as well as the concentration of the individual growth factors, either synergistic or antagonistic effects could result. For example, vascular endothelial growth factor (VEGF) alone is not sufficient to improve healing of critical size bone defects, however by combining VEGF with BMP-4 (bone morphogenetic protein-4), enhanced healing was demonstrated [41]. On the other hand, combined application of osteopontin-1 (OP-1) and BMP-2 did not enhance bone regeneration over single growth factor applications [42]. Simultaneous application of insulin-like growth factor-I (IGF-I) and BMP-2 did not significantly increase alkaline phosphatase activity or calcium content; however, when the cells were first exposed to BMP-2 followed by IGF-I or BMP-2 and IGF-I, the best biological response was achieved, demonstrating the importance the sequence of delivery of the growth factors had on cellular response [43]. By utilizing coprecipitation to incorporate the factors into a biomimetic apatite layer, the spatial localization and therefore the temporal release of multiple growth factors can be better regulated in comparison to superficially adsorbing the factors to the apatite.

Two specific growth factors that have important roles in osteogenic differentiation are BMP-2 and FGF-2 (fibroblastic growth factor-2). BMP-2 is a member of the transforming growth factor (TGF-beta) superfamily. *In vitro*, BMPs regulate growth and differentiation of cells in the osteoblast lineage. BMSCs (bone marrow stromal cells) cultured in medium containing rhBMP-2 demonstrated an increase in the expression of osteopontin (OPN) and increased mineralization in comparison to cells not exposed to

rhBMP-2 [6]. *In vitro*, rhBMP-2 not only induces differentiation of osteoblastic precursors, but it also inhibits myogenic differentiation [44]. *In vivo*, BMP-2 can induce both bone and cartilage tissue formation [45]. BMP-2 is one of the earliest genes that is induced in fracture healing, with a second peak occurring late in the period of osteogenesis [46], which suggests that a simple burst release or sustained release would not be sufficient to elicit optimal results.

Fibroblast growth factors promote cell growth, induce a mitogenic response, stimulate cell migration, and induce differentiation [47]. FGF-2 is a well known angiogenic factor and its angiogenic efficacy can vary with the dose in a nonlinear relationship [48]. However, FGF-2 has also demonstrated a role in osteogenic differentiation. FGF-2 stimulated the replication of osteoprogenitor cells, which then further differentiated into an osteoblastic phenotype, however, prolonged treatment resulted in an inhibitory effect [49]. *In vivo*, FGF-2 coated HA implants induced higher bone formation compared to uncoated implants [50]. Because both of these growth factors have a role in the osteogenic regulatory process, they have been used in combination to elucidate their effects on each other, whether synergistic or antagonistic. FGF-2 stimulated cell growth and osteoblastic differentiation of dexamethasone treated MSCs, and upon exposing cells to both BMP-2 and FGF-2, bone formation was enhanced more than either growth factor individually [51], confirming again the importance of temporal gradients.

1.7 Plasmid DNA Induced Osteogenic Differentiation

An alternative to the usage of growth factors is gene delivery. Plasmid DNA can minimize or eliminate some of the disadvantages of using growth factors, including their short half lives, tissue selectivity, and the risk of toxicity [52]. Transfection of host cells in the defect site by the desired gene will promote secretion of the growth factor, potentially promoting regeneration [3].

Gene therapy can be divided into two general categories: viral and non-viral methods. Viral methods [53-56] include retroviral vectors, adenoviral vectors, and lentiviral vectors. Advantages to using viral vectors include high transfection efficiency for dividing and non-dividing cells, ability to integrate into the host genome, and high levels of expression after cellular transfection. However, there are also disadvantages including high cost, difficulty preparing high titer supplies, limited control over expression, oncogenicity, and high immunogenicity [57, 58].

Non-viral methods [54, 59, 60] encompass the usage of liposomes, cationic lipids, polymers complexed to DNA, or physical methods such as microinjection or gene gun delivery [57]. The advantages of using non-viral methods include the unlimited size of plasmid constructs, low cost, DNA stability under many conditions, and the ability of using delivery systems and carriers [58]. However, there are also disadvantages associated with the non-viral methods including lower transfection efficiency compared to viral methods and a risk of toxicity [2, 57, 58]. Non-viral methods of transfection can occur with both host cells as well as transplanted cells. As cells are recruited to and migrate into the biomaterial carrier, they encounter DNA that is either released or entrapped in the matrix, uptake the plasmid, and release additional biomolecules that

direct cellular behavior [59, 61]. An optimal gene delivery system would involve targeting the desired cell type, promoting internalization by endocytosis, avoiding degradation, and promoting the delivery of plasmid through the nuclear membrane [62]. If transfection is successful, transcription, translation, and finally the expression of the desired protein will occur based on natural mechanisms [63].

DNA can be encapsulated and released from carriers [64, 65]. Other common methods of condensing non-viral DNA for gene transfer use cationic agents such as polymers or lipids. DNA can also be complexed with cationic polymers that can enter cells through charge mediated interactions or receptor mediated endocytosis [57]. Conjugating DNA with a cationic polymer or lipid would protect the DNA from nuclease degradation, minimize the negative surface charge, and target specific cell types through receptor ligand interactions [66]. DNA condensation also leads to a significant increase in mineralized tissue density compared to uncondensed DNA [60]. Disadvantages of this system include possible aggregation, and limited cellular internalization due to the interactions between the DNA and the biomaterial [57, 67].

Cationic lipids have also been widely used for gene transfer. A cationic lipid is composed of a hydrophilic lipid anchor, a linker group, and a positively charged head group. The lipid anchor determines the properties of the lipid bilayer. The linker group determines the stability, biodegradability, and transfection efficiency. The head group interacts with the DNA and determines transfection and the cytotoxicity of the liposome formulation [66]. The term *lipoplex* is used to describe the structure that results when DNA is encapsulated within the lipid. Both positively and negatively charged lipoplexes can be created, however, a positive charge ratio is used most frequently in *in vitro* studies

to assist interactions with cell membranes [66]. Cationic lipid mediated transfection, which has successfully transfected osteoblastic cell lines, is regulated by the dose of lipid used: the higher the dosage, the higher the transfection rate [68].

Another method of gene transfection is calcium phosphate mediated transfection [63, 69]. The DNA is encapsulated within a calcium phosphate precipitate, which is then uptaken by the cell, resulting in gene expression [63]. The advantages to this method include protecting the DNA from degradation and encouraging cellular uptake, however, it exhibits a burst release [63], which may not always be the desired release profile.

By utilizing coprecipitation to incorporate plasmid DNA into a biomimetic apatite layer, which can increase mechanical properties, osteoinductivity and osteoconductivity are combined into a single approach that has the ability to transfect transplanted cells. Increased mechanical properties due to the presence of the mineral may result in increased substrate stiffness. By increasing substrate stiffness, cellular uptake of pDNA-PEI condensates increases [70]. Biomineralized surfaces loaded with DNA supported cell growth and provided high concentrations of DNA in a localized area to cultured cells, and the extent of transfection could be controlled via the composition of the precipitating solution [71]. This technique has the potential to deliver an inductive factor to induce osteogenic differentiation. For example, adenoviral BMP-2 gene transfer was used to transfect BMSCs, which were implanted in femoral defects inducing bone formation [72]. Additionally, direct application of the adenoviral BMP-2 vector induces ectopic bone formation in skeletal muscle [55]. Cationic lipid mediated BMP-2 gene transfer into primary BMSCs resulted in successful healing of critical sized defects [54].

1.8 Global Hypothesis and Specific Aims

This thesis details a bone tissue engineering approach that incorporates osteoconductivity and osteoinductivity into the design of the supporting biomaterial. Osteoconductivity is derived from the formation of a biomimetic apatite layer on a poly(lactic-co-glycolic) acid (PLGA) substrate. The coprecipitation of biomolecules, specifically growth factors and plasmid DNA, with biomimetically prepared apatite address the design criterion of osteoinductivity. Utilizing coprecipitation enables the production of conductive calcium phosphate coatings at physiological temperatures that do not denature inductive factors, and also leads to increased protein loading and more controlled release in comparison to adsorption methods.

The global hypothesis is that the coprecipitation of biomolecules with biomimetically prepared mineral can enhance cellular differentiation compared to superficially adsorbed biomolecules. Specifically, the coprecipitation of plasmid DNA complexed to cationic lipid will increase the transfection efficiency of cells in comparison to polymer incorporation and adsorption methods. The coprecipitation of FGF-2 and BMP-2 with biomimetically prepared mineral in a spatially controlled manner will accelerate the creation of a mineralized extracellular environment on PLGA substrates.

To address the global hypothesis, the following aims were proposed: 1) to demonstrate that coprecipitation can be used to localize a model protein within the mineral in a spatially controlled manner for delivery (Chapter 2); 2) to develop an organic/inorganic hybrid by coprecipitating plasmid DNA complexed with a cationic lipid into the apatite layer nucleated onto polymer substrates (Chapter 3); and 3) to design

an organic/inorganic hybrid by coprecipitating osteogenic growth factors within bone-like apatite that releases the growth factors based upon the criteria provided by the osteogenic response of BMSCs on tissue culture plastic (Chapter 4 and 5).

Chapter 2 details the development of an inorganic/organic hybrid utilizing bovine serum albumin as a model protein. The aim was to determine if utilizing coprecipitation to incorporate protein with the apatite would allow for increased loading in comparison to adsorption, and if changing coprecipitation times would allow for spatial control of the protein through the thickness of the mineral. Spatial localization would therefore allow more control over the temporal exposure of each biomolecule to the cells.

Coprecipitation can be used in both gene and growth factor delivery where release is substrate mediated. Based on the ability of coprecipitation to increase loading in biomimetic apatite, Chapter 3 details the coprecipitation of DNA-lipoplexes in the development of an inorganic/organic hybrid capable of non-viral delivery to cells. By combining the complexation of DNA with a cationic lipid (condensation of DNA) and calcium phosphate coprecipitation (high, homogeneous distribution and retention of DNA on the apatite surface), the transfection efficiency of cells can be increased in comparison to adsorption and polymer incorporation methods.

Before substrate mediated delivery of growth factors can be developed, a determination of the concentration and sequence of delivery of the growth factors of interest, BMP-2 and FGF-2, for optimal differentiation of BMSCs is needed. It was hypothesized that the desired sequence of growth factors that synergistically enhances cellular differentiation of BMSCs would be best achieved by a release of FGF-2 followed by a slower release of BMP-2. In Chapter 4, the concentrations and the sequence of

delivery necessary for these two growth factors to enhance osteogenic differentiation of BMSCs were studied. In Chapter 5, based on the ability of coprecipitation to spatially localize biomolecules within biomimetic apatite, a hybrid delivery system was developed that sequentially delivers FGF-2 and BMP-2 from apatite with the aim of mimicking the osteogenic differentiation of BMSCs on TCPS. Release profiles of the growth factors were determined, as well as the extent of cellular differentiation *in vitro* as regulated by the spatial localization of BMP-2 and FGF-2 within the mineral.

1.9 Summary

The studies contained in this dissertation focused on coprecipitation as a method to incorporate growth factors and plasmid DNA within biomimetically prepared mineral to direct and enhance cellular response. This bone tissue engineering approach encompasses conductivity, via the presence of the apatite mineral, inductivity, provided by the presence of either growth factors or plasmid DNA, while also allowing for better control over the spatial, and therefore the temporal gradients that are necessary for enhancing osteogenic differentiation.

The biological significance of these studies relates to better simulating the environment that cells reside in, due to the action of multiple growth factors or the induction of genes. The clinical significance of these studies relates to the possibility of delivering multiple genes or factors in a safe manner that can be controlled, while simultaneously providing mechanical support, biocompatibility, and biodegradability through the supporting biomaterial potentially accelerating bone regeneration.

Ion Concentration (mM)								
	Na^+	K^+	Mg^{2+}	Ca^{2+}	Cl^-	HCO_3^-	HPO_4^{2-}	SO_4^{2-}
Human blood plasma	142.0	5.0	1.5	2.5	103.0	27.0	1.0	0.5
1 X SBF	145.2	5.0	1.5	2.5	152.0	4.2	1.0	0.5
1 X modified SBF	145.2	6.0	1.5	5.0	157.0	4.2	2.0	0.5
1.5 X SBF	213.0	7.5	2.3	3.8	223.0	6.3	1.5	0.8
2 X SBF	284.0	10.0	3.0	5.0	297.6	8.4	2.0	1.0

Table 1.1: An abbreviated list of commonly used Simulated Body Fluids.

References

1. Gunn C. Bones and Joints: a guide for students. 3rd Edition ed. New York: Churchill Livingstone; 1996.

2. Li RH, Wozney JM. Delivering on the promise of bone morphogenetic proteins. Trends Biotechnol 2001;19:255-265.

3. Tabata Y. Tissue regeneration based on growth factor release. Tissue Eng 2003;9:S5-S15.

4. Bauer TW, Muschler GF. Bone graft materials. An overview of the basic science. Clin Orthop 2000;(371):10-27.

5. Jacobs JJ, Gilbert JL, Urban RM. Current concepts review. Corrosion of metal orthopaedic implants. J Bone Joint Surg Am 1998;80:1554.

6. Huang WB, Carlsen B, Wulur I, Rudkin G, Ishida K, Wu B, et al. BMP-2 exerts differential effects on differentiation of rabbit bone marrow stromal cells grown in two-dimensional and three-dimensional systems and is required for in vitro bone formation in a PLGA scaffold. Exp Cell Res 2004;299:325-334.

7. Seeherman H, Wozney J, Li R. Bone morphogenetic protein delivery systems. Spine 2002;27:S16-S23.

8. Hench LL. Bioceramics - from Concept to Clinic. J Am Ceram Soc 1991;74:1487-1510.

9. Yan W, Nakamura T, Kawanabe K, Nishigochi S, Oka M, Kokubo T. Apatite layer-coated titanium for use as bone bonding implants. Biomaterials 1997;18:1185-1190.

10. Winn SR, Uludag H, Hollinger JO. Sustained release emphasizing recombinant human bone morphogenetic protein-2. Adv Drug Deliv Rev 1998;31:303-318.

11. Kim HM, Kishimoto K, Miyaji F, Kokubo T, Yao T, Suetsugu Y, et al. Composition and structure of the apatite formed on PET substrates in SBF modified with various ionic activity products. J Biomed Mater Res 1999;46:228-235.

12. Hoffman AS. Biologically Functional Materials. In: Ratner BD, Hoffman AS, Schoen FJ, Lemons JE, editors. Biomaterials Science: An Introduction to Materials in Medicine. San Diego: Academic Press, 1996. p. 124-130.

13. Luginbuehl V, Meinel L, Merkle HP, Gander B. Localized delivery of growth factors for bone repair. Eur J Pharm Biopharm 2004;58:197-208.

14. Sumner DR, Turner TM, Urban RM, Leven RM, Hawkins M, Nichols EH, et al. Locally delivered rhTGF-beta(2) enhances bone ingrowth and bone regeneration at local and remote sites of skeletal injury. Journal of Orthopaedic Research 2001;19:85-94.

15. Arm DM, Tencer AF, Bain SD, Celino D. Effect of controlled release of platelet-derived growth factor from a porous hydroxyapatite implant on bone ingrowth. Biomaterials 1996;17:703-709.

16. Campbell AA, Song L, Li XS, Nelson BJ, Bottoni C, Brooks DE, et al. Development, characterization, and anti-microbial efficacy of hydroxyapatite-chlorhexidine coatings produced by surface-induced mineralization. J Biomed Mater Res 2000;53:400-407.

17. Alam MI, Asahina I, Ohmamiuda K, Takahashi K, Yokota S, Enomoto S. Evaluation of ceramics composed of different hydroxyapatite to tricalcium phosphate ratios as carriers for rhBMP-2. Biomaterials 2001;22:1643-1651.

18. Midy V, Rey C, Bres E, Dard M. Basic fibroblast growth factor adsorption and release properties of calcium phosphate. J Biomed Mater Res 1998;41:405-411.

19. Ziegler J, Mayr-Wohlfart U, Kessler S, Breitig D, Gunther KP. Adsorption and release properties of growth factors from biodegradable implants. J Biomed Mater Res 2002;59:422-428.

20. Woo BH, Fink BF, Page R, Schrier JA, Jo YW, Jiang G, et al. Enhancement of bone growth by sustained delivery of recombinant human bone morphogenetic protein-2 in a polymeric matrix (vol 18, pg 1747, 2001). Pharm Res 2003;20:334-334.

21. Lu L, Stamatas GN, Mikos AG. Controlled release of transforming growth factor beta 1 from biodegradable polymer microparticles. J Biomed Mater Res 2000;50:440-451.

22. Perets A, Baruch Y, Weisbuch F, Shoshany G, Neufeld G, Cohen S. Enhancing the vascularization of three-dimensional porous alginate scaffolds by incorporating controlled release basic fibroblast growth factor microspheres. Journal of Biomedical Materials Research Part a 2003;65A:489-497.

23. Ijntema K, Heuvelsland WJM, Dirix C, Sam AP. Hydroxyapatite Microcarriers for Biocontrolled Release of Protein Drugs. Int J Pharm 1994;112:215-224.

24. Shea LD, Smiley E, Bonadio J, Mooney DJ. DNA delivery from polymer matrices for tissue engineering. Nat Biotechnol 1999;17:551-554.

25. Richardson TP, Peters MC, Ennett AB, Mooney DJ. Polymeric system for dual growth factor delivery. Nat Biotechnol 2001;19:1029-1034.

26. Malafaya PB, Silva GA, Baran ET, Reis RL. Drug delivery therapies II. Strategies for delivering bone regenerating factors. Current Opinion in Solid State & Materials Science 2002;6:297-312.

27. Salinas CN, Anseth KS. Mesenchymal stem cells for craniofacial tissue regeneration: designing hydrogel delivery vehicles. J Dent Res 2009;88:681-692.

28. Ruhe PQ, Hedberg EL, Padron NT, Spauwen PHM, Jansen JA, Mikos AG. rhBMP-2 release from injectable poly(DL-lactic-co-glycolic acid)/calcium-phosphate cement composites. Journal of Bone and Joint Surgery-American Volume 2003;85A:75-81.

29. Murphy WL, Peters MC, Kohn DH, Mooney DJ. Sustained release of vascular endothelial growth factor from mineralized poly(lactide-co-glycolide) scaffolds for tissue engineering. Biomaterials 2000;21:2521-2527.

30. Kofron MD, Li XD, Laurencin CT. Protein- and gene-based tissue engineering in bone repair. Curr Opin Biotechnol 2004;15:399-405.

31. Wen HB, de Wijn JR, van Blitterswijk CA, de Groot K. Incorporation of bovine serum albumin in calcium phosphate coating on titanium. J Biomed Mater Res 1999;46:245-252.

32. Wen HB, Wolke JG, de Wijn JR, Liu Q, Cui FZ, de Groot K. Fast precipitation of calcium phosphate layers on titanium induced by simple chemical treatments. Biomaterials 1997;18:1471-1478.

33. Sogo Y, Ito A, Fukasawa K, Kondo N, Ishikawa Y, Ichinose N, et al. Coprecipitation of cytochrome C with calcium phosphate on hydroxyapatite ceramic. Current Applied Physics 2005;5:526-530.

34. Liu YL, Layrolle P, de Bruijn J, van Blitterswijk C, de Groot K. Biomimetic coprecipitation of calcium phosphate and bovine serum albumin on titanium alloy. J Biomed Mater Res 2001;57:327-335.

35. Oyane A, Yokoyama Y, Uchida M, Ito A. The formation of an antibacterial agent-apatite composite coating on a polymer surface using a metastable calcium phosphate solution. Biomaterials 2006;27:3295-3303.

36. Uchida M, Oyane A, Kim HM, Kokubo T, Ito A. Biomimetic coating of laminin-apatite composite on titanium metal and its excellent cell-adhesive properties. Adv Mater 2004;16:1071-+.

37. Stigter M, de Groot K, Layrolle P. Incorporation of tobramycin into biomimetic hydroxyapatite coating on titanium. Biomaterials 2002;23:4143-4153.

38. Liu YL, Hunziker EB, Layrolle P, De Bruijn JD, De Groot K. Bone morphogenetic protein 2 incorporated into biomimetic coatings retains its biological activity. Tissue Eng 2004;10:101-108.

39. Hanada K, Dennis JE, Caplan AI. Stimulatory effects of basic fibroblast growth factor and bone morphogenetic protein-2 on osteogenic differentiation of rat bone marrow-derived mesenchymal stem cells. Journal of Bone and Mineral Research 1997;12:1606-1614.

40. Rodan SB, Wesolowski G, Thomas KA, Yoon KG, Rodan GA. Effects of Acidic and Basic Fibroblast Growth-Factors on Osteoblastic Cells. Connect Tissue Res 1989;20:283-288.

41. Peng H, Wright V, Usas A, Gearhart B, Shen HC, Cummins J, et al. Synergistic enhancement of bone formation and healing by stem cell-expressed VEGF and bone morphogenetic protein-4. J Clin Invest 2002;110:751-759.

42. Ripamonti U, Crooks J, Petit JC, Rueger DC. Periodontal tissue regeneration by combined applications of recombinant human osteogenic protein-1 and bone morphogenetic protein-2. A pilot study in Chacma baboons (Papio ursinus). Eur J Oral Sci 2001;109:241-248.

43. Raiche AT, Puleo DA. In vitro effects of combined and sequential delivery of two bone growth factors. Biomaterials 2004;25:677-685.

44. Yamaguchi A, Katagiri T, Ikeda T, Wozney JM, Rosen V, Wang EA, et al. Recombinant Human Bone Morphogenetic Protein-2 Stimulates Osteoblastic Maturation and Inhibits Myogenic Differentiation Invitro. J Cell Biol 1991;113:681-687.

45. Miyazono K. Bone Morphogenetic Protein Receptors and Actions. In: Bilezikian JP, Raisz LG, Rodan GA, editors. Principles of bone biology. San Diego: Academic Press, 2002. p. 929-942.

46. Cho TJ, Gerstenfeld LC, Einhorn TA. Differential temporal expression of members of the transforming growth factor beta superfamily during murine fracture healing. Journal of Bone and Mineral Research 2002;17:513-520.

47. Hurley MM, Marie PJ, Florkiewicz RZ. Fibroblast Growth Factor (FGF) and FGF Receptor Families in Bone. In: Bilezikian JP, Raisz LG, Rodan GA, editors. Principles of bone biology. San Diego: Academic Press, 2002. p. 825-851.

48. Norrby K. Basic fibroblast growth factor and de novo mammalian angiogenesis. Microvasc Res 1994;48:96-113.

49. Canalis E, Centrella M, Mccarthy T. Effects of Basic Fibroblast Growth-Factor on Bone-Formation Invitro. J Clin Invest 1988;81:1572-1577.

50. Schnettler R, Alt V, Dingeldein E, Pfefferle HJ, Kilian O, Meyer C, et al. Bone ingrowth in bFGF-coated hydroxyapatite ceramic implants. Biomaterials 2003;24:4603-4608.

51. Hanada K, Dennis JE, Caplan AI. Stimulatory effects of basic fibroblast growth factor and bone morphogenetic protein-2 on osteogenic differentiation of rat bone marrow-derived mesenchymal stem cells. J Bone Miner Res 1997;12:1606-1614.

52. Putney SD, Burke PA. Improving protein therapeutics with sustained-release formulations. Nat Biotechnol 1998;16:153-157.

53. Jin QM, Anusaksathien O, Webb SA, Rutherford RB, Giannobile WV. Gene therapy of bone morphogenetic protein for periodontal tissue engineering. J Periodontol 2003;74:202-213.

54. Park J, Ries J, Gelse K, Kloss F, von der Mark K, Wiltfang J, et al. Bone regeneration in critical size defects by cell-mediated BMP-2 gene transfer: a comparison of adenoviral vectors and liposomes. Gene Ther 2003;10:1089-1098.

55. Musgrave DS, Bosch P, Ghivizzani S, Robbins PD, Evans CH, Huard J. Adenovirus-mediated direct gene therapy with bone morphogenetic protein-2 produces bone. Bone 1999;24:541-547.

56. Hu W, Elkasabi Y, Chen H, Zhang Y, Lahann J, Hollister SJ, et al. The use of reactive polymer coatings to facilitate gene delivery from poly (ε-caprolactone) scaffolds. Biomaterials 2009;30:5785-5792.

57. Partridge KA, Oreffo ROC. Gene delivery in bone tissue engineering: Progress and prospects using viral and nonviral strategies. Tissue Eng 2004;10:295-307.

58. Bonadio J, Goldstein SA, Levy RJ. Gene therapy for tissue repair and regeneration. Adv Drug Deliv Rev 1998;33:53-69.

59. Bonadio J, Smiley E, Patil P, Goldstein S. Localized, direct plasmid gene delivery in vivo: prolonged therapy results in reproducible tissue regeneration. Nat Med 1999;5:753-759.

60. Huang YC, Simmons C, Kaigler D, Rice KG, Mooney DJ. Bone regeneration in a rat cranial defect with delivery of PEI-condensed plasmid DNA encoding for bone morphogenetic protein-4 (BMP-4). Gene Ther 2005;12:418-426.

61. Jang JH, Shea LD. Controllable delivery of non-viral DNA from porous scaffolds. J Controlled Release 2003;86:157-168.

62. Pouton CW, Seymour LW. Key issues in non-viral gene delivery. Adv Drug Deliv Rev 1998;34:3-19.

63. Kofron MD, Laurencin CT. Development of a calcium phosphate co-precipitate/poly(lactideco-glycolide) DNA delivery system: release kinetics and cellular transfection studies. Biomaterials 2004;25:2637-2643.

64. Hirosue S, Muller BG, Mulligan RC, Langer R. Plasmid DNA encapsulation and release from solvent diffusion nanospheres. J Controlled Release 2001;70:231-242.

65. Leong KW, Mao HQ, Truong-Le VL, Roy K, Walsh SM, August JT. DNA-polycation nanospheres as non-viral gene delivery vehicles. J Controlled Release 1998;53:183-193.

66. Segura T, Shea LD. Materials for non-viral gene delivery. Annual Review of Materials Research 2001;31:25-46.

67. Pannier AK, Shea LD. Controlled release systems for DNA delivery. Molecular Therapy 2004;10:19-26.

68. Kim SW, Ogawa T, Tabata Y, Nishimura I. Efficacy and cytotoxicity of cationic-agent-mediated nonviral gene transfer into osteoblasts. Journal of Biomedical Materials Research Part a 2004;71A:308-315.

69. Jordan M, Schallhorn A, Wurm FM. Transfecting mammalian cells: Optimization of critical parameters affecting calcium-phosphate precipitate formation. Nucleic Acids Res 1996;24:596-601.

70. Kong HJ, Liu JD, Riddle K, Matsumoto T, Leach K, Mooney DJ. Non-viral gene delivery regulated by stiffness of cell adhesion substrates. Nature Materials 2005;4:460-464.

71. Shen H, Tan J, Saltzman WM. Surface-mediated gene transfer from nanocomposites of controlled texture. Nature Materials 2004;3:569-574.

72. Lieberman JR, Daluiski A, Stevenson S, Wu L, McAllister P, Lee YP, et al. The effect of regional gene therapy with bone morphogenetic protein-2-producing bone-marrow cells on the repair of segmental femoral defects in rats. J Bone Joint Surg Am 1999;81:905-917.

Chapter 2

Spatial Control of Protein Within Biomimetically Nucleated Mineral[1]

2.1 Introduction

The clinical basis for bone regeneration is the correction of bone defects caused from trauma, congenital malformations, and progressively deforming skeletal disorders. Bone tissue engineering provides an alternative to bone grafting and direct usage of growth factors to regenerate bone. An ideal bone tissue engineering approach would incorporate osteoconductivity and osteoinductivity into the design of the supporting biomaterial, as well as biocompatibility, degradability, mechanical integrity, and the ability to support cell transplantation.

Direct bonding between implants and bone, the ultimate goal of osteoconductivity, occurs if a layer of bone-like mineral forms on the surface of the implant [1]. It has therefore been hypothesized that formation of bone-like mineral layer within the pores of a tissue engineering scaffold may enhance the conduction of host cells into scaffolds [2], and also enhance osteogenic differentiation of transplanted cells seeded on scaffolds [3]. Such a biomimetic system maintains porosity, which is important to cell migration, as well as biocompatibility, mechanical integrity, and degradability [1, 2]. While the scaffold serves as a carrier for the growth factor [4], the bone-like mineral

[1] Published as Luong, LN et al., Biomaterials 2006; 27:1175-1186

system enhances the osteoconductivity and mechanical properties of the scaffold and serves as a platform for all three tissue engineering approaches.

Osteoinductive properties can be integrated into a scaffold using methods to immobilize proteins to surfaces such as adsorption, cross-linking, covalent binding, and entrapment, each of which results in different loading efficiencies and levels of protein retention [5]. Growth factors have been adsorbed to calcium phosphate ceramic surfaces, allowing these materials to serve as delivery systems [6, 7]. Variations of protein adsorption onto bioceramics include dispersing a growth factor over the surface of porous hydroxyapatite [8, 9], adsorbing antibiotic to each new layer of mineral deposited [10], and binding ceramic pellets together with gel with the growth factor adsorbed to the surface of the pellets [11]. These techniques are dependent on two factors: the substrate, and the specific growth factor used. The release profile of a surface adsorbed growth factor is rapid release, followed by a slower release based on the chemical and/or physical attraction between the material and the growth factor adsorbed [12, 13]. In some cases, however, a more sustained release or a pulsatile release is required for a growth factor to be effective.

Coprecipitation of proteins and calcium phosphate is another method that has been used to incorporate growth factors on metal substrates, such as titanium alloy implants [14-16]. An important advantage to this approach is the ability to produce calcium phosphate coatings at a physiological temperature, therefore minimizing conditions that would change the biological activity of the factors [17, 18]. Coprecipitation leads to a more controlled protein release in comparison to adsorption methods, as well as increases the protein loading capacity [14]. Coprecipitation of

bovine serum albumin, tobramycin, or recombinant human bone morphogenetic protein 2 and calcium phosphate onto titanium resulted in the retention of biological activity [14, 15, 19]. The main disadvantage of this system is the thickness of the coating created, which can be as thick as 50 μm [14]. If porous scaffolds were used as the platform for tissue engineering and growth factor release, the thick coatings could obscure the pores, restricting transport and cellular access, and possibly access to the growth factor.

In this study, we examined coprecipitation and surface adsorption schemes with respect to their abilities to control the spatial quantity and localization of a model protein, bovine serum albumin (BSA), that is incorporated into a biomimetic apatite layer nucleated onto polylactic-co-glycolic acid (PLGA) films. Protein incorporation was characterized by determining: 1) its presence in the film; 2) the quantity of protein incorporated; 3) the effects of rinsing on protein retention; 4) the morphology of the mineral with protein incorporated; and 5) the localization of the protein.

2.2 Materials and Methods

2.2.1 PLGA film preparation

The films (approximately 30-80 μm thick) were prepared using 5 wt. % PLGA, 85:15 PLA:PGA ratio (Alkermes), in chloroform solution. The films were cast in 10 cm glass Petri dishes, then covered with aluminum foil and air dried for at least 24 hours under a fume hood. The films were cut into 2 X 2 cm^2 squares and etched in 0.5 M NaOH for seven minutes per side. They were rinsed with Millipore water before use.

2.2.2 Modified simulated body fluid and proteins used

A modified simulated body fluid (mSBF, which contains 2X the concentration of Ca^{2+} and HPO_4^{2-} as standard SBF) was used to mineralize the films [20]. mSBF consists of the dissolution of the following reagents in Millipore water: 141 mM NaCl, 4.0 mM KCl, 0.5 mM $MgSO_4$, 1.0 mM $MgCl_2$, 4.2 mM $NaHCO_3$, 5.0 mM $CaCl_2 \cdot 2H_2O$, and 2.0 mM KH_2PO_4, whereas standard SBF contains 2.5 mM $CaCl_2 \cdot 2H_2O$, and 1.0 mM KH_2PO_4. mSBF was prepared at 25°C and titrated to pH 6.8 using NaOH to avoid homogeneous precipitation of calcium phosphate. BSA was obtained from Sigma-Aldrich (A3294). Fluorescein-isothiocyanate (FITC)-labeled BSA was used in the protein localization experiments (Sigma-Aldrich, A9771).

2.2.3 Protein incorporation methods

In order to compare coprecipitation versus adsorption and quantities of protein loaded via the different protein incorporation methods, the following groups were examined: (1) 6 days coprecipitation of apatite and BSA; (2) 3 days apatite mineralization, 3 days BSA adsorption; (3) 3 days apatite mineralization, 3 days coprecipitation of apatite and BSA; (4) 3 days apatite mineralization, 2 days BSA adsorption, 1 day apatite mineralization; (5) 3 days apatite mineralization, 2 days coprecipitation of apatite and BSA, 1 day apatite mineralization; (6) 3 days apatite mineralization, 3 days acid etched BSA adsorption (10 mM EDTA); and (Control) 6 days apatite mineralization.

For mineralization, films were submerged in 40 ml of mSBF. Coprecipitation was accomplished by submerging the films in 40 ml of mSBF containing 200 μg/ml of BSA. Both mineralization and coprecipitation were carried out at 37°C and the solutions

were exchanged daily in order to replenish the ion concentration to supersaturated levels. For the samples subjected to adsorption, 0.25 ml of phosphate buffered saline (PBS) containing 200 μg/ml BSA was pipetted onto each film per day of adsorption. For Group 6, the protein was adsorbed to the surface using 10 mM ethylenediaminetetraacetic acid (EDTA), a technique which is based on higher protein retention to etched surfaces [9].

2.2.4 Protein presence

The incorporation of BSA was determined using Fourier Transform Infrared Spectroscopy (Spectrum BX FT-IR, Perkin-Elmer). The calcium phosphate coatings were scraped off each of the samples (n=2) using a ratio of approximately 300:1 of KBr to sample coating. A pellet was then prepared from this mixture. FT-IR spectra were recorded from 400 to 4000 cm^{-1} and baseline corrected.

2.2.5 Protein quantification

BSA was quantified using a Micro-Bicinchoninic acid (BCA) assay or BCA assay (Pierce, IL), depending on the concentration range. Samples (n=7) were demineralized in 10 mM HCl. The samples were placed on a magnetic stir plate and agitated at 300 rpm for three days. The samples were incubated in reagents containing Na_2CO_3, $NaHCO_3$, bicinchoninic acid, $Na_2C_4H_4O_6 \cdot 2H_2O$ in 0.1 M NaOH, and 4% cupric sulfate, provided in the kit at 60ºC for one hour for the Micro-BCA assay, or for half hour for the BCA assay.

Absorbance was measured using a UV spectrophotometer (SmartSpec 3000, BioRad) at 562 nm, and BSA concentration was determined based on standards. The BSA concentration in each of the groups was normalized to mineralized control concentrations.

2.2.6 Protein retention

To remove excess protein, samples were rinsed by gently dipping each film (n=7) in Millipore water for 10 s. Samples were dried in a fume hood and placed in a vacuum desiccator until analyses were performed. Protein presence was confirmed using FT-IR, and protein concentration was quantified using the BCA assay kits.

2.2.7 Mineral and mineral/protein coating morphology

Mineral morphology with and without BSA was examined using scanning electron microscopy (Philips XL30 FEG Scanning Electron Microscope). Sample films (n=2) were coated with a thin layer of gold and examined at 3 kV.

High resolution transmission electron microscopy (HRTEM, Jeol 2010) was operated at an acceleration voltage of 200 kV to examine the crystal orientation of the mineral deposited on the polymer substrate. Rectangular glass plates, 2 X 2 cm^2 and 1 mm thick were coated with PLGA and used as a substrate for apatite deposition. Samples with BSA incorporated via coprecipitation and samples without BSA incorporated were examined. Samples with BSA incorporation were coprecipitated for 7-8 days and samples without BSA were mineralized for 7-8 days. Additional days of coprecipitation or mineralization were needed in order to produce flakes that were appropriate for analyses. Calcium phosphate flakes were removed by breaking or dissolving PLGA between the calcium phosphate and the glass plate. The flakes were placed over a 1 mm diameter hole on a Cu grid. The grids were ion-milled on a liquid nitrogen stage at 5 kV using an incidence angle of 11-12°. Ion-milling was performed below -100°C in order to prevent damage to the sample [21]. The specimen rotation drive rod was submerged in liquid nitrogen for at least one hour prior to ion milling. To

obtain a large but thin area on the mineralized film, a laser terminator was used to terminate power.

2.2.8 Protein localization

To visualize the spatial distribution of BSA in the different sample groups, a ratio of 7:1 of BSA:FITC-labeled BSA was used. Protein incorporation groups 1, 2, 3, 5, and the control group were studied (n=3/group). Samples were produced by coating the surface of 2 X 2 cm^2 glass cover slips with 5 % wt. PLGA, 85:15 PLA:PGA ratio. The cover slips were dried in a fume hood and protein was incorporated as previously stated. After the incubation period, the samples were rinsed in three washes of Millipore water and dried in a fume hood. A small section was cut from the film and placed on a cover slide. A cover slip was glued on top of the sample and then the slide was viewed using confocal microscopy (Nikon TE 3000 Inverted Microscope) at an excitation wavelength of 488 nm. Using the BioRad Radiance 2000 LaserSharp imaging program, a series of images was taken in 2 μm intervals through the thickness of the film (approximately 100 μm) using 60X magnification oil immersion. A side depth profile through the thickness of the mineral layer on each of the films was obtained by stacking the series of images.

2.2.9 Statistical analysis

BCA assay results were analyzed with significance defined as $p<0.05$. The Kruskal-Wallis One Way ANOVA on Ranks was used to analyze the effects of protein incorporation method on the amount of BSA within the mineral. The Student-Newman-Keuls post hoc comparison test was used for pair-wise comparisons. To determine the effects of rinsing, unrinsed and rinsed samples from each experimental group were analyzed via t-tests.

2.3 Results

2.3.1 Coprecipitation incorporated protein into the biomimetic mineral coating

The FT-IR spectra of all of the biomimetic mineral coatings show phosphate absorption bands of hydroxyapatite at ca. 1031, 600, and 561 cm^{-1}, and a carbonate peak at 1456 cm^{-1} (Figure 2.1) [22]. An amide peak is shown for all three coprecipitated groups at 1652 cm^{-1} (Figure 2.1) [23]. An additional smaller amide peak was also detected at 1539 cm^{-1} [23]. A peak at ca. 1635 cm^{-1}, near one of the amide peaks, is apparent in the mineralized control as well as the surface adsorbed samples, and is associated with the presence of water or octacalcium phosphate [22].

2.3.2 Coprecipitation resulted in significantly higher incorporation

The different protein incorporation methods resulted in significantly different amounts loaded into the films, $p<0.001$ (Figure 2.2). The results are provided as the concentration (µg/ml) of protein in 10 mM HCl (demineralization solution). All three coprecipitation groups (1, 3, 5) have significantly higher amounts of protein ($p<0.05$) in comparison to the three surface adsorption groups (2, 4, 6) (Figure 2.2). When comparing the coprecipitation groups, protein loading was also significantly higher for Group 3 (3 day mineralization, 3 day coprecipitation) compared to Group 1 (6 day coprecipitation), and Group 5 (3 day mineralization, 2 day coprecipitation, 1 day mineralization), $p<0.05$. When comparing the surface adsorption groups, protein loading was significantly less for Group 4 (3 day mineralization, 2 day surface adsorption, 1 day mineralization) compared to Group 2 (3 day mineralization, 3 day surface adsorption) and Group 6 (3 day mineralization, 3 day surface adsorption using acid), $p<0.05$.

2.3.3 Coprecipitation leads to higher protein retention in comparison to adsorption

After rinsing to remove excess protein from the surface, amide peaks were still apparent in the spectra of the coprecipitated samples (Figure 2.3). The amide (1652 and 1539 cm^{-1}), carbonate (1456 cm^{-1}), and phosphate (1031, 600, and 531 cm^{-1}) peaks that were present in the unrinsed samples were also denoted in spectra of most of the coprecipitation rinsed samples. The amide peak intensity decreased for Group 3 (3 day mineralization, 3 day coprecipitation), and for Group 5 (3 day mineralization, 2 day coprecipitation, 1 day mineralization) after rinsing (e.g. compare the peak at 1652 cm^{-1} in Figure 2.3 to Figure 2.1).

While rinsing significantly affects protein retention in the surface adsorbed samples, there was no significant difference in retention when the coprecipitated samples were rinsed (Table 2.1). The efficiency of protein retention of each group was determined by obtaining the ratios of the quantity loaded after rinsing to the quantity loaded before rinsing. A ratio of approximately 1 is indicative of high protein retention after rinsing. A ratio much less than 1 is indicative of low protein retention. Two surface adsorption groups (Groups 2 and 6) showed significantly lower protein loaded onto the films after rinsing ($p<0.001$). The one exception was Group 4 (3 day mineralization, 2 day surface adsorption, 1 day mineralization), $p=0.126$.

2.3.4 Protein coprecipitation changed mineral morphology

Incorporation of BSA via coprecipitation lead to changes in the plate-like mineral morphology observed in mineralized controls, while BSA incorporation via surface adsorption did not change the plate-like mineral (Figure 2.4). Control samples (6 day mineralization) exhibited plate-like morphology that is well defined with sharp edges

(Figure 2.4, Control). Differences in morphology were found between the surface adsorbed and the coprecipitated samples. For the 6 day coprecipitation (Panel 1) and the 3 day mineralization, 3 day coprecipitation samples (Panel 3), the crystal plates were more rounded and there was less growth out of plane of the substrate due to the incorporation of BSA into the mineral. For the 3 day mineralization, 3 day coprecipitation samples (Panel 3), changes were apparent due to the absence of definable sharp plate edges. The 3 day mineralization, 2 day coprecipitation, 1 day mineralization sample (Panel 5), where the last day of treatment was mineralization without protein addition, showed similar plate-like structures to the control. The presence of the pipetted PBS/BSA solution on the mineral surface in the 3 day mineralization, 3 day adsorbed sample is characterized by the smooth material that appears on the left hand side of the image (Panel 2). Although the presence of PBS/BSA was not as apparent in the 3 day mineralization, 2 day surface adsorption, 1 day mineralization sample (Panel 4), the plate-like structures were similar to the control. The plate-like structures were not rounded like the structures that were present in the 6 day coprecipitation sample (Panel 1) or in the 3 day mineralization, 3 day coprecipitation samples (Panel 3). The acid etched sample (Panel 6) shows complete coverage of the acid/protein over the entire surface of each nucleation site resulting in smooth coverage.

HRTEM images of the films (A) without and (B) with BSA coprecipitation displayed plate-like apatite (Figure 2.5). The size, shape, and distribution of the apatite crystals did not appear to be affected by the presence of BSA. However, a careful examination of the samples revealed that the coprecipitated apatite consisted of locally parallel layers, all parallel to the long axis of the plates (Figure 2.5 B, marked with

arrows) whereas the layers were not visible in the samples without BSA coprecipitation (e.g. Figure 2.5A). Diffraction patterns from the samples (A) without and (B) with BSA coprecipitation exhibited differences in the crystallographic orientations. The (002) ring observed in the samples without BSA (A) is not visible in BSA coprecipitated samples (B).

2.3.5 Coprecipitation allows for control over the localization of the protein

For the 6 day coprecipitation sample (Group 1), fluorescence was present throughout the thickness of the mineral layer (Figure 2.6, Panel 1). At the bottom of the mineral layer (layer closest to the polymer substrate), fluorescence occurred in the center of each nucleation site, and increased in intensity as more mineral and protein were deposited. In Group 2 (3 day mineralization, 3 day surface adsorption) little of the protein was adsorbed to the surface of the mineralization sites. Also, because the protein was surface adsorbed, the fluorescence was only on the surface of the mineral. Images closer to the polymer substrate show the fluorescence surrounding a dark circular center. Group 3 (3 day mineralization, 3 day coprecipitation) demonstrated a similar principle of coprecipitation to Group 2. The images closest to the substrate show fluorescence surrounding a dark center; towards the top of the mineral layer, fluorescence was exhibited throughout the entire mineralization site. For Group 5 (3 day mineralization, 2 day coprecipitation, 1 day mineralization), fluorescence occurred as a shell closer to the polymer substrate. At the surface of the mineral (top image), darker circles were also present and fluorescence was less intense. The additional dark circles were due to the additional day of mineralization that occurred for those samples. The mineralization that

occurred on the last day had no protein incorporated; therefore fluorescence should not be present.

Side depth profiles were obtained by stacking the images acquired through the 100 μm thickness of mineral and substrate show fluorescence through the thickness (Figure 2.7). Consistent fluorescence occurred over a flat surface in the 6 day coprecipitation samples (Panel 1), which is not the case for the other groups. The 3 day mineralization, 3 day coprecipitation sample (Panel 3), and the 3 day mineralization, 2 day coprecipitation, 1 day mineralization sample (Panel 5) both showed an uneven fluorescence due to the mineral nucleation sites that occurred before FITC-labeled BSA was incorporated. In the 3 day mineralization, 3 day surface adsorption sample (Panel 2) fluorescence is also uneven, again due to the presence of the mineral nucleation sites that do not contain FITC-labeled BSA.

2.4 Discussion

There are various ways to immobilize proteins to surfaces, including physical adsorption, cross-linking, covalent binding, and entrapment. These methods have varying loading efficiency and varying levels of protein retention with manipulation [5]. Physical adsorption leads to low levels of loading while entrapment maintains high levels of loading; protein retention is low for physical adsorption and high for entrapment techniques. While coprecipitation of mineral and protein has been investigated using titanium alloy implants and supersaturated calcium phosphate solutions, it has not been investigated on a polymer substrate. The focus of this study has been on the use of mSBF and BSA to form a thin organic/inorganic layer on an organic film at a physiological pH,

temperature, and pressure, leading to spatially controlled protein localization within the mineral layer. Using BSA as the model protein, we have demonstrated that more protein can be incorporated into a mineral layer nucleated onto PLGA films via coprecipitation than via surface adsorption, and coprecipitation also allows for more control over protein localization in comparison to surface adsorption. By being able to control protein loading and spatial localization, it is hypothesized that a desired biological response can be elicited due to the resultant protein or growth factor release profile.

The presence of the amide bands in the FT-IR spectra showed that BSA was incorporated into both the coprecipitated and the surface adsorbed mineral, with a slight difference in amide intensity. The presence of phosphate and carbonate groups confirmed the presence of a carbonated apatite mineral [22].

Coprecipitation incorporates significantly more protein into a biomimetic apatite layer than surface adsorption. BSA is an acidic protein that is negatively charged at a pH of 6.8, therefore electrostatic interactions are important [24]. Through the interactions of its COOH groups, BSA binds to the Ca^{2+} on the surface of the mineral [24]. Another possibility is a conformational change upon attachment of BSA to the mineral surface, resulting in the exposure of NH_3^+ groups, and therefore interactions between BSA and mineral would occur with the phosphate groups [24]. These interactions lead to higher incorporation via coprecipitation because mineral and protein were deposited together through the thickness of the mineral layer, whereas in adsorption, these interactions were limited to the surface.

The significant increase in protein quantity when using 3 day mineralization, 3 day coprecipitation in comparison to a 6 day coprecipitation suggests that the preliminary

mineral layer that was deposited increases the affinity of the protein, thus increasing its incorporation. BSA is a negatively charged protein, and PLGA a hydrophobic polymer. The mineral layer is both positively and negatively charged, and with the presence of this layer the protein can better interact with the biomaterial surface. In the current study, once BSA has been incorporated onto the mineral surface, it increases the affinity for additional calcium phosphate deposition through its interactions with Ca^{2+}. The initial precipitated mineral serves to attract more BSA to the surface [25], resulting in a cyclical process. With the 6 day coprecipitation group, the preliminary mineral layer is absent, therefore protein cannot be deposited as easily due to the absence of Ca^{2+} molecules.

There was no significant difference in protein loaded between 6 day (Group 1) and 2 day (Group 5) coprecipitation. Thus, by premineralizing the films, fewer days of coprecipitation are needed to achieve the same amount of protein loaded. The significant decrease in protein amount between the 3 day mineralization, 2 day surface adsorption, 1 day mineralization group and the 3 day mineralization, 3 day adsorption group indicates that a polymer film that has protein adsorbed loses a majority of the protein once it is placed into solution due to weak surface interactions.

Coprecipitation resulted in significantly higher retention of protein following rinsing (Figure 2.3 & Table 2.1). These data point to a stronger interaction of the protein with the mineral surface when coprecipitation is utilized. Higher protein retention is also the result of distributing the protein through the thickness of the apatite layer via coprecipitation, whereas in adsorption, the protein is bound to just the apatite surface. With surface adsorption, a large percentage of the protein is lost to solution once the

sample is rinsed, suggesting that the BSA desorbs from the mineral layer and is distributed back into solution[24].

By coprecipitating protein into the mineral, the morphology of the mineral changed. BSA coats the surface of the mineral and alters the plate-like structures. BSA is chemically bound into or onto calcium phosphate, as indicated by the change in morphology and composition of the crystals in this study, as well as the absence of BSA release without the dissolution of calcium phosphate [17].

The addition of BSA, especially higher concentrations, results in a decrease in the crystallinity of the calcium phosphate precipitates [26]. Decreasing crystallinity of the calcium phosphate decreases protein release rates, which can contribute to better control of release kinetics [27]. The reason for the difference in the crystallographic orientation between the mineralized samples and the coprecipitated samples may be attributed to the interaction between BSA and crystallographic structure of apatite. With coprecipitation, protein may be incorporated into the three dimensional crystal latticework [14]. A model was recently suggested regarding the interaction between aspartic acid and apatite crystals, which proposed that aspartic acid was enclosed inside a fourfold carbonate substituted apatite unit cell [28]. Based on the analysis of the HRTEM images and the diffraction patterns, BSA also has an influence on the crystal structure during the nucleation and growth of the mineral. Apatite growth can be influenced by the presence of protein because of the strong affinity between Ca^{2+} and protein. Since the spatial distribution of Ca^{2+} is orientation dependent, the preferential growth orientation can be modified by the presence of BSA.

With coprecipitation, the localization of the protein throughout the mineral layer can be controlled by changing the coprecipitation scheme. By using a 6 day coprecipitation process, the protein is incorporated throughout the mineral layer, whereas with adsorption the protein is only on the surface of the mineral (Figure 2.6 & Figure 2.7). In coprecipitation, the mineral is depositing with the protein, therefore the protein is being incorporated simultaneously with the mineral. The different coprecipitation schemes that were examined in this study show that the spatial localization of the protein can be controlled by controlling the start and extent of coprecipitation.

The control of protein localization could be manipulated to control the release kinetics of growth factors or other biomolecules. By changing the number of days of coprecipitation, or times at which protein is added to the mineralizing solution, the release kinetics of a growth factor can be varied. Multiple growth factors or plasmid DNA could also be incorporated into the bone-like mineral layer and/or the polymer substrate. Bone-like mineral will increase osteoconductivity and mechanical properties [2, 3], while growth factors or plasmid DNA will increase inductivity. DNA [29] and other proteins [12, 15] bind to apatite crystals through affinity binding. By controlling the loading quantity and localization of the protein through the mineral thickness, a desired release profile can be achieved. Protein release kinetics from coprecipitation samples differ in comparison to surface adsorbed samples. The burst release profile at early time points from adsorbed samples is minimized, suggesting that the protein has become an integral part of the mineral layer [14].

2.5 Conclusion

At standard temperature and pressure, coprecipitation processes were used to incorporate a model protein, BSA, into a biomimetic carbonated apatite mineral nucleated onto PLGA films. Coprecipitation of apatite and protein increased the quantity of protein incorporated into the apatite, in comparison to surface adsorption of protein following apatite deposition. This study also showed that coprecipitation allows for higher protein retention following rinsing, in comparison to adsorption. Furthermore, coprecipitation of protein along with apatite allowed for control over the localization of protein through the apatite thickness. The higher protein loading of this biomaterial system, and ability to spatially control the location of protein within the apatite, along with the provision of osteoinductivity and osteoconductivity, are important requirements for designing a desired protein release profile and effective delivery system of biological agents for bone regeneration.

Acknowledgements

I would like to thank the co-authors on this research, David Kohn, Sun Ig Hong, Rusha Patel, and Mark Outslay. This research is supported by NIH DE 015411, DE 13380, and the National Science Foundation Graduate Research Fellowship. The authors would like to thank the University of Michigan Electron Microbeam Analysis Laboratory for the use of their scanning electron microscope. The authors would also like to thank Sharon Miller and Laura Darjatmoko for their aid in manuscript revision and helpful advice.

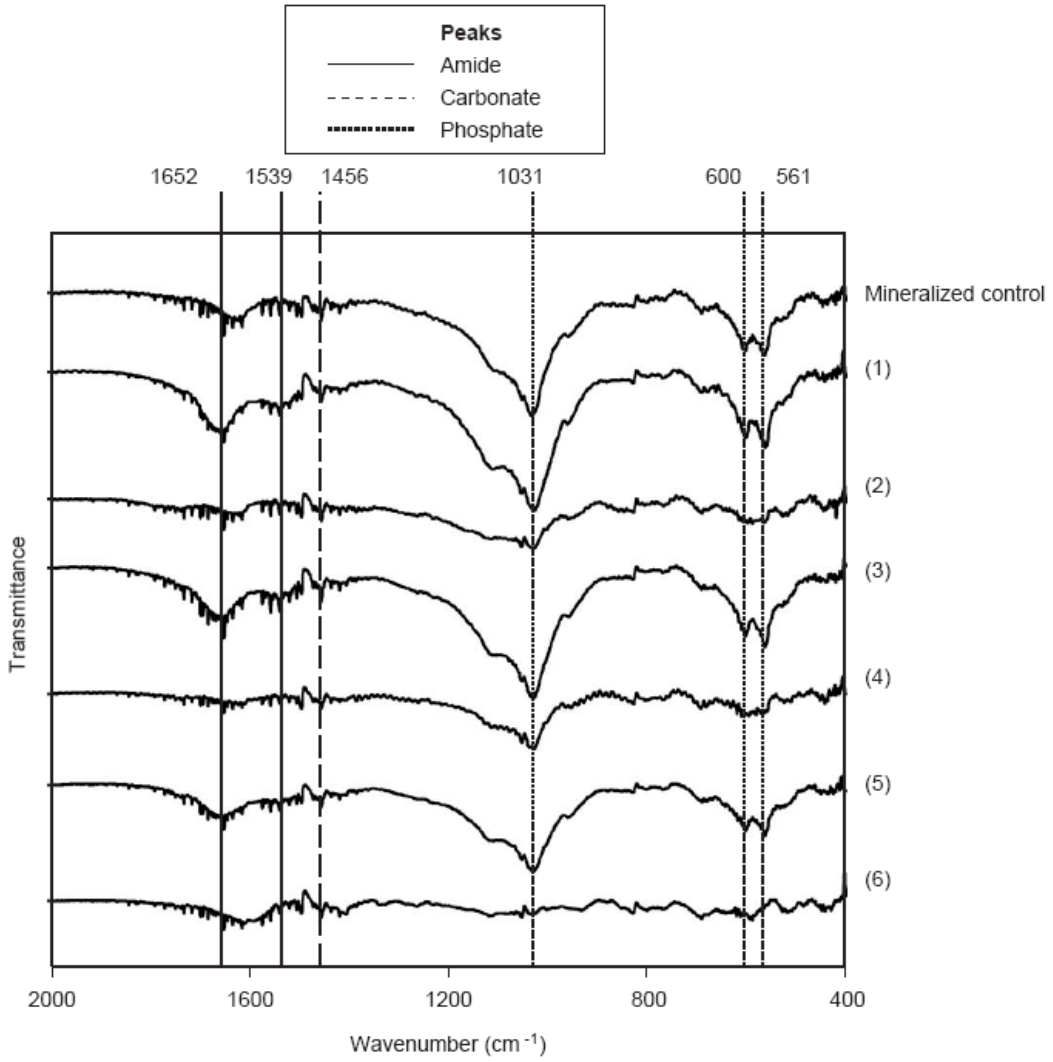

Figure 2.1: Representative FT-IR spectra for the mineral-protein samples formulated via each of the following techniques: mineralized control, (1) 6 day coprecipitation, (2) 3 day mineralization, 3 day adsorption, (3) 3 day mineralization, 3 day coprecipitation, (4) 3 day mineralization, 2 day adsorption, 1 day mineralization, (5) 3 day mineralization, 2 day coprecipitation, 1 day mineralization, and (6) 3 day mineralization, 3 day acid etched adsorption. The phosphate (1031, 600, 561 cm-1) peaks are denoted by dotted lines, a carbonate (1456 cm-1) peak is denoted by a dashed line, and the amide (1652 and 1539 cm-1) peaks are denoted by solid lines. Amide peaks are shown for all three coprecipitation groups.

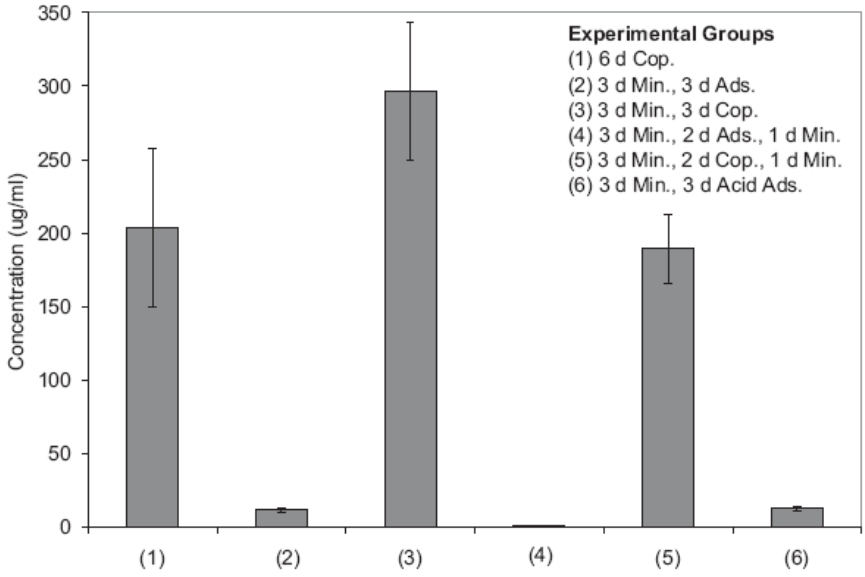

Groups	6 d Cop.	3 d Min., 3 d Ads.	3 d Min., 3 d Cop.	3 d Min., 2 d Ads., 1 d Min.	3 d Min., 2 d Cop., 1 d Min.	3 d Min., 3 d Acid
6 d Cop.						
3 d Min., 3 d Ads.						
3 d Min., 3 d Cop.						
3 d Min., 2 d Ads., 1 d Min.						
3 d Min., 2 d Cop., 1 d Min.						
3 d Min., 3 d Acid						

Figure 2.2: Protein quantification for the mineral-protein samples via the following methods of protein incorporation: (1) 6 day coprecipitation, (2) 3 day mineralization, 3 day adsorption, (3) 3 day mineralization, 3 day coprecipitation, (4) 3 day mineralization, 2 day adsorption, 1 day mineralization, (5) 3 day mineralization, 2 day coprecipitation, 1 day mineralization, and (6) 3 day mineralization, 3 day acid etched adsorption. The results are provided as a protein concentration (μg/ml) in 10 mM HCl. Different incorporation methods resulted in significantly different amounts of protein loaded into the films, $p<0.001$. In the table, pair-wise comparisons of each of the groups were performed using the Student-Newman-Keuls post hoc test, significance is $p<0.05$ for the grey boxes. The white boxes show no significant difference between the two groups compared. The coprecipitation groups had a significantly higher quantity of protein loaded into the mineralized films in comparison to the surface adsorption groups.

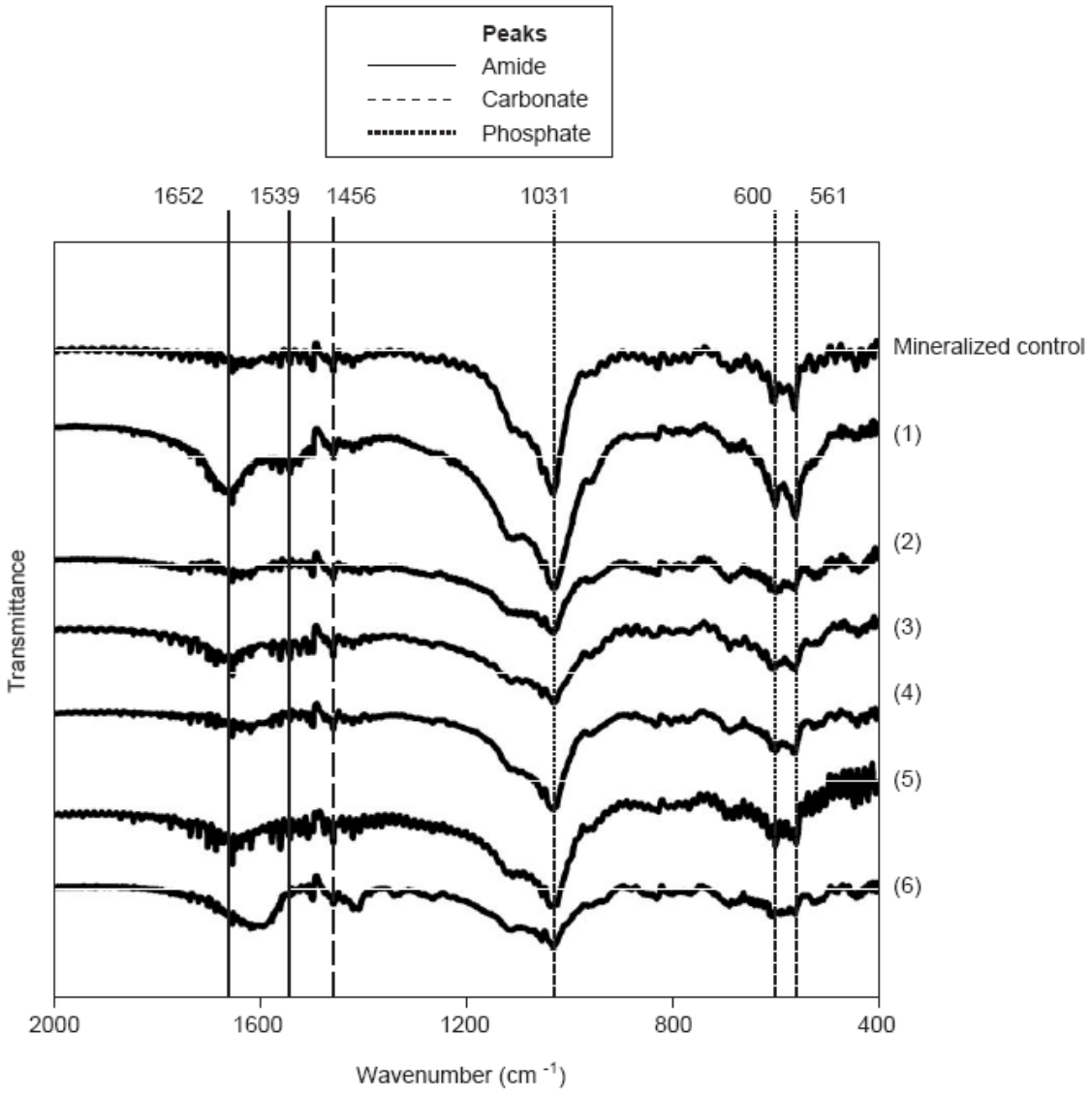

Figure 2.3: Representative FT-IR spectra after rinsing for the mineral-protein samples formulated via each of the following techniques: mineralized control, (1) 6 day coprecipitation, (2) 3 day mineralization, 3 day adsorption, (3) 3 day mineralization, 3 day coprecipitation, (4) 3 day mineralization, 2 day adsorption, 1 day mineralization, (5) 3 day mineralization, 2 day coprecipitation, 1 day mineralization, and (6) 3 day mineralization, 3 day acid etched adsorption. The phosphate (1031, 600, 561 cm-1) peaks are denoted by dotted lines, a carbonate (1456 cm-1) peak is denoted by a dashed line, and the amide (1652 and 1539 cm-1) peaks are denoted by solid lines. The amide peak at 1652 cm-1 decreased for Groups 3 and 5 following rinsing.

Protein retention after rinsing

Groups	Ratio (rinsed/ unrinsed)	St. dev. of ratios	Significance
(1) 6 d Cop.	1.23	0.43	0.148
(2) 3 d Min., 3 d Ads.	0.22	0.09	<0.001
(3) 3 d Min., 3 d Cop.	0.97	0.17	0.597
(4) 3 d Min., 2 d Ads., 1 d Min.	0.66	0.47	0.126
(5) 3 d Min., 2 d Cop., 1 d Min.	1.10	0.16	0.119
(6) 3 d Min., 3 d Acid Ads.	0.38	0.12	<0.001

Table 2.1: Ratios of the amount of protein incorporated in the rinsed to unrinsed samples were calculated. Significant differences between the rinsed and unrinsed samples were determined using t-tests. All coprecipitation groups showed no significant difference between unrinsed and rinsed sample results, while the surface adsorption groups showed a more significant difference ($p<0.001$) from unrinsed to rinsed samples for two groups.

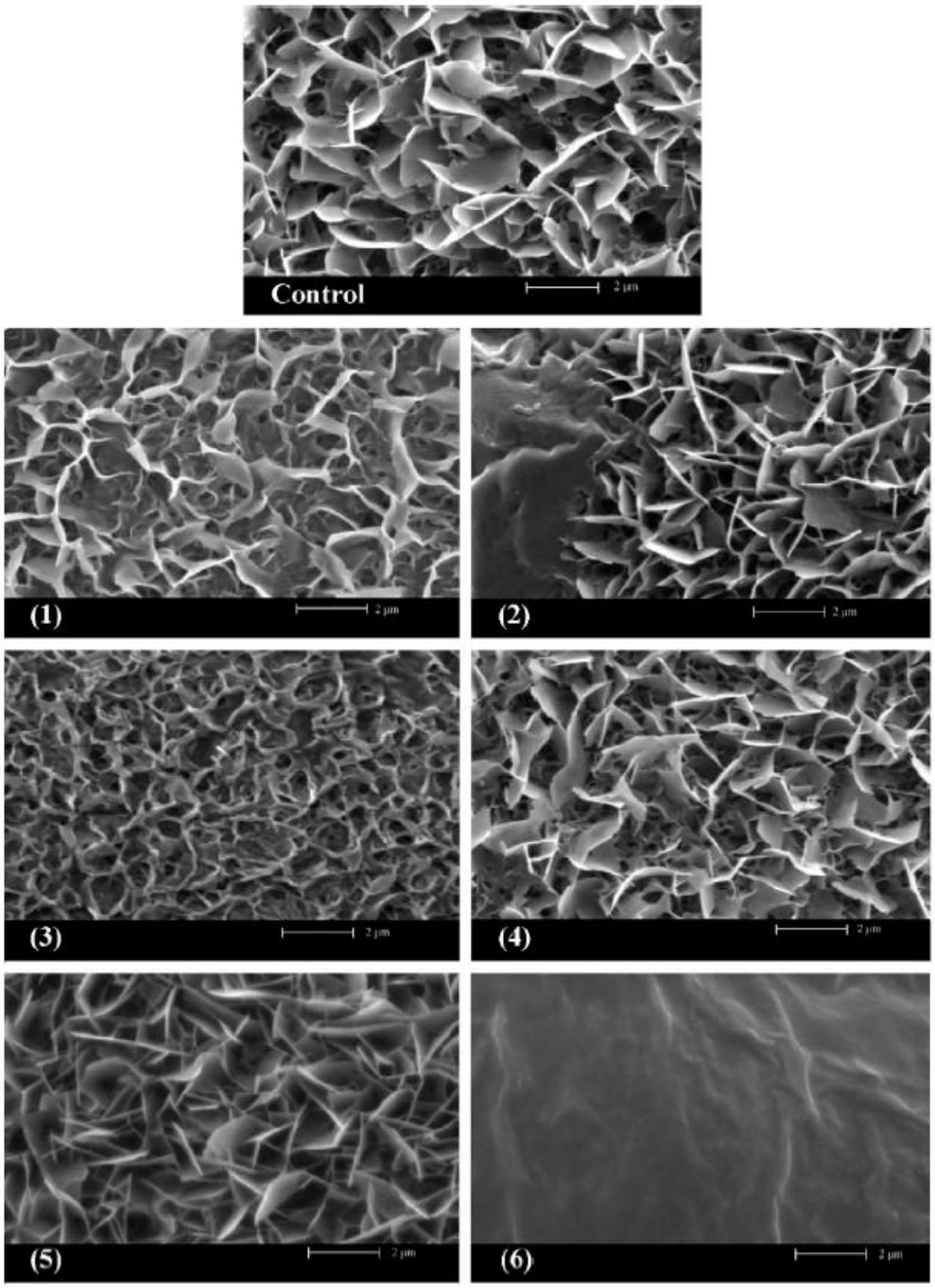

Figure 2.4: SEM images of representative samples examined from each of the following groups (magnification 10,000X): (Control) 6 Day mineralization, (1) 6 day coprecipitation, (2) 3 day mineralization, 3 day adsorption, (3) 3 day mineralization, 3 day coprecipitation, (4) 3 day mineralization, 2 day adsorption, 1 day mineralization, (5) 3 day mineralization, 2 day coprecipitation, 1 day mineralization, and (6) 3 day mineralization, 3 day acid etched adsorption. BSA incorporation via coprecipitation leads to changes in the plate-like mineral structure that is observed in the control, while BSA incorporation does not change the mineral morphology.

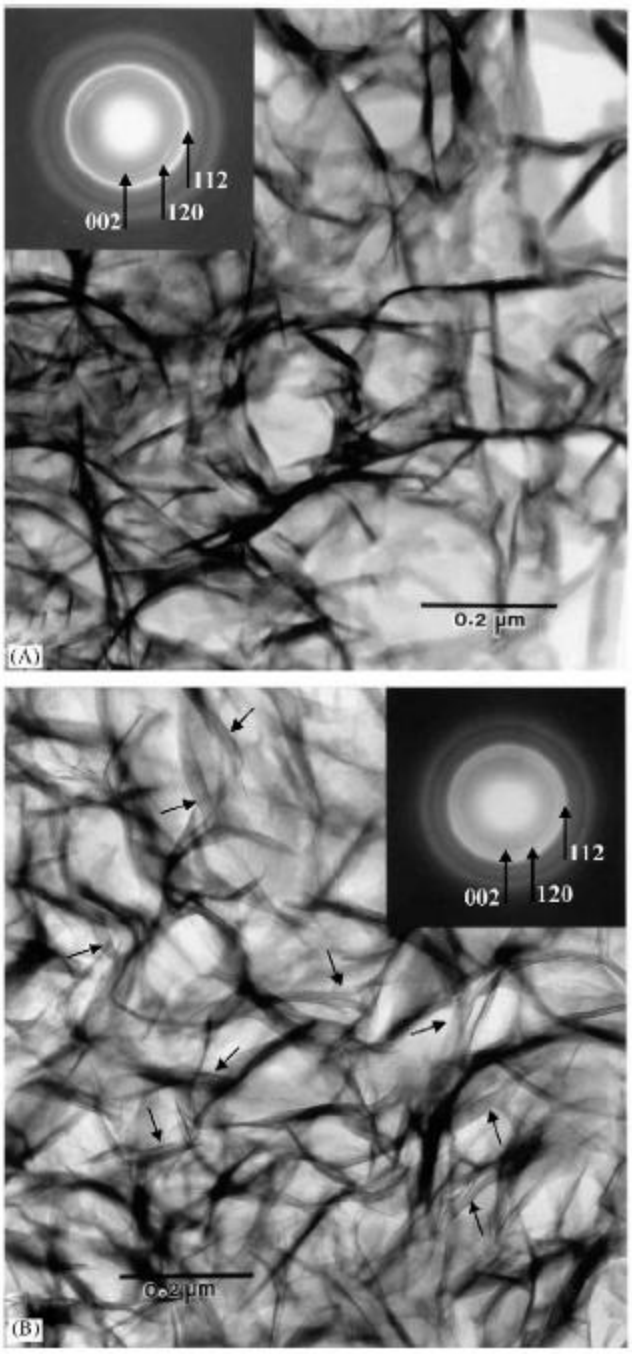

Figure 2.5: Transmission electron microscope images of the mineral crystals: (A) Mineralized sample without BSA and diffraction pattern showing the presence of the (002) ring, (B) Mineralized sample with BSA via coprecipitation and diffraction pattern showing the absence of the (002) ring. Arrows in (B) mark apatite that consists of locally parallel layers, all parallel to the long axis of the plates. Arrows in the diffraction patterns of (A) and (B) mark the diffraction rings. The size, shape, and distribution of the crystals do not appear to be affected by the presence of the protein; however, there are differences exhibited in the orientation of the crystals.

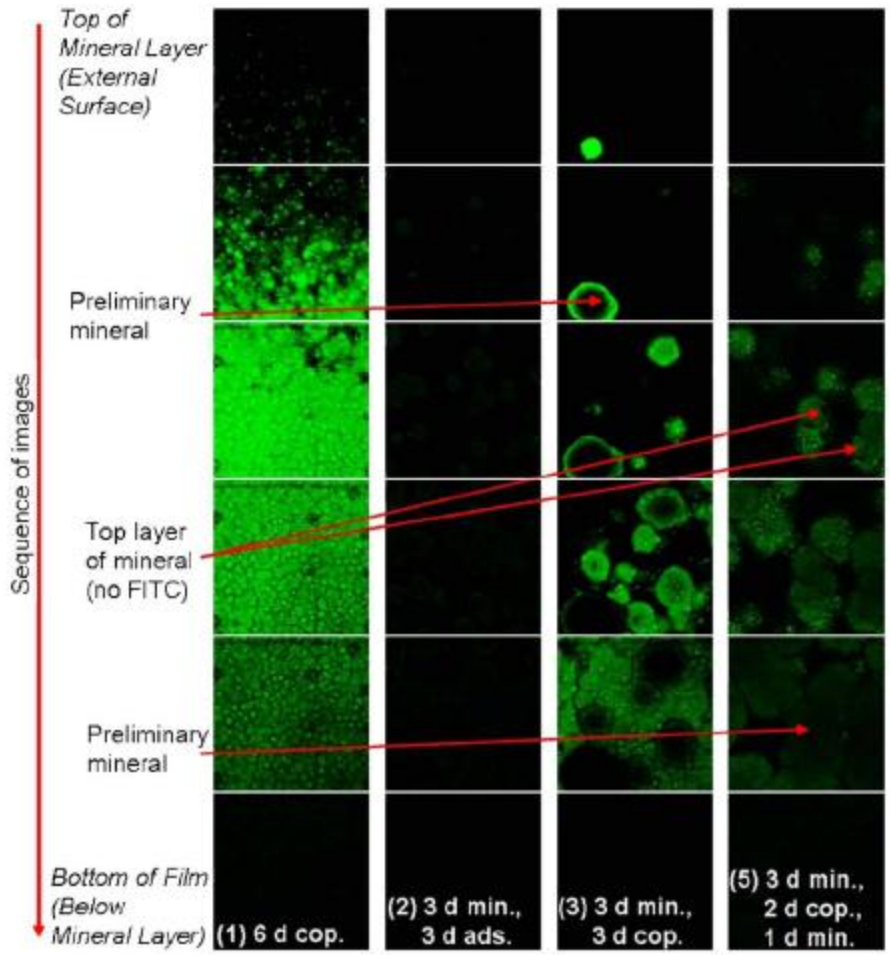

Figure 2.6: Images through the thickness of the mineral layer containing FITC-labeled BSA taken using confocal microscopy. Spatial distribution of the protein through the thickness of the mineral layer is exhibited for the following incorporation techniques: (1) 6 day coprecipitation, (2) 3 day mineralization, 3 day adsorption, (3) 3 day mineralization, 3 day coprecipitation, and (5) 3 day mineralization, 2 day coprecipitation, 1 day mineralization. Fluorescence can be seen where coprecipitation or adsorption had occurred. The 6 day and 3 day coprecipitation groups were taken at the same gain and offset while the 3 day adsorption and 2 day coprecipitation groups were taken at a higher gain and offset in order to image the fluorescence. Control over the spatial distribution of the protein is shown by the presence of fluorescence through the thickness of the mineral for the different coprecipitation groups.

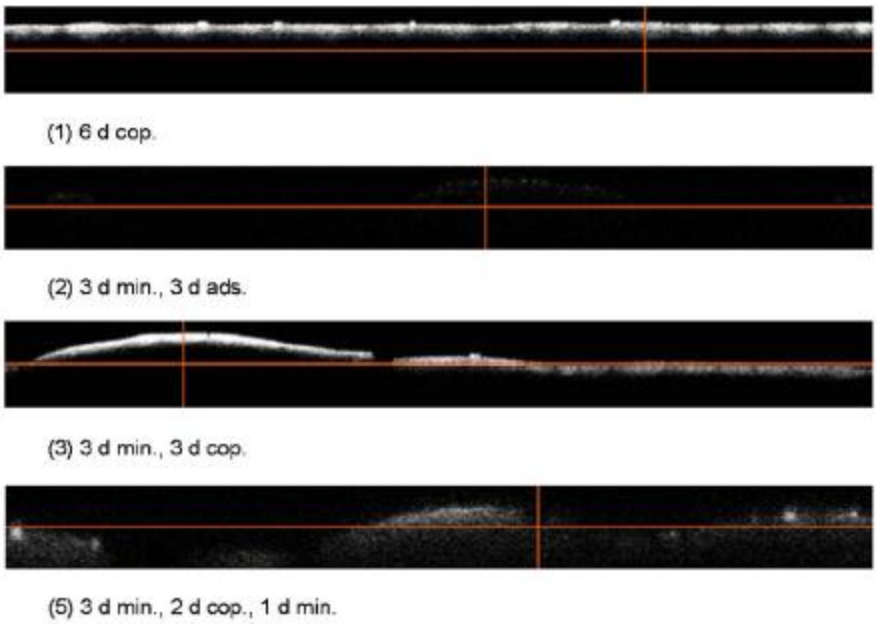

Figure 2.7: Side depth profiles through the thickness of the mineral were obtained by stacking each series of images from Fig. 6, resulting in an image of the cross section of the film through the mineral layer and polymer substrate. The following groups were examined: (1) 6 day coprecipitation, (2) 3 day mineralization, 3 day adsorption, (3) 3 day mineralization, 3 day coprecipitation, and (5) 3 day mineralization, 2 day coprecipitation, 1 day mineralization. The side depth profiles show minimal protein incorporation for the adsorption group, whereas, all three of the coprecipitation groups show protein incorporation at varying locations through the thickness of the mineral.

References

1. Hench LL. Bioceramics - from Concept to Clinic. J Am Ceram Soc 1991;74:1487-1510.

2. Murphy WL, Kohn DH, Mooney DJ. Growth of continuous bonelike mineral within porous poly(lactide-co-glycolide) scaffolds in vitro. J Biomed Mater Res 2000;50:50-58.

3. Kohn DH, Shin K, Hong SI, Jayasuriya AC, Leonova EV, Rossello RA, et al. Self-Assembled Mineral Scaffolds as Model Systems for Biomineralization and Tissue Engineering. In: Proceedings of the Eighth International Conference on the Chemistry and Biology of Mineralized Tissues; W. J. Landis and J. Sodek, editors. Toronto, Canada: University of Toronto Press; 2005.

4. Murphy WL, Peters MC, Kohn DH, Mooney DJ. Sustained release of vascular endothelial growth factor from mineralized poly(lactide-co-glycolide) scaffolds for tissue engineering. Biomaterials 2000;21:2521-2527.

5. Hoffman AS. Biologically Functional Materials. In: Ratner BD, Hoffman AS, Schoen FJ, Lemons JE, editors. Biomaterials Science: An Introduction to Materials in Medicine. San Diego: Academic Press, 1996. p. 124-130.

6. Ripamonti U, Ma S, Reddi AH. The Critical Role of Geometry of Porous Hydroxyapatite Delivery System in Induction of Bone by Osteogenin, a Bone Morphogenetic Protein. Matrix 1992;12:202-212.

7. Ripamonti U, Yeates L, Vandenheever B. Initiation of Heterotopic Osteogenesis in Primates after Chromatographic Adsorption of Osteogenin, a Bone Morphogenetic Protein, onto Porous Hydroxyapatite. Biochem Biophys Res Commun 1993;193:509-517.

8. Sumner DR, Turner TM, Urban RM, Leven RM, Hawkins M, Nichols EH, et al. Locally delivered rhTGF-beta(2) enhances bone ingrowth and bone regeneration at local and remote sites of skeletal injury. Journal of Orthopaedic Research 2001;19:85-94.

9. Arm DM, Tencer AF, Bain SD, Celino D. Effect of controlled release of platelet-derived growth factor from a porous hydroxyapatite implant on bone ingrowth. Biomaterials 1996;17:703-709.

10. Campbell AA, Song L, Li XS, Nelson BJ, Bottoni C, Brooks DE, et al. Development, characterization, and anti-microbial efficacy of hydroxyapatite-chlorhexidine coatings produced by surface-induced mineralization. J Biomed Mater Res 2000;53:400-407.

11. Alam MI, Asahina I, Ohmamiuda K, Takahashi K, Yokota S, Enomoto S. Evaluation of ceramics composed of different hydroxyapatite to tricalcium phosphate ratios as carriers for rhBMP-2. Biomaterials 2001;22:1643-1651.

12. Midy V, Rey C, Bres E, Dard M. Basic fibroblast growth factor adsorption and release properties of calcium phosphate. J Biomed Mater Res 1998;41:405-411.

13. Ziegler J, Mayr-Wohlfart U, Kessler S, Breitig D, Gunther KP. Adsorption and release properties of growth factors from biodegradable implants. J Biomed Mater Res 2002;59:422-428.

14. Liu YL, Layrolle P, de Bruijn J, van Blitterswijk C, de Groot K. Biomimetic coprecipitation of calcium phosphate and bovine serum albumin on titanium alloy. J Biomed Mater Res 2001;57:327-335.

15. Stigter M, de Groot K, Layrolle P. Incorporation of tobramycin into biomimetic hydroxyapatite coating on titanium. Biomaterials 2002;23:4143-4153.

16. Liu Y, Hunziker EB, Randall NX, de Groot K, Layrolle P. Proteins incorporated into biomimetically prepared calcium phosphate coatings modulate their mechanical strength and dissolution rate. Biomaterials 2003;24:65-70.

17. Wen HB, de Wijn JR, van Blitterswijk CA, de Groot K. Incorporation of bovine serum albumin in calcium phosphate coating on titanium. J Biomed Mater Res 1999;46:245-252.

18. Wen HB, Wolke JG, de Wijn JR, Liu Q, Cui FZ, de Groot K. Fast precipitation of calcium phosphate layers on titanium induced by simple chemical treatments. Biomaterials 1997;18:1471-1478.

19. Liu YL, Hunziker EB, Layrolle P, De Bruijn JD, De Groot K. Bone morphogenetic protein 2 incorporated into biomimetic coatings retains its biological activity. Tissue Eng 2004;10:101-108.

20. Murphy WL, Mooney DJ. Bioinspired growth of crystalline carbonate apatite on biodegradable polymer substrata. J Am Chem Soc 2002;124:1910-1917.

21. Lee KH, Hong SI. Interfacial and twin boundary structures of nanostructured Cu-Ag filamentary composites. J Mater Res 2003;18:2194-2202.

22. Koutsopoulos S. Synthesis and characterization of hydroxyapatite crystals: A review study on the analytical methods. J Biomed Mater Res 2002;62:600-612.

23. Xie J, Riley C, Kumar M, Chittur K. FTIR/ATR study of protein adsorption and brushite transformation to hydroxyapatite. Biomaterials 2002;23:3609-3616.

24. Wassell DTH, Hall RC, Embery G. Adsorption of Bovine Serum-Albumin onto Hydroxyapatite. Biomaterials 1995;16:697-702.

25. Marques P, Serro AP, Saramago BJ, Fernandes AC, Magalhaes MCF, Correia RN. Mineralisation of two phosphate ceramics in HBSS: role of albumin. Biomaterials 2003;24:451-460.

26. Dorozhkin SV, Dorozhkina EI. The influence of bovine serum albumin on the crystallization of calcium phosphates from a revised simulated body fluid. Colloids and Surfaces a-Physicochemical and Engineering Aspects 2003;215:191-199.

27. Barroug A, Kuhn LT, Gerstenfeld LC, Glimcher MJ. Interactions of cisplatin with calcium phosphate nanoparticles: in vitro controlled adsorption and release. J Orthop Res 2004;22:703-708.

28. Sarig S. Aspartic acid nucleates the apatite crystallites of bone: a hypothesis. Bone 2004;35:108-113.

29. Okazaki M, Yoshida Y, Yamaguchi S, Kaneno M, Elliott JC. Affinity binding phenomena of DNA onto apatite crystals. Biomaterials 2001;22:2459-2464.

Chapter 3

Gene Delivery via DNA Incorporation Within a Biomimetic Apatite Coating[2]

3.1 Introduction

The clinical basis for developing strategies to regenerate bone is the healing of bone defects caused from trauma, congenital malformations, and progressively deforming skeletal disorders. Bone tissue engineering provides an alternative to bone grafting and direct usage of growth factors to regenerate bone. An ideal bone tissue engineering approach would incorporate osteoconductivity and osteoinductivity potential into the design of the supporting biomaterial, as well as biocompatibility, degradability, mechanical integrity, and the ability to support cell transplantation.

Direct bonding between implants and bone, the ultimate goal of osteoconductivity, can occur if a layer of bone-like mineral forms on the surface of the implant [1]. It has therefore been hypothesized that formation of a bone-like mineral layer within the pores of a tissue engineering scaffold may enhance the conduction of host cells into scaffolds [2], and also enhance osteogenic differentiation of cells transplanted on scaffolds [3]. The bone-like mineral enhances the osteoconductivity and mechanical properties of the scaffold and can serve as a cell transplantation vehicle [2]. Bone-like mineral coatings can also serve as carriers for inductive agents [2, 4], providing a platform for the three tissue engineering approaches of conduction, induction, and cell transplantation.

[2] Published as Luong, LN et al., Biomaterials 2009; 30: 6696-7004

The coprecipitation of biological factors and bone-like mineral has been used to incorporate growth factors on metal substrates, such as titanium alloy implants [5-7]. An important advantage to coprecipitation is the ability to form calcium phosphate coatings at a physiological temperature, minimizing conditions that would degrade the biological activity of the factors [8-11]. For example, the biological activity of bovine serum albumin, tobramycin, and recombinant human bone morphogenetic protein 2 (BMP-2) is retained when each of these biomolecules is coprecipitated with calcium phosphate onto titanium [6, 7, 12]. More specifically, BMP-2 coprecipitated into biomimetic apatite coatings can induce ectopic bone formation *in vivo* [13]. The ability to increase the loading efficiency and to control the spatial localization of proteins within bone-like mineral coatings has also been demonstrated utilizing coprecipitation [14].

Gene therapy is one approach to achieve the design objective of integrating inductivity into a material. Gene delivery provides an alternative to utilizing proteins, and has advantages over protein delivery, including a longer half-life, and lower expense [15]. The incorporation of genes into cells can be achieved virally and non-virally [16-19]. However, viral approaches present disadvantages, including the risk of mutations, insert size limitations, and viral-induced immune responses [15]. An alternative is the use of non-viral methods, such as naked DNA, cationic polymers, and cationic lipids [16, 20, 21]. While non-viral methods are less efficient than viral techniques, they are more promising in terms of accommodating larger genes of interest, lower immunogenicity, and the potential for tissue targeting [15, 22]. An optimal non-viral gene delivery system will fulfill the following design objectives: 1) the carrier should avoid aggregation or negative interactions with the extracellular matrix, 2) the carrier should condense the

DNA to facilitate cellular internalization, and 3) cellular processes to transcribe and translate the gene of interest should not be inhibited [15].

Non-viral gene delivery has been achieved by complexing DNA with cationic lipids [17], as well as precipitating DNA with calcium phosphate [23, 24]. However, the two approaches of cationic lipids and calcium phosphate precipitation have not been combined. Cationic lipids are typically composed of a positively charged head group, a hydrophobic chain, and a linker group [25]. The positively charged lipids interact with the negatively charged DNA chains, resulting in complexes. The cellular uptake of these complexes depends on their stability and size [25]. For example, Lipofectamine 2000®, which is a lipid based transfection agent for eukaryotic cells, protects the DNA from enzymatic digestion from DNase treatment [26], whereas plasmid DNA alone is prone to degradation by nucleases [15]. DNA-Lipoplexes are therefore successful in cellular transfection, both *in vitro* and *in vivo* [27, 28].

The precipitation of DNA/calcium phosphate nanocomposites has also been successful in inducing transfection of cell lines, due to the concentrated quantity of DNA localized in the immediate cellular environment [20, 24]. The precipitation of a calcium phosphate coating onto a polymer scaffold increases the stiffness of the scaffold [2] and increased substrate stiffness increases cellular uptake of DNA condensates [29]. These advantages of calcium phosphates can be combined with the advantages of cationic lipids by coprecipitating coatings of calcium phosphate and DNA-Lipoplexes onto a biomaterial substrate.

In this study, we developed an organic/inorganic hybrid by coprecipitating plasmid DNA encoding for the β-galactosidase gene complexed with a cationic lipid

(Lipofectamine 2000®) and biomimetic apatite onto a polymer substrate. The lipid condenses the DNA, better enabling cellular uptake, while the coprecipitation of DNA-Lipoplexes with mineral localizes high, homogeneously dispersed concentrations of DNA in the immediate cellular environment. We hypothesized that this combinatorial inductive/conductive system would result in enhanced transfection efficiency compared to DNA-Lipoplexes adsorbed to the mineral surface and DNA coprecipitated without Lipofectamine 2000®. To test this hypothesis, experiments were conducted to address: 1) DNA-Lipoplex presence in mineral, 2) DNA-Lipoplex stability (vs. coprecipitation time), and 3) transfection efficiency (determined with C3H10T1/2 cells) as a function of coprecipitation time, DNA-Lipoplex concentration, and DNA incorporation method.

3.2 Materials and Methods

3.2.1 PLGA film preparation

The films were prepared using 5 wt. % PLGA, 85:15 PLA:PGA ratio (Alkermes), in chloroform solution. The films (approximately 200-300 μm thick) were cast onto 15 mm round glass coverslips, covered with aluminum foil and air dried for at least 24 hours under a fume hood. Prior to mineralization, the films were etched in 0.5 M NaOH for seven minutes. They were rinsed thoroughly with Millipore water before use.

3.2.2 Modified simulated body fluid

A modified simulated body fluid (mSBF, which contains 2X the concentration of Ca^{2+} and HPO_4^{2-} as standard SBF) was used to mineralize the films [14]. mSBF consists of the following reagents dissolved in Millipore water: 141 mM NaCl, 4.0 mM KCl, 0.5 mM $MgSO_4$, 1.0 mM $MgCl_2$, 4.2 mM $NaHCO_3$, 5.0 mM $CaCl_2 \cdot 2H_2O$, and 2.0 mM

KH_2PO_4. mSBF was prepared at 25°C and titrated to pH 6.8 using NaOH to avoid homogeneous precipitation of calcium phosphate.

3.2.3 Plasmid DNA preparation and purification

Plasmid DNA encoding for β-galactosidase (β-gal) was produced via the transformation of E. Coli competent cells (Promega #L2001). Plasmid DNA purification was completed using the protocol provided by Qiagen. Cells were harvested from 500 ml of LB broth. Following centrifugation and cell lysis, the purified DNA was precipitated by isopropanol. DNA pellets were washed with ethanol, dried, resuspended in TE buffer at pH 8.0, and stored at -20°C.

3.2.4 Complexing plasmid DNA to Lipofectamine 2000®

DNA-Lipofectamine 2000® complexes (DNA-Lipoplex) were prepared in polypropylene centrifuge tubes according to the protocol provided by the manufacturer (Molecular Probes, Invitrogen). The ratio of complexation was 3 µl of Lipofectamine 2000® per µg of plasmid DNA. Briefly, the DNA and the Lipofectamine 2000® were individually diluted in Opti-MEM Reduced Serum Medium and gently mixed. The samples were then incubated for 5 minutes at room temperature, after which they were combined together. The DNA-Lipofectamine 2000® mixture was then incubated for 20 minutes at room temperature.

3.2.5 Mineralization and DNA incorporation methods

Four types of samples were prepared: PLGA coated with mineral, PLGA with DNA incorporated, PLGA coated with mineral and coprecipitated DNA-Lipoplexes, and PLGA coated with mineral and DNA-Lipoplexes adsorbed to the mineral surface. PLGA covered glass slips were submerged into each Petri dish containing 50 ml of

mSBF. Mineralization was carried out for 3 to 4 days at 37°C and the solutions were exchanged daily in order to replenish the ion concentration to supersaturated levels. For coprecipitation of mineral-DNA and mineral-DNA-Lipoplexes, the mineralization scheme to deposit the precursor mineral layer was the same (i.e. the starting point for coprecipitation was similar). Samples were removed from the Petri dishes after mineralization and placed into 24 well plates. An mSBF solution containing DNA-Lipoplexes or DNA alone was then added to the samples (1 ml per sample). Concentration and coprecipitation time were dependent on the experiment performed as detailed in Sections 3.2.6 to 3.2.10. Coprecipitation was carried out at 37°C; the samples were placed on a rotational shaker to evenly distribute the complexes (approximately 50 rpm). For the DNA incorporated into PLGA, the DNA was added to the 5 wt. % PLGA, 85:15 PLA:PGA ratio (Alkermes), in chloroform solution. The films were cast onto 15 mm round glass coverslips (250 µl), covered with aluminum foil and air dried for at least 24 hours under a fume hood. DNA-Lipoplexes incorporated into PLGA was not included due to the inability to achieve the required composition of DNA-Lipoplexes in PLGA/chloroform solution. For DNA-Lipoplex adsorption to mineral, the complexes were prepared in the Opti-MEM media and pipetted onto the surface of the mineralized substrate.

3.2.6 Plasmid DNA incorporation and effects on mineral morphology

Effects of DNA incorporation on mineralization were examined using scanning electron microscopy (Philips XL30 FEG Scanning Electron Microscope). The following groups were examined: 1) Mineralized controls, 2) Plasmid DNA coprecipitated with mineral onto films, 3) Plasmid DNA-Lipoplex adsorbed to mineralized films, and 4)

Plasmid DNA-Lipoplex coprecipitated with mineral onto films. Films were coated with a thin layer of gold and examined at 3 kV.

3.2.7 Verification of Plasmid DNA presence and spatial distribution

The spatial distribution of the DNA was determined using a fluorescence microscope (Nikon TE 3000 Inverted Microscope). The following groups were examined: 1) Mineralized controls, 2) Plasmid DNA incorporated into PLGA, 3) Plasmid DNA coprecipitated with mineral, 4) Plasmid DNA-Lipoplex adsorbed to mineralized films, and 5) Plasmid DNA-Lipoplex coprecipitated with mineral. For this qualitative assessment, ten µg of plasmid DNA was used per sample. For the coprecipitation groups, 10 µg was the DNA concentration in solution and the samples were incubated at 37°C for 24 h. Samples were then removed and dried in the chemical fume hood. Bisbenzimide Hoescht (Sigma-Aldrich) was used to determine the spatial distribution of the plasmid DNA, while DiO Cell Labeling Solution (MicroProbes, Invitrogen) was used to determine the presence of the Lipofectamine 2000®. Briefly, a 1:500 dilution of Hoescht and a 1:200 dilution of DiO solution were made using 1X PBS. Samples were placed into 24 well plates, and rewet with ddH_2O, which was then removed. Staining solution was placed over the samples; the plate was covered with aluminum foil and incubated for 30 minutes at 37°C. Solution was then removed and the samples were rinsed 4 to 5 times with ddH_2O. Samples were placed on glass microscope slides with GelMount (Biomedia) as a mounting medium. Samples were imaged on the same day on a fluorescence microscope with emission wavelengths of 420 and 510-560 nm for DNA and Lipofectamine 2000®, respectively.

3.2.8 Plasmid DNA stability and Plasmid DNA- Lipofectamine 2000® complex stability

To determine the stability of the complexes formed, gel electrophoresis (based on size) and transfection efficiency at varying timepoints (6, 12, 24 and 48 h) were examined. All samples were prepared in polypropylene tubes. At first, the stability of the plasmid DNA in water was examined to determine its intrinsic stability. The protocol was then repeated to examine DNA – Lipofectamine 2000® complexation in Opti-Mem. The tubes were placed in an incubator at 37°C. Samples were then removed at each timepoint and frozen (DNA in water) or stored at 4°C (DNA-Lipoplex in Opti-Mem). Samples were placed in wells in a 0.6% agarose gel containing ethidium bromide. Freshly thawed (no previous incubation) plasmid DNA and plasmid DNA conjugated to Lipofectamine 2000® were prepared as controls. Samples were loaded and run for 75 minutes at 80V, and images were obtained and analyzed using a Fluor S MultiImager (Bio-Rad, CA).

To determine plasmid DNA-Lipoplex stability in the mSBF during and after the precipitation of the apatite and complexes with respect to time of coprecipitation, a second set of experiments was performed using the mouse embryonic fibroblast cell line C3H10T1/2 (provided by Dr. Franceschi, University of Michigan). The C3H10T1/2 cell line was chosen due to its capability of differentiating along the osteogenic lineage with either exogenous protein or via gene transfection [30, 31]. Samples (n=4) were prepared as stated in Section 3.2.5 using coprecipitation times of (6, 12, 24, and 48 h). The baseline concentration for the samples was 10 µg in 1 ml of mSBF per sample. At each

incubation timepoint, the samples were removed and rinsed with HBSS (Hanks buffered saline solution).

MEMα medium (Invitrogen) containing 10% fetal bovine serum (FBS) without antibiotics was prepared, and one day before transfection, the cells were replated at a density of 50,000 in 1 ml of media. The plates were gently rocked to evenly distribute the cells on the surface of the films and placed in the incubator at 37°C. The media was exchanged after 24 hours. The total time allowed for transfection was 48 hours. Media was aspirated and the cells were washed with PBS.

Cells were fixed for 15 min with a 0.25% v/v glutaraldehyde solution and then rinsed gently 3 times with PBS. X-gal staining solution containing N,N-DMF, $MgCl_2$, $K_4Fe(CN)_6$ $3H_2O$, and $K_3Fe(CN)_6$ was added to each well containing cells and incubated at 37° C between 14-16 hours. The X-gal solution was then removed and the samples were rinsed 2-3 times with PBS. Samples were removed and placed onto microscope slides and mounted using GelMount. Samples were then observed under the light microscope. Fifteen random locations per sample were imaged, and then positively stained cells were counted. The average number of stained cells per location was then applied to the entire area of the well resulting in the total number of cells that were stained. The cellular transfection efficiency is based on the total number of stained cells in the well divided by the initial seeding density of 50,000 cells.

3.2.9 Effect of plasmid DNA concentration on transfection efficiency

To determine the plasmid DNA-Lipoplex concentration needed to obtain the highest transfection efficiency, coprecipitation and adsorption were examined. For coprecipitation, the concentration was varied (0, 10, 20, or 40 μg) in 1 ml of 1X mSBF.

For adsorption, the adsorption solution contained 0, 10, 20, or 40 µg of DNA-Lipoplexes. Samples (n=4) were prepared as stated in Section 3.2.5. Coprecipitated and mineralized control samples were incubated at 37 °C. The DNA-Lipoplexes were adsorbed onto mineralized films during the corresponding coprecipitation time period. After 6 h, the samples were removed and rinsed with HBSS. The C3H10T1/2 cell seeding density was 50,000 per sample with 1 ml of media. Fixing, staining, and analysis were the same as stated in Section 3.2.8.

3.2.10 Effect of plasmid DNA incorporation technique on transfection efficiency

The transfection efficiencies of the following methods of DNA incorporation were examined: 1) PLGA only, 2) Plasmid DNA incorporated into PLGA, 3) Mineralized controls, 4) Plasmid DNA coprecipitated with mineral, 5) Plasmid DNA-Lipoplex adsorbed to mineral, and 6) Plasmid DNA-Lipoplex coprecipitated with mineral. The DNA or DNA-Lipoplex concentration was 40 µg (in 1X mSBF, adsorption solution, or in PLGA). Samples (n=4) were prepared as stated in Section 3.2.5. All of the samples containing mineral and controls (except adsorption) were incubated at 37 °C. The DNA-Lipoplexes were adsorbed during the corresponding coprecipitation time period. After 6 h, the samples were removed and rinsed with HBSS. The cell seeding density was 50,000 per sample with 1 ml of media. Fixing, staining, and analysis were the same as stated in Section 3.2.8.

3.2.11 Statistical analysis

The Kruskal-Wallis One Way ANOVA on Ranks and/or ANOVA were used to analyze the differences in transfection efficiency of the C3H10T1/2 cells with variations

in coprecipitation time, DNA-Lipoplex concentration, and incorporation method. The Student Newman Keuls post hoc comparison test was used for pair-wise comparisons.

3.3 Results

3.3.1 Presence and localization of DNA and DNA-Lipoplexes in biomimetic apatite

At low magnification, the macroscopic mineral morphology was similar for all sample groups. The nucleation sites were approximately 10-15 μm in diameter (Figure 3.1). However, at higher magnification, morphological differences were more apparent. Mineralization resulted in the deposition of plate-like structures (Figure 3.2a). The coprecipitation of DNA and adsorption of DNA-Lipoplexes did not change the morphology of the plates (Figure 3.2b,c) from that of the mineralized controls. Incorporation of DNA-Lipoplexes via coprecipitation (Figure 3.2d) resulted in plate-like crystals that were covered by a "fibrous" coating (black arrows in inset), thickening the plate-like structures (white arrows), compared to samples in which only DNA was coprecipitated or the mineralized controls.

The presence of both the plasmid DNA and the lipid transfection agent within the mineralized substrate was verified (Figure 3.3). The mineralized controls that did not contain DNA or cationic lipid, did not exhibit fluorescence (Figure 3.3, a-b). Incorporating DNA into PLGA resulted in the detection of bubbles from DNA staining, but no staining for the lipid transfection agent was detected (Figure 3.3, c-d). Plasmid DNA incorporation via coprecipitation resulted in an even distribution of DNA fluorescence over the entire substrate, and also demonstrated an absence of the lipid transfection agent (no red fluorescence) (Figure 3.3, e-f). The superficial adsorption of

the DNA-Lipoplexes onto the surface of the mineralized films resulted in fluorescence for both DNA and lipid, however the areas of fluorescence are localized and limited (Figure 3.3, g-h). Only for the DNA-Lipoplex coprecipitation samples was an even distribution of fluorescence demonstrated for both DNA and lipid (Figure 3.3, i-j). The surface adsorption and coprecipitation of DNA-Lipoplexes demonstrated the colocalization of the DNA and the lipid as actual complexes in addition to free plasmid DNA that was not bound to complexes.

3.3.2 Plasmid DNA stability in water and DNA-Lipoplex complexation in medium

The plasmid DNA encoding for the β-galactosidase gene has a base-pair length of 7504 bp. As incubation time in water increased, the stability of the plasmid DNA decreased (Figure 3.4, a-b). As the band (ca. 6557), which is representative of the supercoiled form of the plasmid DNA, decreased in intensity with increasing incubation time, another secondary band (between 9416 and 23130 bp, representing nicked circular form of DNA) formed and increased in intensity with increasing incubation time (Figure 3.4, a-b). DNA stability is demonstrated by these changes in supercoiled and nicked circular DNA, where the supercoiled form is preferred for gene transfection.

The formation of the DNA-Lipoplexes in Opti-Mem was visually confirmed via gel electrophoresis (Figure 3.4c). The complexation of the plasmid DNA to the transfection agent was almost complete, due to the absence of bands in all lanes containing the DNA-Lipoplexes. Due to size-exclusion effects, the complexes remained in the wells. The bright outlines surrounding the wells containing the DNA-Lipoplexes compared to the lane containing only DNA (outline is not present) are also represented by the intensity profiles of 2 lanes: DNA 0 h and DNA-Lipo 48 h (Figure 3.4d). The two peaks denote

the top and bottom edges of the wells, and the intensities were higher for the DNA-Lipoplex lane compared to the DNA only lane (highest peak representing the DNA is shown in the inset image), which suggests the size exclusion effect.

3.3.3 Effects of coprecipitation time on DNA-Lipoplex stability

The ability of these complexes to be uptaken by the cells and then translated was not affected by the coprecipitation time (Figure 3.5). There were no significant differences among the four coprecipitation time periods ($p=0.084$). Based on the results from DNA stability (Figure 3.4) the time of coprecipitation was limited to 6 hours for the remaining experiments.

3.3.4 Effects of adsorption/coprecipitation concentration on DNA-Lipoplex transfection

Varying the concentrations of the DNA-Lipoplexes during adsorption and coprecipitation resulted in significantly different transfection efficiencies, $p=0.004$ and $p<0.001$ respectively (Figure 3.6). Significantly different transfection efficiencies ($p<0.05$) existed between adsorption concentrations, except between 20 µg and 40 µg, with the highest transfection efficiency corresponding to a concentration of 10 µg. Significantly different transfection efficiencies ($p\leq0.009$) existed between coprecipitation concentrations, except between 10 µg/ml and 20 µg/ml, with the highest transfection efficiency corresponding to a DNA-Lipoplex concentration of 40 µg/ml. Coprecipitation resulted in significantly higher transfection efficiencies than adsorption for 20 µg/ml and 40 µg/ml ($p<0.05$).

3.3.5 Effects of incorporation method on DNA-Lipoplex transfection

Varying the incorporation method for the DNA resulted in significantly different transfection efficiencies, $p<0.001$ (Figure 3.7). The coprecipitation of DNA-Lipoplexes resulted in the highest transfection efficiency compared with all groups ($p<0.05$). The transfection efficiency of the DNA-Lipoplex adsorption group was significantly increased when compared with all groups ($p<0.05$), except the DNA-Lipoplex coprecipitation group. The higher transfection efficiency of the DNA-Lipoplex adsorption group compared to the DNA only coprecipitation group suggests that the addition of the cationic lipid enhances transfection. Higher transfection efficiency for coprecipitation compared to adsorption suggests higher availability of the complexes on the surface of the apatite.

3.4 Discussion

The focus of this study has been on the development of an organic/inorganic hybrid that incorporates plasmid DNA complexed with a cationic lipid into biomimetic apatite via coprecipitation. This hybrid can be formed at physiological pH, temperature, and pressure. The advantages of combining the methods of calcium phosphate based transfection and cationic lipid assisted transfection are many fold: the biomimetic mineral increases substrate stiffness and osteoconductivity in addition to serving as a carrier for the DNA which increases osteoinductivity. The presence of the lipid condenses the DNA, making cellular internalization easier (Figure 3.7), while the deposition of apatite with the DNA-complexes provides for higher, homogeneously distributed concentrations of DNA available for cellular uptake (Figure 3.3).

Coprecipitation of the DNA-Lipoplexes displayed the highest transfection efficiency compared to all other incorporation techniques, including coprecipitation of the plasmid alone (Figure 3.7). The transfection efficiency of the adsorbed DNA-Lipoplexes was higher than that of coprecipitated DNA (Figure 3.7), which is suggestive of the enhancement in transfection that the cationic lipid complexation provides. This increase in transfection efficiency with cationic lipid is possibly caused by the change in charge and size of the DNA [32, 33]. A cationic lipid agent can promote the condensation of DNA particles, protect the DNA from degradation, and enhance cellular uptake [22, 34]. Transport across the nucleus is limited to particle diameters less than 26 nm [35]. After condensation using cationic lipids, diameters of approximately 23 nm have resulted [32], thus enhancing cellular internalization. For example, polyethyleneimine (PEI), a cationic polymer, enables DNA encoding for bone morphogenetic protein 4 to condense, which significantly increases the mineral density of regenerated bone compared to uncondensed DNA [16].

Transfection efficiency is also DNA-Lipoplex concentration dependent. For coprecipitation, higher concentrations of DNA-Lipoplexes tended towards higher transfection efficiencies (Figure 3.6). However for adsorption, the reverse was true. The different trends in transfection efficiency may be due to the ability of coprecipitation to better retain the complexes on the mineral compared to adsorption [14], suggesting the presence of a stronger interaction between the complexes and apatite during coprecipitation. This enhanced retention of DNA-Lipoplexes at the apatite surface with coprecipitation leads to a higher surface density, which enhances transfection efficiency [20, 34, 36]. With adsorption, the lower transfection efficiencies may be the result of

DNA-Lipoplexes aggregating at higher concentrations without the opportunity for the complexes to be evenly dispersed (Figure 3.3). Alternatively, there may be a lower affinity between the complexes and the apatite surface during adsorption compared to coprecipitation, therefore less complexes adsorb.

DNA stability is essential for the retention of biological activity and DNA topology may serve an important role in transfection ability. Plasmid DNA can be found in different forms, the most common of which are supercoiled, nicked circular, and linearized [37]. The supercoiled form is the most condensed conformation; nicked circular results in the loss of the supercoiling capability; and linearized DNA forms when the strands are cleaved. Over the time of incubation in water, DNA stability decreased, resulting in less of the supercoiled form of DNA and more of the nicked circular form (Figure 3.4). Supercoiled DNA, when complexed to a cationic polymer exhibits higher transfection efficiencies compared to nicked circular or linearized DNA forms [38]. Therefore, longer coprecipitation times could lead to lower transfection efficiencies due to the change in DNA conformation. Complexation in medium was demonstrated to be complete by the absence of bands since free DNA that did not complex would be visible as a band [26]. Incubation in medium over time did not result in the dissociation between the DNA and the cationic lipid. Stability of the DNA-Lipoplexes was also tested by assessing the transfection efficiency using C3H10T1/2 cells at four coprecipitation times. There was no significant difference in transfection efficiency with increasing time of incubation (Figure 3.5). To minimize the possibility of DNA instability (Figure 3.4a), the coprecipitation time for future experiments was limited to 6 hours. Additionally, a precursor layer of mineral was applied before initiating the coprecipitation process since

longer periods of incubation of the DNA-Lipoplexes in mSBF may cause DNA instability, and therefore decrease the transfection efficiency. In general, the supercoiled form of DNA is preferred for gene transfections; however, the presence of nicked circular DNA may not always decrease transfection efficiency in specific cases [39].

By coprecipitating the DNA-Lipoplexes into the mineral, the morphology of the mineral changed, while adsorption of DNA-Lipoplexes or coprecipitation of just DNA did not change the plate-like mineral (Figure 3.2). The distinctive morphological features resulting from the coprecipitation of the DNA-Lipoplexes with apatite demonstrate the interactions that occur between the complexes and the mineral plates. The presence of a "fibrous" coating (Figure 3.2d) is most likely due to the presence of the cationic lipid, because the coprecipitation of DNA alone resulted in minimal differences in apatite morphology compared to the mineralized controls. Condensation via cationic particles can result in the formation of toroids or rods [40, 41], which is a possible cause for the "fibrous" coating displayed on the plate-like mineral. Even after thorough rinsing, the DNA-Lipoplexes were still retained on the apatite especially for the coprecipitation groups (Figure 3.3). Coprecipitation may therefore lead to DNA-Lipoplex incorporation into the three dimensional crystal latticework resulting in the morphological changes observed. It is probable that the interaction is between the positively charged Ca ions within the apatite and the negatively charged backbone of the DNA [42]. It has also been hypothesized that affinity binding can occur between DNA and hydroxyapatite crystals [42]. The interaction between the DNA-Lipoplexes and the mineral via coprecipitation may enhance the availability of these complexes for cellular uptake. In addition to better retention, coprecipitation also distributes protein through the thickness of the apatite

compared to just placing it at the apatite surface as is the case with adsorption [14]. Therefore, coprecipitation offers an added advantage of prolonging delivery.

Transfection efficiencies are low (~5-12%), which is typical of a non-viral gene delivery method when compared to viral delivery methods. However, utilizing non-viral gene delivery is advantageous in regards to ease of reproduction without the risk of mutation [22]. Different methods of cationic carrier based gene delivery (lipid, gelatin, and PEI) have transfection efficiencies ranging from ca. 3% to 18%, which are dependent on both the method of delivery and the cell type utilized [43]. Generally, the transfection efficiencies that are typical of all non-viral methods are not high enough for *in vivo* gene therapy. However, lipid based gene transfection has induced new bone tissue *in vivo* with and without cell transplantation [17, 28, 44]. Therefore, DNA-Lipoplex coprecipitation has the potential to become a viable method for gene therapy.

Transfection efficiency is controlled by a combination of factors, including cell type, DNA topology, mechanism of cellular internalization, and cytoplasmic barriers including degradation via nucleases [20, 36, 45, 46]. More established cell lines are easier to transfect compared to primary cells [43]. Cells in the mitotic phase exhibit decreased uptake of DNA complexed to cationic lipids in comparison to cells in the interphase [45]. Cell cycle varies between cell types, therefore the use of a different cell line may lead to higher transfection efficiencies. The transfection efficiency of supercoiled plasmid DNA is higher compared to nicked circular or linear plasmid DNA when injected into the cytoplasm, however if these forms are directly introduced to the nucleus, this dependency is absent [46]. Therefore DNA stability in the cytoplasm is important to achieving successful transfection and must be considered since cells must uptake the DNA into the

cytoplasm before they can enter the nuclear pore complexes. There is potential for developing a better cationic agent than Lipofectamine 2000® that can better protect the plasmid DNA from degradation in the cytoplasm, thereby increasing the transfection efficiency. Endocytosis is hypothesized to be the manner in which DNA complexed to nanoparticles is internalized by the cellular environment [36]. When endocytosis is inhibited, transfection efficiency is reduced [36]. Therefore, the transfection efficiencies demonstrated in this study could be improved if the endocytosis pathway by which the DNA-Lipoplexes enter the cells is ascertained, since there are there are several possible pathways of entry into the cells [45, 47]. The development of an improved cationic agent that targets and enhances the type of endocytosis utilized by the cells could also increase transfection efficiency.

There are a number of material factors that can be used to increase transfection efficiency. DNA and calcium phosphate coprecipitation is influenced by concentrations of calcium and phosphate, DNA concentrations, temperature, and reaction time [23]. The mSBF contained Mg, which may have impeded the coprecipitation of the DNA-Lipoplexes resulting in relatively low transfection efficiencies. Changing the composition of the mineralizing solutions by removing Mg could alter the transfection efficiency [20]. Concentrations of calcium and phosphate in solution may also affect the concentration of DNA-Lipoplexes that coprecipitate with the calcium phosphate [23]. Therefore, changing the supersaturation of the mSBF could change the transfection efficiency. Changing the composition of the mineralization solution can also change the rate of DNA release [20], which suggests that apatite dissolution affects DNA release. The differences in transfection efficiency can also be influenced by the surface

morphology and DNA retention at the mineral surface. Additionally, the ratio of DNA to lipid and type of lipid can be altered. In cationic lipid mediated transfection, the higher the lipid dosage, the higher the transfection efficiency [43]. In this study, a commercial lipid agent was used as a model for developing a DNA-Lipoplex coprecipitation system. Designing a cationic lipid that can better protect supercoiled DNA, increase cellular internalization, and prevent degradation from occurring upon uptake would further the development of a feasible non-viral gene delivery method.

3.5 Conclusion

At standard temperatures, pressures and physiological pH, coprecipitation was used to incorporate plasmid DNA complexed with a cationic lipid into a biomimetic apatite. The stability of the plasmid DNA-Lipoplexes is retained during coprecipitation and the complexes are colocalized on the mineralized polymer substrates. DNA-Lipoplex coprecipitation resulted in a higher transfection efficiency in comparison to other methods of delivery, including adsorption of DNA-Lipoplexes. By combining the methods of calcium phosphate based precipitation and cationic lipid assisted transfection, a gene delivery method was developed that has the ability to combine osteoconductivity and osteoinductivity. The coprecipitation of DNA-Lipoplexes into biomimetically nucleated apatite has the potential to be used in bone regeneration and allows for more control over the cellular behavior *in vivo*.

Acknowledgements

I would like to thank the co-authors on this research, David Kohn and Kristen McFalls. This research is supported by NIH DE 015411, DE 13380, and the Tissue Engineering and Regeneration Grant T32 DE 07057. The authors would like to thank the University of Michigan Electron Microbeam Analysis Laboratory for the use of their scanning electron microscope. The authors would also like to thank Viral Patel for aid in plasmid DNA preparation and purification.

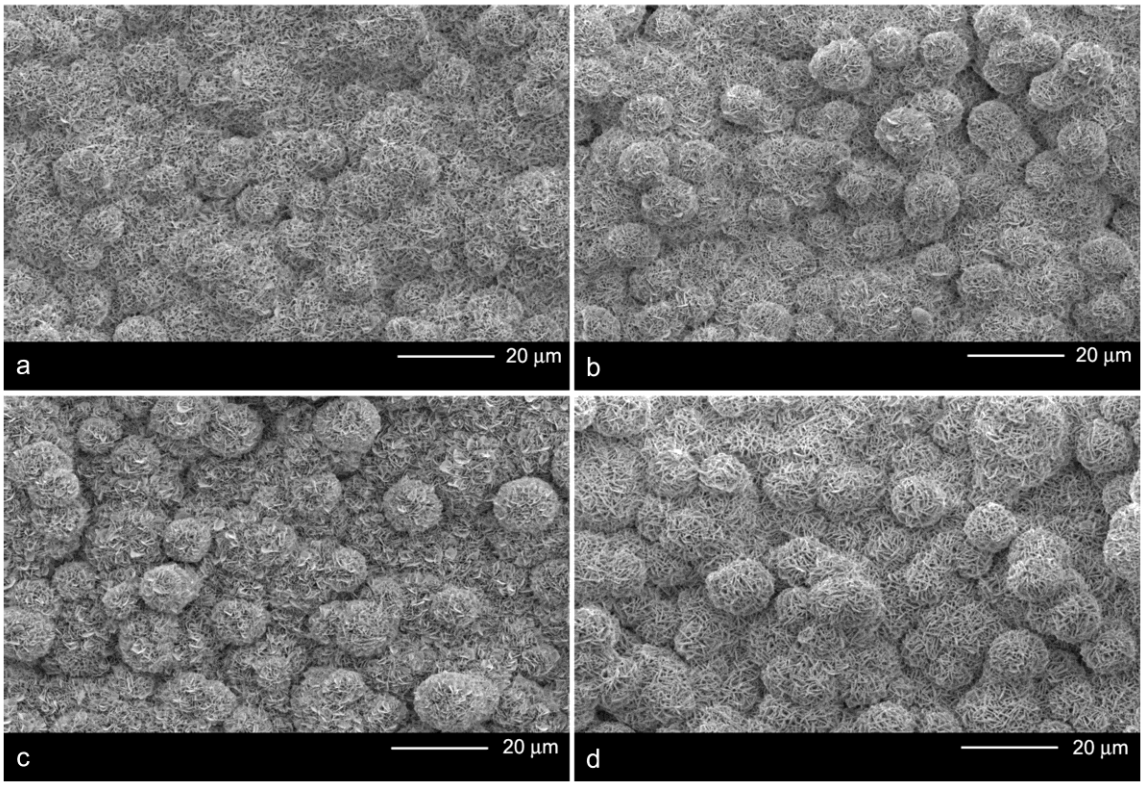

Figure 3.1: Low magnification SEM images of the bone-like mineral surface following different DNA incorporation methods: a) Mineralized control b) Plasmid DNA coprecipitation c) DNA-Lipoplex adsorption and d) DNA-Lipoplex coprecipitation. Neither coprecipitation group demonstrated a difference in the size of the mineral nucleation sites as compared to the mineralized controls.

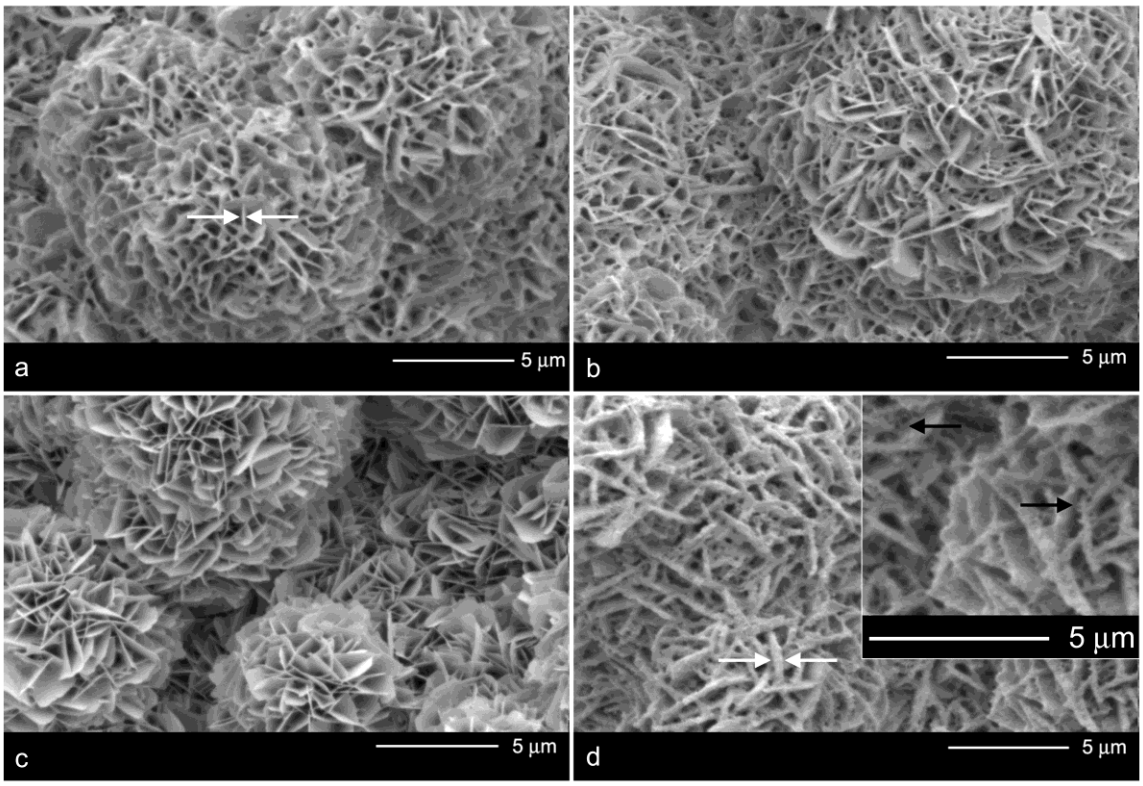

Figure 3.2: High magnification SEM images of the bone-like mineral surface following different DNA incorporation methods: a) Mineralized control b) Plasmid DNA coprecipitation c) DNA-Lipoplex adsorption and d) DNA-Lipoplex coprecipitation. DNA-Lipoplex incorporation via coprecipitation leads to the thickening (white arrows) of the plate-like mineral structures. The "fibrous" coating (black arrows in inset) is most likely due to presence of the cationic lipid because the coprecipitation of DNA alone resulted in minimal changes in apatite morphology.

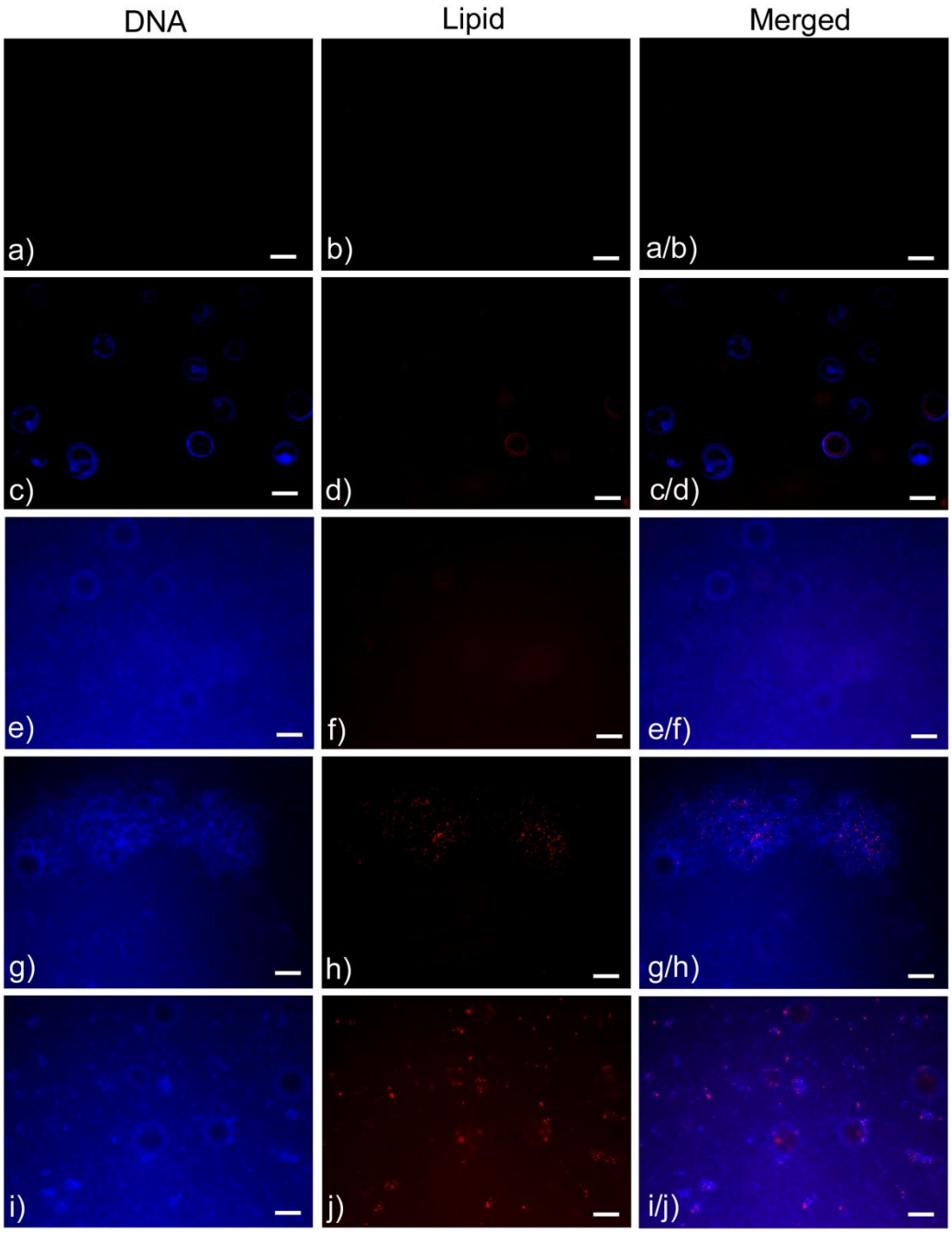

Figure 3.3: Fluorescence images of DNA and lipid agent components from representative samples from each of the following groups: a-b) Mineralized controls, c-d) Plasmid DNA incorporated into PLGA, e-f) Plasmid DNA coprecipitated with mineral, g-h) Plasmid DNA-Lipoplex adsorbed to mineralized films, and i-j) Plasmid DNA-Lipoplex coprecipitated with mineral. Distribution of both the plasmid DNA and the lipid transfection agent on the bone-like mineral was demonstrated by the colocalization of the fluorescent staining (after thorough rinsing) in the adsorption and coprecipitation groups and the absence of staining in the mineralized controls. Scale bars represent 100 μm.

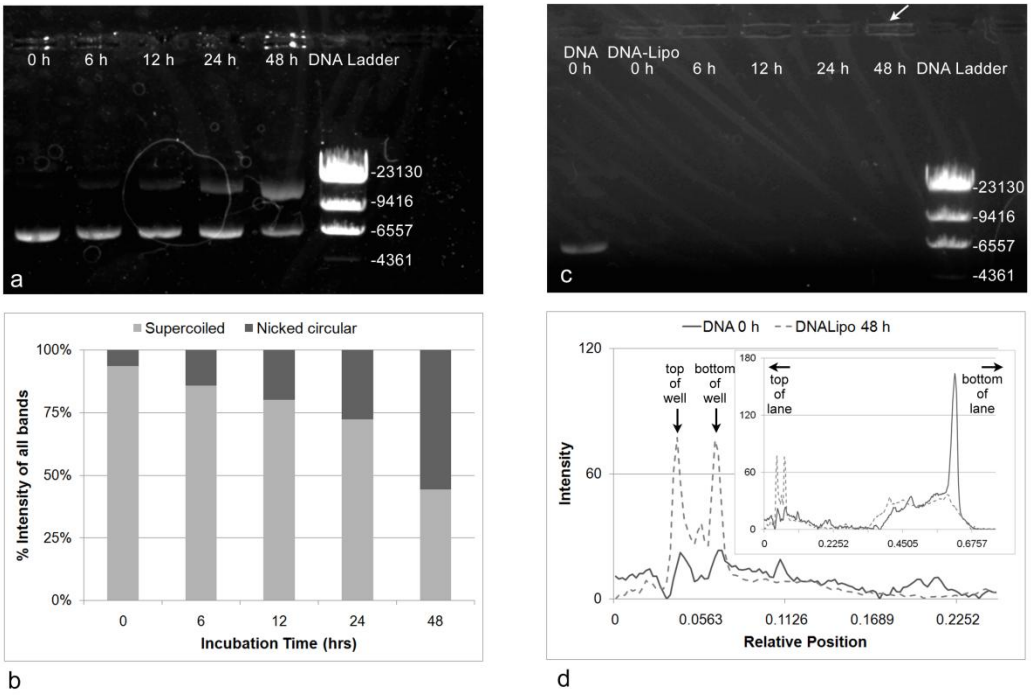

Figure 3.4: Plasmid DNA stability in water, as indicated by a) gel electrophoresis and b) quantification of relative percentages of different forms of DNA. The total intensity of all bands of interest (supercoiled and nicked circular DNA) is equivalent to 100% at each incubation time. Stability of DNA decreases with increasing incubation time as demonstrated by the increasing intensity of the top band (between 23130 and 9416, nicked circular form of DNA) and decreasing intensity of the bottom band, ca. 6557 (supercoiled form of the plasmid DNA). c) DNA-Lipoplex stability in Opti-Mem. Complexation of the DNA and lipid was almost complete due to the absence of bands in these groups. Due to size exclusion, the complexes were not able to leave the wells, resulting in the brightness (white arrow) surrounding the wells. d) Intensity profiles for 2 lanes of the gel: DNA 0 h and DNA-Lipo 48 h demonstrate that the peaks that appear for these wells represent the edges of the wells. Peak intensities for the DNA-Lipoplexes are higher compared to DNA only. Profile intensities for the entire lanes are shown in the inset image.

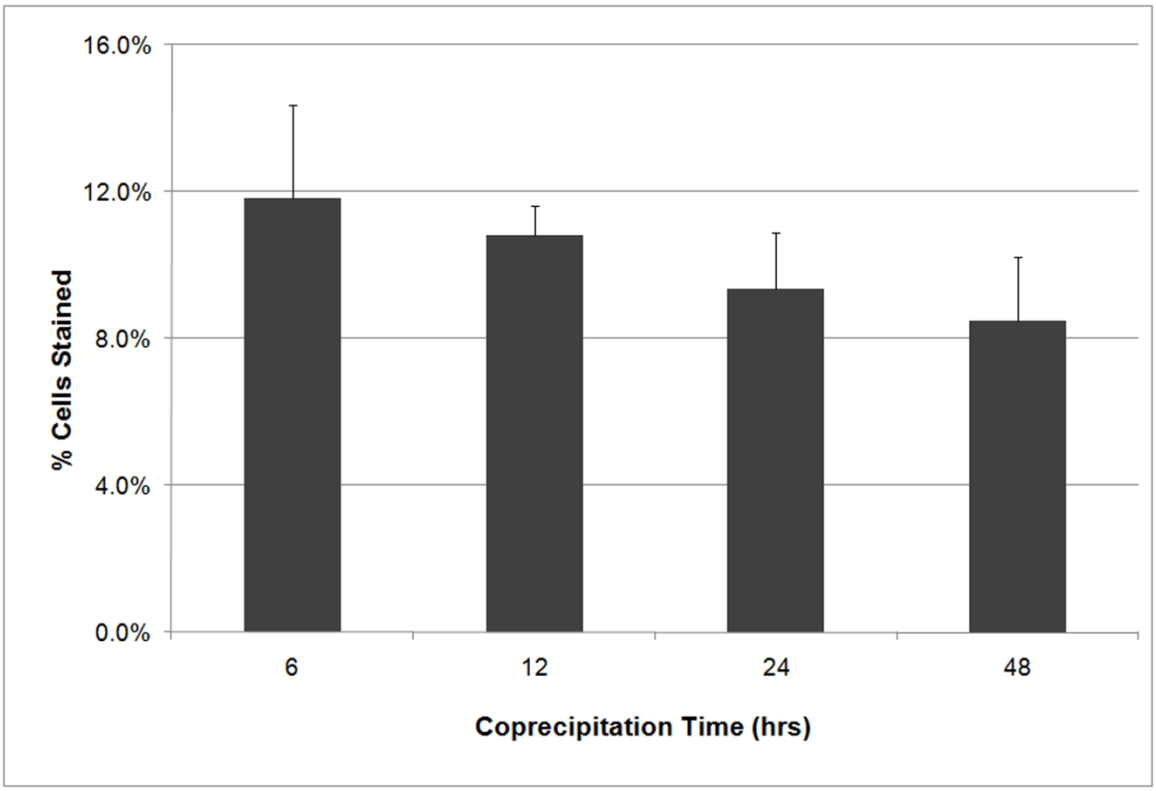

Figure 3.5: Transfection efficiency of DNA-Lipoplexes based on the period of coprecipitation: 6 h, 12 h, 24 h, and 48 h. No significant differences in transfection efficiency existed between coprecipitation times (ANOVA, n=4, p=0.084).

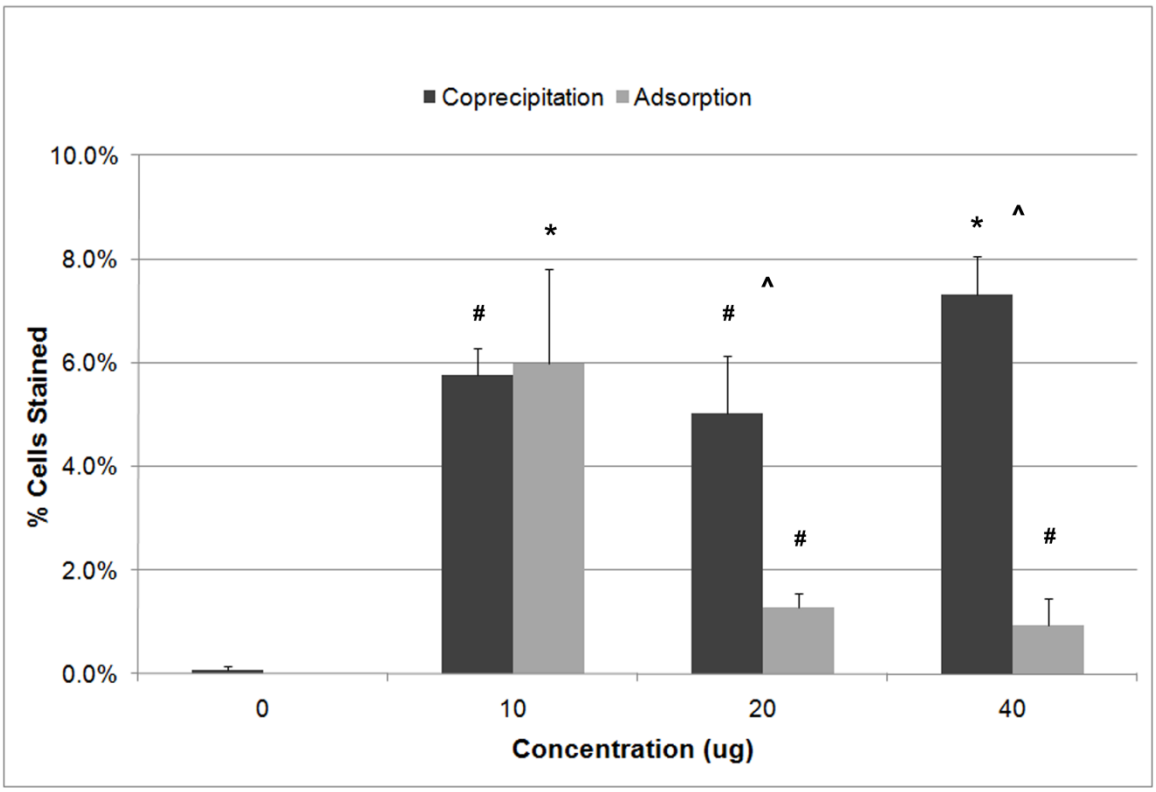

Figure 3.6: Significant differences in transfection efficiencies with concentration of DNA-Lipoplexes were demonstrated for adsorption and coprecipitation groups, $p=0.004$ (ANOVA on Ranks, $n=4$) and $p<0.001$ (ANOVA, $n=4$) respectively. Highest transfection efficiency resulted when 10 µg was adsorbed (SNK, $p<0.05$ relative to other adsorption concentrations) and 40 µg/ml was coprecipitated (SNK, $p\leq0.009$ relative to other coprecipitation concentrations). Comparison of adsorption and coprecipitation at the same concentrations demonstrated a higher efficiency for the coprecipitation groups at 20 µg and 40 µg (SNK, $p<0.05$ for both concentrations). The higher retention of complexes on the apatite surface for the coprecipitation group leads to a higher surface density, and therefore results in a higher transfection efficiency. ^ represents $p<0.05$ between coprecipitation and adsorption at a given concentration, # represents $p<0.05$ in comparison to the concentration of 0, and * represents $p<0.05$ in comparison to all other concentrations within the same technique (either adsorption or coprecipitation).

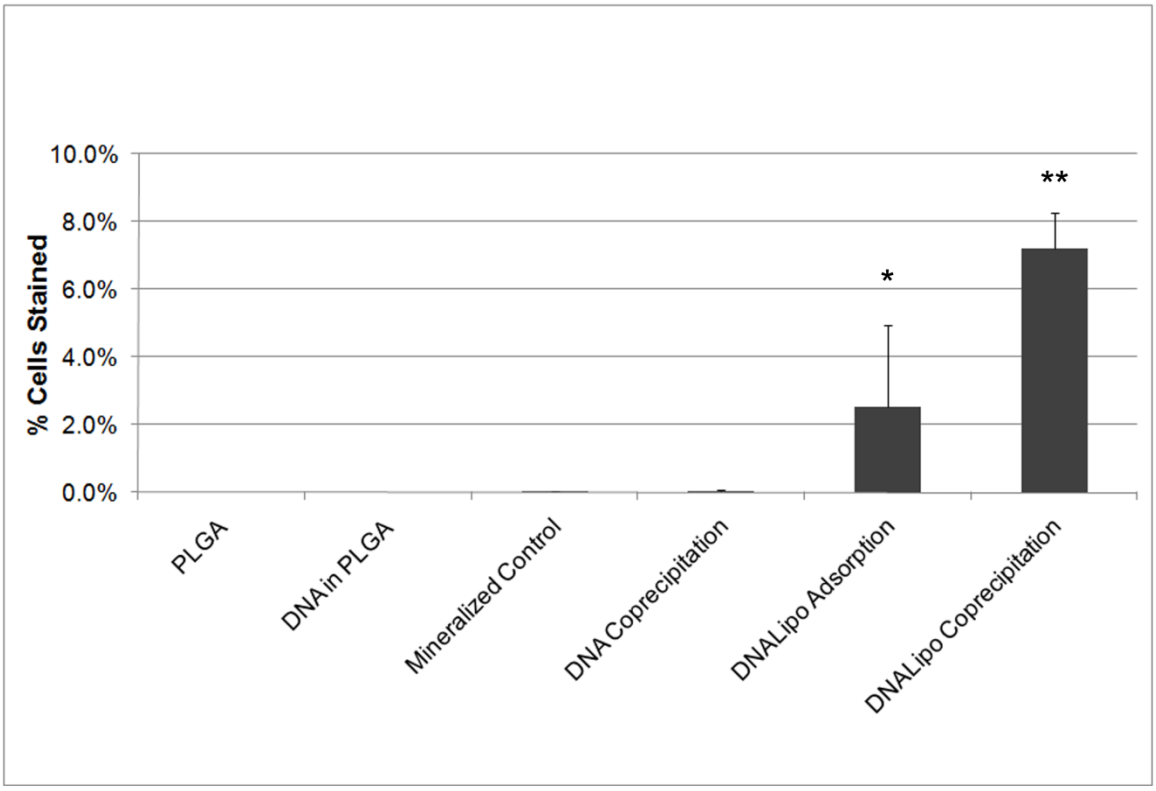

Figure 3.7: DNA-Lipoplex coprecipitation resulted in the highest transfection efficiency compared to all other groups (SNK, n=4, $p<0.05$). The higher transfection efficiency of the DNA-Lipoplex adsorption group compared to the DNA only coprecipitation group suggests that the addition of the cationic lipid enhances transfection. Higher transfection efficiency for coprecipitation compared to adsorption suggests higher retention of the complexes on the surface of the apatite. * represents $p<0.05$ in comparison to each of the groups to the left, ** represents $p<0.05$ in comparison to each of the groups to the left.

References

1. Hench LL. Bioceramics - from Concept to Clinic. J Am Ceram Soc 1991;74:1487-1510.

2. Murphy WL, Kohn DH, Mooney DJ. Growth of continuous bonelike mineral within porous poly(lactide-co-glycolide) scaffolds in vitro. J Biomed Mater Res 2000;50:50-58.

3. Kohn DH, Shin K, Hong SI, Jayasuriya AC, Leonova EV, Rossello RA, et al. Self-Assembled Mineral Scaffolds as Model Systems for Biomineralization and Tissue Engineering. In: Proceedings of the Eighth International Conference on the Chemistry and Biology of Mineralized Tissues; W. J. Landis and J. Sodek, editors. Toronto, Canada: University of Toronto Press; 2005.

4. Murphy WL, Peters MC, Kohn DH, Mooney DJ. Sustained release of vascular endothelial growth factor from mineralized poly(lactide-co-glycolide) scaffolds for tissue engineering. Biomaterials 2000;21:2521-2527.

5. Liu Y, Hunziker EB, Randall NX, de Groot K, Layrolle P. Proteins incorporated into biomimetically prepared calcium phosphate coatings modulate their mechanical strength and dissolution rate. Biomaterials 2003;24:65-70.

6. Stigter M, de Groot K, Layrolle P. Incorporation of tobramycin into biomimetic hydroxyapatite coating on titanium. Biomaterials 2002;23:4143-4153.

7. Liu YL, Layrolle P, de Bruijn J, van Blitterswijk C, de Groot K. Biomimetic coprecipitation of calcium phosphate and bovine serum albumin on titanium alloy. J Biomed Mater Res 2001;57:327-335.

8. Wen HB, Wolke JG, de Wijn JR, Liu Q, Cui FZ, de Groot K. Fast precipitation of calcium phosphate layers on titanium induced by simple chemical treatments. Biomaterials 1997;18:1471-1478.

9. Wen HB, de Wijn JR, Cui FZ, de Groot K. Preparation of calcium phosphate coatings on titanium implant materials by simple chemistry. J Biomed Mater Res 1998;41:227-236.

10. Wen HB, van den Brink J, de Wijn JR, Cui FZ, de Groot K. Crystal growth of calcium phosphate on chemically treated titanium. J Cryst Growth 1998;186:616-623.

11. Wen HB, de Wijn JR, van Blitterswijk CA, de Groot K. Incorporation of bovine serum albumin in calcium phosphate coating on titanium. J Biomed Mater Res 1999;46:245-252.

12. Liu YL, Hunziker EB, Layrolle P, De Bruijn JD, De Groot K. Bone morphogenetic protein 2 incorporated into biomimetic coatings retains its biological activity. Tissue Eng 2004;10:101-108.

13. Liu Y, de Groot K, Hunziker EB. BMP-2 liberated from biomimetic implant coatings induces and sustains direct ossification in an ectopic rat model. Bone 2005;36:745-757.

14. Luong LN, Hong SI, Patel RJ, Outslay ME, Kohn DH. Spatial control of protein within biomimetically nucleated mineral. Biomaterials 2006;27:1175-1186.

15. Partridge KA, Oreffo ROC. Gene delivery in bone tissue engineering: Progress and prospects using viral and nonviral strategies. Tissue Eng 2004;10:295-307.

16. Huang YC, Simmons C, Kaigler D, Rice KG, Mooney DJ. Bone regeneration in a rat cranial defect with delivery of PEI-condensed plasmid DNA encoding for bone morphogenetic protein-4 (BMP-4). Gene Ther 2005;12:418-426.

17. Park J, Ries J, Gelse K, Kloss F, von der Mark K, Wiltfang J, et al. Bone regeneration in critical size defects by cell-mediated BMP-2 gene transfer: a comparison of adenoviral vectors and liposomes. Gene Ther 2003;10:1089-1098.

18. Schek RM, Hollister SJ, Krebsbach PH. Delivery and protection of adenoviruses using biocompatible hydrogels for localized gene therapy. Mol Ther 2004;9:130-138.

19. Leong KW, Mao HQ, Truong-Le VL, Roy K, Walsh SM, August JT. DNA-polycation nanospheres as non-viral gene delivery vehicles. J Control Release 1998;53:183-193.

20. Shen H, Tan J, Saltzman WM. Surface-mediated gene transfer from nanocomposites of controlled texture. Nat Mater 2004;3:569-574.

21. Shea LD, Smiley E, Bonadio J, Mooney DJ. DNA delivery from polymer matrices for tissue engineering. Nat Biotechnol 1999;17:551-554.

22. Mountain A. Gene therapy: the first decade. Trends Biotechnol 2000;18:119-128.

23. Jordan M, Schallhorn A, Wurm FM. Transfecting mammalian cells: Optimization of critical parameters affecting calcium-phosphate precipitate formation. Nucleic Acids Res 1996;24:596-601.

24. Kofron MD, Laurencin CT. Development of a calcium phosphate co-precipitate/poly(lactideco-glycolide) DNA delivery system: release kinetics and cellular transfection studies. Biomaterials 2004;25:2637-2643.

25. Lv HT, Zhang SB, Wang B, Cui SH, Yan J. Toxicity of cationic lipids and cationic polymers in gene delivery. J Control Release 2006;114:100-109.

26. Yi SW, Yune TY, Kim TW, Chung H, Choi YW, Kwon IC, et al. A cationic lipid emulsion/DNA complex as a physically stable and serum-resistant gene delivery system. Pharm Res 2000;17:314-320.

27. Gao X, Huang L. A novel cationic liposome reagent for efficient transfection of mammalian cells. Biochem Biophys Res Commun 1991;179:280-285.

28. Park J, Lutz R, Felszeghy E, Wiltfang J, Nkenke E, Neukam FW, et al. The effect on bone regeneration of a liposomal vector to deliver BMP-2 gene to bone grafts in peri-implant bone defects. Biomaterials 2007;28:2772-2782.

29. Kong HJ, Liu JD, Riddle K, Matsumoto T, Leach K, Mooney DJ. Non-viral gene delivery regulated by stiffness of cell adhesion substrates. Nat Mater 2005;4:460-464.

30. Gazit D, Turgeman G, Kelley P, Wang E, Jalenak M, Zilberman Y, et al. Engineered pluripotent mesenchymal cells integrate and differentiate in regenerating bone: A novel cell-mediated gene therapy. J Gene Med 1999;1:121-133.

31. Shea CM, Edgar CM, Einhorn TA, Gerstenfeld LC. BMP treatment of C3H10T1/2 mesenchymal stem cells induces both chondrogenesis and osteogenesis. J Cell Biochem 2003;90:1112-1127.

32. Blessing T, Remy JS, Behr JP. Monomolecular collapse of plasmid DNA into stable virus-like particles. Proc Natl Acad Sci U S A 1998;95:1427-1431.

33. Banerjee R, Das PK, Srilakshmi GV, Chaudhuri A, Rao NM. Novel series of non-glycerol-based cationic transfection lipids for use in liposomal gene delivery. J Med Chem 1999;42:4292-4299.

34. Segura T, Shea LD. Surface-tethered DNA complexes for enhanced gene delivery. Bioconjug Chem 2002;13:621-629.

35. Dworetzky SI, Lanford RE, Feldherr CM. The effects of variations in the number and sequence of targeting signals on nuclear uptake. J Cell Biol 1988;107:1279-1287.

36. Luo D, Saltzman WM. Enhancement of transfection by physical concentration of DNA at the cell surface. Nat Biotechnol 2000;18:893-895.

37. Schmidt T, Friehs K, Schleef M, Voss C, Flaschel E. Quantitative analysis of plasmid forms by agarose and capillary gel electrophoresis. Anal Biochem 1999;274:235-240.

38. Cherng JY, Schuurmans-Nieuwenbroek NM, Jiskoot W, Talsma H, Zuidam NJ, Hennink WE, et al. Effect of DNA topology on the transfection efficiency of poly((2-dimethylamino)ethyl methacrylate)-plasmid complexes. J Control Release 1999;60:343-353.

39. Chancham P, Hughes JA. Relationship between plasmid DNA topological forms and in vitro transfection. J Liposome Res 2001;11:139-152.

40. Hansma HG, Golan R, Hsieh W, Lollo CP, Mullen-Ley P, Kwoh D. DNA condensation for gene therapy as monitored by atomic force microscopy. Nucleic Acids Res 1998;26:2481-2487.

41. Golan R, Pietrasanta LI, Hsieh W, Hansma HG. DNA toroids: Stages in condensation. Biochemistry (N Y) 1999;38:14069-14076.

42. Okazaki M, Yoshida Y, Yamaguchi S, Kaneno M, Elliott JC. Affinity binding phenomena of DNA onto apatite crystals. Biomaterials 2001;22:2459-2464.

43. Kim SW, Ogawa T, Tabata Y, Nishimura I. Efficacy and cytotoxicity of cationic-agent-mediated nonviral gene transfer into osteoblasts. J Biomed Mater Res A 2004;71A:308-315.

44. Park MS, Kim SS, Cho SW, Choi CY, Kim BS. Enhancement of the osteogenic efficacy of osteoblast transplantation by the sustained delivery of basic fibroblast growth factor. J Biomed Mater Res B Appl Biomater 2006;79B:353-359.

45. Prasad TK, Rangaraj N, Rao NM. Quantitative aspects of endocytic activity in lipid-mediated transfections. FEBS Lett 2005;579:2635-2642.

46. Remaut K, Sanders NN, Fayazpour F, Demeester J, De Smedt SC. Influence of plasmid DNA topology on the transfection properties of DOTAP/DOPE lipoplexes. J Control Release 2006;115:335-343.

47. Wasungu L, Hoekstra D. Cationic lipids, lipoplexes and intracellular delivery of genes. J Control Release 2006;116:255-264.

Chapter 4

Bone Marrow Stromal Cell Response to the Sequential Delivery of FGF-2 and BMP-2

4.1 Introduction

The clinical basis for bone regeneration is the correction of bone defects caused from trauma, congenital malformations, and progressively deforming skeletal disorders. Bone tissue engineering provides an alternative to bone grafting and direct usage of growth factors to regenerate bone. Bone tissue engineering uses engineering design to strategically integrate cells, an extracellular matrix (ECM) analogue, and signaling molecules to induce bone regeneration: [1]. An ideal bone tissue engineering approach would incorporate osteoinductivity and osteoconductivity into the design of the supporting biomaterial, as well as biocompatibility, degradability, mechanical integrity, and the ability to support cell transplantation.

Osteoinductive properties can be integrated into a tissue engineering system by immobilization of biomolecules to a biomaterial surface, or encapsulation within a biomaterial. Growth factors are proteins that regulate cellular signals and can stimulate or inhibit cellular migration, adhesion, proliferation, and differentiation. A single growth factor can act on different cells with varying effects, and can also influence the activation of other growth factors in a synergistic or antagonistic manner. While the use of one growth factor is beneficial to eliciting cellular attachment, proliferation and/or

differentiation [2-4], the biological environment is not limited to the activation of a single growth factor. To better simulate the microenvironment that cells are subjected to *in vivo*, exposure to multiple biological agents with a spatial and temporal gradient would be ideal. For example, vascular endothelial growth factor (VEGF) alone is not sufficient to heal of critical size defects, however by combining VEGF with bone morphogenetic protein 4 (BMP-4) enhanced healing was demonstrated [5]. On the other hand, combined delivery of osteopontin-1 (OP-1) and bone morphogenetic protein 2 (BMP-2) did not enhance bone regeneration over delivery of each of these factors individually [6]. Simultaneous exposure of rat BMSCs to IGF-I (insulin growth factor I) and BMP-2 did not significantly increase alkaline phosphatase expression or amount of calcium secreted, the optimized result was exposure to BMP-2 followed by IGF-I, demonstrating the importance of timing and the sequence of delivery of the growth factors on cellular response [7].

To provide the design parameters for the development of a delivery system for bone engineering, two growth factors chosen due to their important roles in osteogenic differentiation were BMP-2 and fibroblastic growth factor 2 (FGF-2). BMP-2 is a member of the transforming growth factor (TGF-β) superfamily. *In vitro*, BMPs regulate the growth and differentiation of cells in the osteoblast lineage. Osteogenic differentiation of BMSCs cultured in medium containing rhBMP-2 was demonstrated by a marked increase in the expression of osteopontin and increased mineralization in comparison to cells not exposed to rhBMP-2 [4]. In vitro, rhBMP-2 not only induces differentiation of osteoblastic precursors, but it also inhibits myogenic differentiation [8]. BMP-2 is one of the earliest genes that is induced in fracture healing, with a second peak

occurring late in the period of osteogenesis [9], which suggests that a simple burst release or sustained release would not be sufficient to elicit an osteogenic response.

Fibroblast growth factors promote cell growth, induce a mitogenic response, stimulate cell migration, and induce differentiation [10]. FGF-2 is a well known angiogenic factor, and it also plays a role in osteogenic differentiation. FGF-2 can stimulate the replication of osteoprogenitor cells, which then further differentiate into an osteoblastic phenotype, however, prolonged treatment resulted in an inhibitory effect [11]. Because both BMP-2 and FGF-2 regulate osteogenesis, they have been used in combination. FGF-2 stimulated cell growth and osteoblastic differentiation of dexamethasone treated MSCs, and upon exposing cells to both BMP-2 and FGF-2, bone formation was enhanced more than either growth factor individually [12], confirming again the importance of temporal gradients.

The long term aim is to provide design criteria for a delivery system based on the effects of exposure of BMP-2 and FGF-2 on BMSCs. The concentrations and sequence of BMP-2 and FGF-2 defined to optimally differentiate BMSCs cultured on tissue culture polystyrene (TCPS) in this study will be applied to the development of a delivery system based on coprecipitation of bone-like mineral and one or both of these growth factors. Delivering the growth factors from a mineralized substrate is a tissue engineering approach that combines osteoinductivity, provided by the inclusion of the growth factors, and osteoconductivity, provided by the presence of biomimetically precipitated apatite.

To build toward this long term objective, the effects of individual and sequential delivery of BMP-2 and FGF-2 on osteogenic differentiation of murine BMSCs were examined with the aim of providing a design basis for a multiple growth factor delivery

system. It was hypothesized that low concentrations of FGF-2 would increase cell number while high concentrations of BMP-2 would enhance osteogenic differentiation. It was also hypothesized that the sequence of FGF-2 followed by the administration of BMP-2 would best enhance the osteogenic activity of the BMSCs compared to the delivery of each of the growth factors independently. DNA content, alkaline phosphatase activity (ALP), osteocalcin serum content, and mineralization were analyzed over a 3 week time period for cells plated on TCPS with the addition of FGF-2 (2.5, 10, 40 ng/ml) or BMP-2 (50, 150, 450 ng/ml) for 6 days for the individual growth factors and FGF-2 (2.5 ng/ml) and BMP-2 (300 ng/ml) for the sequential administration.

4.2 Materials and Methods

4.2.1 Murine bone marrow stromal cell extraction and cell culture

Six week old C57BL6 mice were utilized for BMSC extraction. Freshly extracted long bones (6 per mouse) were suspended in Hank's Balanced Salt Solution (HBSS). The metaphyses of each bone were cut (to allow for an opening to the marrow cavity), and 2 bones were placed into a 200 µl pipette tip and then placed in a microcentrifuge tube. Tubes were spun for 8-12 sec up to a maximum speed of 2000 rpm [13]. An 18 gauge needle was used to gently agitate the cell pellets. Cell pellets were then pooled and split into T75 flasks. Media was exchanged and non-adhesive cells were removed after 5 days. Media was exchanged every 3 days until cells reached confluency, at which time cells were split 1:3 and replated. After reaching confluency, cells were counted and replated in 24 well plates.

Growth medium for primary cell culture and plating was composed of 10% FBS, 1% penicillin-streptomycin, and MEMα medium. During growth factor administration, the growth medium was supplemented with 10^{-8} M dexamethasone for six days. After this time period, osteogenic medium was utilized which was growth medium supplemented with dexamethasone, 50 mg/L L-ascorbic acid-phosphate, and 10 mM β-glycerol phosphate hydrate disodium salt.

4.2.2 Single growth factor optimization

The growth factors rhBMP-2 and rhFGF-2 were obtained from Peprotech (Rocky Hill, NJ). FGF-2 was reconstituted in 5 mM Tris buffer containing BSA. BMP-2 was reconstituted in sterile water containing BSA.

Cells were plated into 24 well-plates (n=4 per group) at a density of 40,000 cells per well and allowed to attach for 24 h. Medium was then removed and replaced with growth medium containing dexamethasone and growth factor (FGF-2 at 0, 2.5, 10, and 40 ng/ml or BMP-2 at 0, 50, 150, and 450 μg/ml) which was designated as Day 1. The media containing growth factor was then replaced on Day 4. On Day 7, and every 3 days thereafter , the medium was replaced with osteogenic medium.

4.2.3 Multiple growth factor optimization

Cells were plated into 24 well-plates (n=5 per group) at a density of 50,000 cells per well and allowed to attach for 24 h. Medium was then removed and replaced with growth medium containing dexamethasone and growth factors on Days 1 and 4 (Table 4.1). On Day 7, and every 3 days thereafter, the medium was replaced with osteogenic medium.

4.2.4 DNA content

To determine DNA content and ALP activity, cells were washed twice with HBSS and harvested utilizing a buffer containing 10 mM Tris-HCl, 0.2% Igepal, and 2 mM PMSF in ethanol. Samples were then placed at -80^{o}C for later analysis.

For DNA determination, samples were thawed, and homogenized on ice. Samples were then centrifuged at 12,500 rpm for 10 min at 4^{o}C. The Quant-iT Picogreen kit (Molecular Probes, Eugene, OR) was used to determine DNA content according to the protocol adapted from the manufacturer. Samples were prepped in duplicate, and the fluorescence (480 nm excitation and 520 nm emission) was determined using a microplate reader and DNA quantity was determined by using standard curves. DNA content was determined for all timepoints.

4.2.5 Alkaline phosphatase (ALP) activity

Thawed homogenized samples were then vortexed with assay buffer (glycine, $MgCl_2$), harvest buffer, and p-nitrophenyl-phosphate (PnPP) substrate solution (Sigma, St. Louis, MO) and incubated at 37^{o}C for 15 min. The reaction was then terminated by adding 0.1 N NaOH and samples were placed in a 96 well-plate. A standard curve using alkaline phosphatase from calf intestine (Roche, Indianapolis, IN) was used to compare the activity and absorbance was determined at 405 nm. Values were then normalized to DNA content. ALP activity was determined for all timepoints.

4.2.6 Osteocalcin (OCN) content

Media was removed and frozen every 3 days in microcentrifuge tubes for OCN analysis. The serum OCN content was determined using a mouse OCN EIA kit (Biomedical Technologies, Stoughton, MA) according to manufacturer's protocol.

Samples were thawed and placed into the 96 well-plate. A standard curve was also prepared ranging from 0 ng/ml to 50 ng/ml. After reaction termination, measure the absorbance at 450 nm immediately.

4.2.7 Von Kossa Staining

To determine mineralization, the BMSC cultures were stained with silver nitrate. Briefly, media was removed from the wells, and submerged in Z-fix for 30 min. The wells were gradually rehydrated using EtOH/H_2O mixtures, and then rinsed with H_2O. The wells were exposed to UV light, stain was removed, and wells were imaged using a dissection microscope. Image analysis of % stained area was obtained using ImageJ (NIH).

4.2.8 Statistical analysis

One way ANOVA was used to analyze DNA content, ALP activity, OCN content, and von Kossa staining of the BMSC cells with regards to growth factor concentration, and growth factor sequence. Tukey or Dunnett's T3 post hoc comparison tests were used for pair-wise comparisons.

4.3 Results

4.3.1 FGF-2 has a proliferative effect on BMSCs, while BMP-2 does not

The addition of BMP-2 to BMSCs did not have a significant effect on DNA content (Figure 4.1a). For 150 and 450 ng/ml of BMP-2, DNA content increased from Day 8 to Day 15 ($p<0.001$ and $p=0.013$ respectively). The addition of FGF-2 to BMSCs had a proliferative effect (Figure 4.1b). At Day 8 (ANOVA, $p=0.002$) and Day 15 (ANOVA, $p<0.001$), there was significantly higher DNA content for groups that had

been treated with FGF-2 (2.5, 10, and 40 ng/ml) compared to the untreated controls. However, there was not a significant dose dependent response with increasing the FGF-2 concentration from 2.5 ng/ml to 40 ng/ml. For 2.5 and 40 ng/ml of FGF-2, DNA levels were significantly higher at Day 15 compared to Day 8 ($p<0.05$). At Day 22, DNA levels were significantly lower for all FGF-2 concentrations compared to their respective DNA levels at Day 8 ($p<0.05$).

4.3.2 BMP-2 has a dose dependent enhancement of ALP activity, while FGF-2 has a dose dependent inhibitive effect

At Day 8, ALP activity (normalized to DNA content) was significantly higher (ANOVA, $p=0.004$) for cells treated with 450 ng/ml BMP-2 compared to both the untreated controls (Tukey, $p=0.006$) and cells treated with 50 ng/ml BMP-2 (Tukey, $p=0.008$) (Figure 4.2a). A lower concentration of BMP-2 (150 ng/ml) did not result in significantly higher amounts of ALP activity compared to untreated controls, suggesting a minimum concentration has to be reached before osteogenic enhancement occurs.

FGF-2 also had a significant effect on ALP activity (ANOVA) of BMSCs, however, the effect is inhibitive when compared to the untreated controls (Figure 4.2b). At Day 8, normalized ALP was significantly lower for all FGF-2 concentrations compared to the controls ($p<0.05$). At Day 15, normalized ALP activity was significantly lower for 2.5, 10, and 40 ng/ml (Tukey, $p<0.01$) compared to untreated controls. For Day 22, ALP activity for 2.5 ng/ml was significantly higher compared to 10 and 40 ng/ml (Dunnett's T3, $p<0.01$). Exposing BMSCs to FGF-2 at higher concentrations delays or even inhibits osteogenic activity.

4.3.3 BMP-2 administration significantly enhances late stage differentiation, while FGF-2 inhibits

In later stages of osteogenic differentiation, osteocalcin secretion (Figure 4.3) is higher for cells that were treated with higher concentrations of BMP-2 (ANOVA, $p=0.036$). At Day 22, BMSCs treated with a BMP-2 concentration of 450 ng/ml secreted significantly more osteocalcin than control cells (Tukey, $p=0.045$) and marginally more than cells treated with 50 ng/ml BMP-2 (Tukey, $p=0.056$). For 450 ng/ml of BMP-2, OCN secretion at Day 22 was significantly compared to OCN levels on Day 16, and Day 19 ($p<0.05$). In contrast, for the groups treated with FGF-2 at increasing concentrations, osteocalcin secretion levels were not significantly different (data not shown).

At Day 22, the % mineral coverage for cells treated with 150 ng/ml of BMP-2 was marginally higher than the untreated cells (Dunnett's T3, $p=0.104$) (Figure 4.4 and Figure 4.5). Adding FGF-2 at any concentration inhibits mineral deposition. The control cells demonstrated some mineral deposition, however, the difference with varying FGF-2 concentration was not statistically significant.

4.3.4 Effects of BMP-2 and FGF-2 sequence on DNA content

The concentrations that were used in the sequential exposure experiments were based on the results from the individual exposure of each growth factor. For the sequential experiments, 2.5 ng/ml of FGF-2 and 300 ng/ml of BMP-2 were used. Since FGF-2 increases DNA content, but inhibits osteogenic differentiation, the minimum concentration was chosen to increase the number of cells that can be osteogenically induced (Figure 4.1). For BMP-2, a concentration of 300 ng/ml was chosen due to cost limitations and the necessity for a concentration of BMP-2 that was higher than the 150

ng/ml threshold for significant results (Figure 4.2). Due to the cell layers contracting for some of the treatment groups, the time points at which DNA, ALP, OCN, and mineral deposition were examined differed from the times in the individual growth factor experiments (8, 11, 13 d).

The duration of FGF-2 exposure significantly affects the total DNA content (Figure 4.6). At Day 8, F/F, F/BF, and BF/BF had significantly higher DNA levels compared to the untreated controls and the groups that delivered BMP-2 first (Tukey, $p<0.05$). At Day 11, B/F, F/F, and BF/BF had higher DNA content compared to the DNA level for the group that only delivered BMP-2 (Dunnett's T3, $p<0.05$). At Day 13, the groups that delivered FGF-2 first (F/F, F/B, F/BF, BF/BF) had significantly higher DNA content compared to B/B and B/F where BMP-2 is delivered first (Tukey, $p<0.05$). Groups that delivered FGF-2 the entire time period tended towards having higher DNA levels. Most groups that delivered FGF-2 second also trended towards having higher DNA levels.

4.3.5 Effects of BMP-2 and FGF-2 sequence on ALP activity

Delivering BMP-2 alone led to the highest ALP levels (Figure 4.7). However, taken in conjunction with relatively low DNA levels compared with other groups (Figure 4.6), this suggests that a smaller population of cells had enhanced osteogenic activity. Delivering FGF-2 alone also resulted in a low level of ALP expression. However, when both growth factors were delivered, the effects of BMP-2 and FGF-2 did vary depending on the sequence of delivery (ANOVA, $p<0.001$). At Day 8, ALP levels for F/F and F/BF are significantly lower compared to all other groups. The sequential delivery of BMP-2 and FGF-2 in either order led to significantly higher ALP levels compared to

delivering both factors simultaneously on Day 8 (Dunnett's T3, $p<0.05$). Delivery of FGF-2 first, and then BMP-2 resulted in higher ALP levels compared to delivery of BMP-2 first, followed by FGF-2. Inclusion of FGF-2 resulted in significantly lower levels in all groups except B/BF and F/B. Groups that were not exposed to FGF-2 for the entire 6 days had higher ALP levels compared to all of the other groups. At Day 11, F/B still demonstrated higher ALP compared to all groups except the untreated cells and B/BF (Dunnett's T3, $p<0.05$). At Day 13, F/B continued to demonstrate high ALP levels compared to all groups except the controls and B/BF (Dunnett's T3, $p<0.05$). Untreated cells, B/B, and F/B had significantly higher ALP levels compared to BF/BF. Even though cells were subjected to the same two growth factors, the sequence of delivery did significantly affect osteogenic differentiation.

4.3.6 Effects of BMP-2 and FGF-2 sequence on late stage osteogenic differentiation

The different sequences of delivery also had an impact on OCN secretion (ANOVA, $p<0.001$) (Figure 4.8a). F/B, B/BF, and BF/BF had higher levels of OCN compared to F/F and F/BF (Dunnett's T3, $p<0.05$). When both growth factors were delivered, delivering BMP-2 the entire 6 days led to higher OCN levels compared to delivering FGF-2 during the entire time period (B/BF compared to F/BF), which suggests that if the cells had not contracted early, the differences between the groups would have increased since OCN is a late marker for differentiation.

Mineral deposition also demonstrated dependence on when the growth factors were administered (ANOVA, $p<0.001$) (Figure 4.8b). Groups that delivered FGF-2 the entire 6 days had lower mineral coverage, including the simultaneous delivery of FGF-2 and BMP-2 (Dunnett's T3, $p<0.05$). Delivering FGF-2 first followed by BMP-2 had

higher mineral coverage compared to the delivery of both factors simultaneously. Additionally, B/BF also had higher mineral coverage compared to simultaneous delivery, suggesting that the delivery of BMP-2 the entire 6 days can override the inhibitive effects of delivering FGF-2 to osteogenic activity.

4.4 Discussion

The aim of this study was to provide design criteria for the development of a delivery system in which the concentration and timing of release of multiple growth factors can be controlled. The aim was accomplished by investigating the effects of BMP-2 and FGF-2 on osteogenic differentiation of murine BMSCs. The first objective was to determine the concentrations of the growth factors required, and the second was to determine the impact that the sequence in which the factors are delivered have on osteogenic differentiation.

BMP-2 is a potent osteogenic factor that has effects on different stages of osteoblastic maturation ranging from osteoblast progenitor cells to more mature osteoblasts [8]. Pertaining to DNA content, BMP-2 did not have a significant effect even at higher doses (Figure 4.1). BMP-2 demonstrated a dose dependent increase in ALP, OCN and mineral deposition (Figure 4.2a, Figure 4.3, and Figure 4.5a), which suggests that a higher concentration of BMP-2 may increase ALP, OCN and mineral deposition even further. With a more mature osteoblastic cell line, this dose dependent increase is absent [8], however, the presence of more osteoprogenitor cells in a base population could lead to the dose dependency demonstrated here. Based on the concentrations

examined, 450 ng/ml is most appropriate for further experimentation, however, due to cost limitations, 300 ng/ml was chosen for the sequential delivery experiments.

FGF-2, as a well known mitogenic factor, increased DNA content for all concentrations compared to the untreated controls (Figure 4.1b), however dose dependency was not demonstrated. FGF-2 plays an active mitogenic role for various cells types including endothelial, fibroblastic, and smooth muscle cells. *In vitro*, FGF-2 also has a mitogenic effect on preosteoblastic cells [14]. The effect that FGF-2 has on osteogenic differentiation *in vivo* is biphasic, high concentrations also result in an inhibitory effect on bone regeneration [15]. This inhibitory effect may be due to the differentiation stage of the cell population in question [16]. In this study, FGF-2 has a significant negative impact on both early and late stage osteogenic differentiation (Figure 4.2, Figure 4.3, and Figure 4.5). Even at a low concentration of 2.5 ng/ml, there was an inhibitory effect on ALP, OCN and mineral deposition. A concentration of 2.5 ng/ml was determined to be most appropriate for the dual growth factor experiments in order to balance the proliferative properties of FGF-2 with its delaying effect on osteogenic differentiation.

Using a concentration of 2.5 ng/ml for FGF-2 and 450 ng/ml for BMP-2, different growth factor sequences were administered to BMSCs (Table 4.1). Treatment sequences that delivered FGF-2 for the entire 6 day time period demonstrated higher DNA content while sequences that delivered BMP-2 for the same 6 day time period did not lead to a significant increase in DNA levels (Figure 4.6), which implies that a more prolonged treatment of FGF-2 increases cell number better than treating the cells for a shorter period of time. However, the inclusion of FGF-2, even at a low concentration of 2.5 ng/ml

results in a marked decrease in osteogenic activity (Figure 4.7 and Figure 4.8), even with a shorter time period of administration. The groups in which FGF-2 was administered for the entire 6 day time period, had the lowest levels of osteogenic activity (ALP, OCN, and mineral deposition), compared to the groups that only delivered FGF-2 for 3 days. FGF-2 induced osteogenic enhancement could be dependent on the stage of cellular differentiation, where late administration of FGF-2 can lead to matrix mineralization but no change in cell growth [16]. *In vivo*, nanogram levels of FGF-2 with BMP-2 can synergistically increase osteogenic differentiation, but on a microgram level serve to inhibit bone regeneration, demonstrating biphasic bioactivity [17].

Differences in the delivery sequence had a significant impact on the osteogenic activity of the BMSCs. Delivering FGF-2 first, followed by BMP-2 led to higher ALP levels and mineral deposition compared to simultaneous delivery of BMP-2 and FGF-2 (Figure 4.7, Figure 4.8b). Bone chamber studies have also shown a high inhibition due to a simultaneous delivery of BMP-2 and FGF-2 [18]. For OCN expression, FGF-2 followed by BMP-2 was not significantly different from from simultaneous exposure. The comparable OCN levels suggests that due to the binding affinity of OCN for apatite [19], the OCN secreted from the cultured cells may have adsorbed to the mineralized nodules formed, especially in the case of FGF-2 followed by BMP-2 where mineral coverage was significantly higher compared to simultaneous exposure (Figure 4.8).

The importance of sequential administration of FGF-2 and BMP-2 is also supported by finding that FGF-2 followed by BMP-2 resulted in higher ALP activity and possibly higher mineral deposition than the reverse order of administration. Delivering BMP-2 the entire 6 days, and FGF-2 in the latter 3 days also resulted in relatively high

osteogenic activity compared to the simultaneous delivery of both growth factors (Figure 4.7 and Figure 4.8). This is most likely due to the continuous presence of BMP-2, which is a potent inducer of osteoblastic differentiation. There are a few possible theories for the efficacy of the sequential exposure of FGF-2 followed by BMP-2. First, FGF-2 may serve to increase the efficacy of BMP-2 induction by stimulating precursor cells to enter the early stages of osteogenic differentiation [20-22]. Second, by treating cells with FGF-2 early, the population of osteoprogenitor cells that can be induced by BMP-2 to undergo the later stages of osteogenic differentiation is increased [12, 22]. In the another theory, the increase in osteogenic activity with sequential exposure may be due to FGF-2 selectively increasing the number of cells that have already expressed BMP-2 receptors or increasing the expression of a specific receptor, BMPR-1B, which would potentiate BMP-2 induction [12, 23]. Selective BMP-2 receptor dependency was suggested to be a possible cause for ectopic bone formation induced by delivering low doses of FGF-2 with BMP-2 [23].

From this study, we have demonstrated the importance of the sequence of growth factor delivery in enhancing osteogenic differentiation. By understanding the response of BMSCs to FGF-2 and BMP-2, we can design a substrate based delivery system to mimic these responses (Chapter 5), especially since cells in their surrounding microenvironment would respond to spatial and temporal gradients that growth factors exhibit *in vivo*. The hybrid delivery system based on coprecipitation has the potential to deliver any number of growth factors in order to better mimic the cellular environment. Coprecipitation potentiates the integration of the mechanical support and conductivity of apatite with the

inductivity of biomolecules in a hybrid delivery system that can better control the sequential delivery of multiple biomolecules.

4.5 Conclusion

To best design a delivery system for multiple growth factors, the biological basis for the delivery of two growth factors was characterized. BMP-2 and FGF-2 were chosen and osteogenic differentiation was evaluated as a means of measuring the importance of sequential delivery. From the individual growth factor experiments, low concentrations of FGF-2 resulted in higher cell number while high concentrations of BMP-2 best enhanced osteogenic activity. The sequence of delivery of BMP-2 and FGF-2 had a significant impact on osteogenic differentiation. The delivery of FGF-2 followed by BMP-2 or even the delivery of BMP-2 followed by the delivery of both BMP-2 and FGF-2 enhanced osteogenic differentiation compared to the simultaneous delivery of both factors. In Chapter 5, the results of the biological response of BMSCs to the two growth factors will be applied in the development of a coprecipitation based delivery system with the aim of mimicking the cellular response.

Acknowledgements

This research is supported by NIH DE 015411, DE 13380, and the Tissue Engineering and Regeneration Grant T32 DE 07057. I would like to thank Janani Ramaswamy and Erin McNerny for their support and advice during this work.

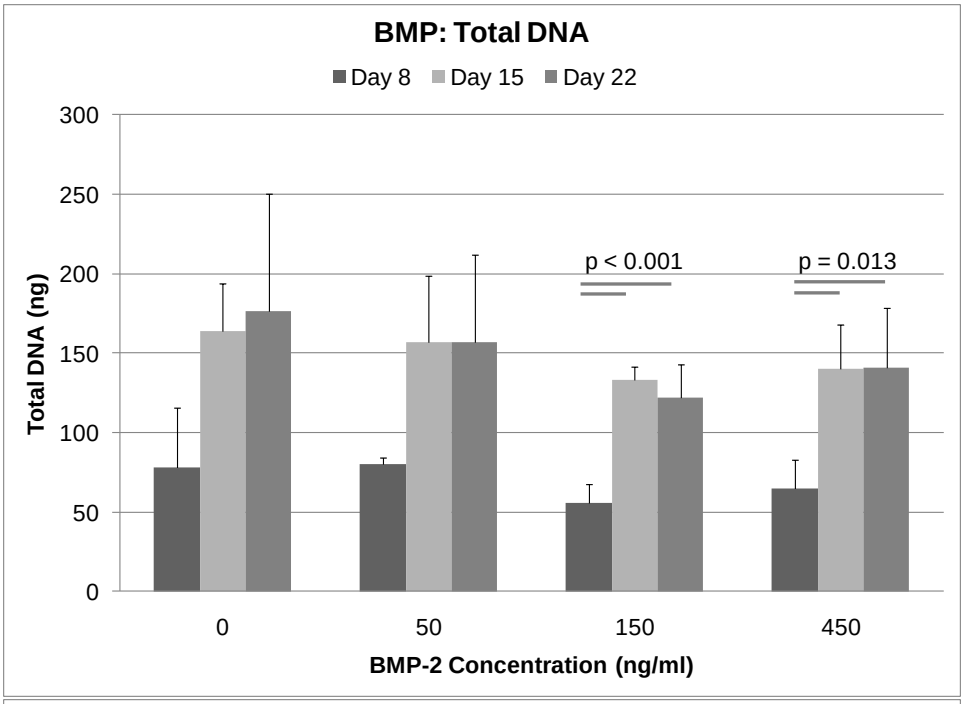

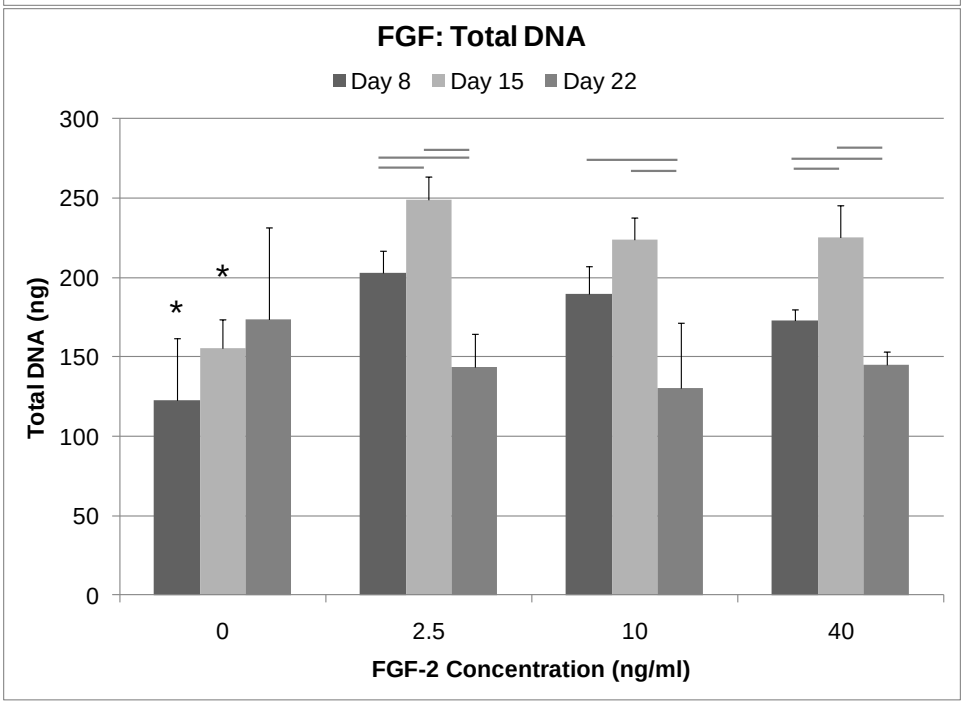

Figure 4.1: Total DNA quantified using Picogreen. A) There was no significant difference in DNA amounts with varying concentrations of BMP-2 (n=4) as determined by ANOVA at the respective timepoints. B) All concentrations of FGF-2 demonstrated higher DNA content compared to the untreated cells for Day 8 and Day 15 (* indicates $p<0.05$) as determined by ANOVA at the respective time points. The bars represent significance between timepoints within the same concentration treatment.

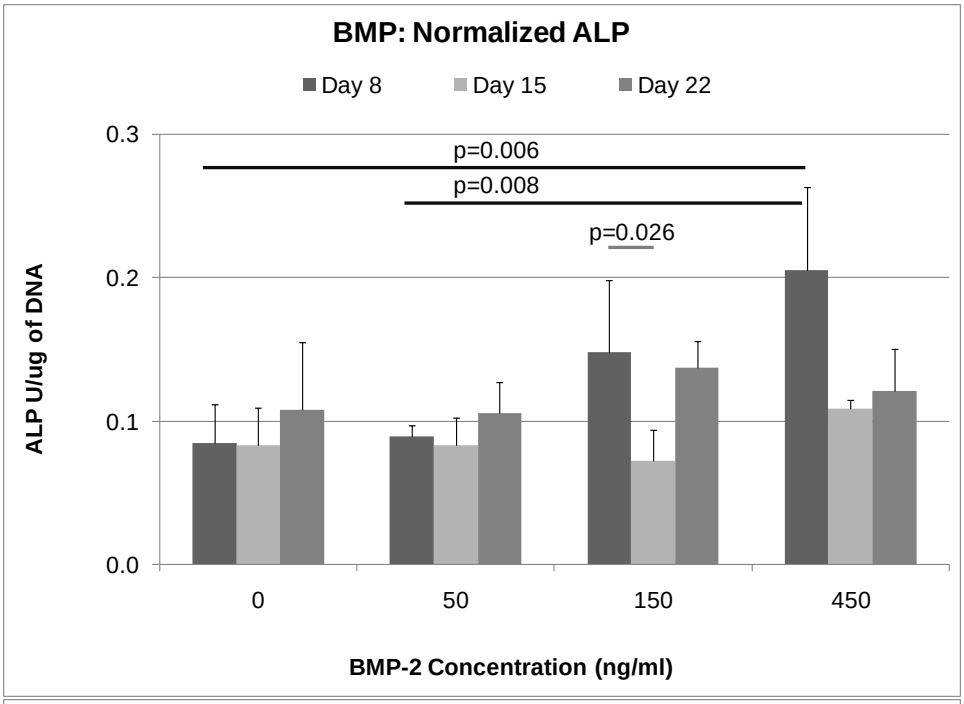

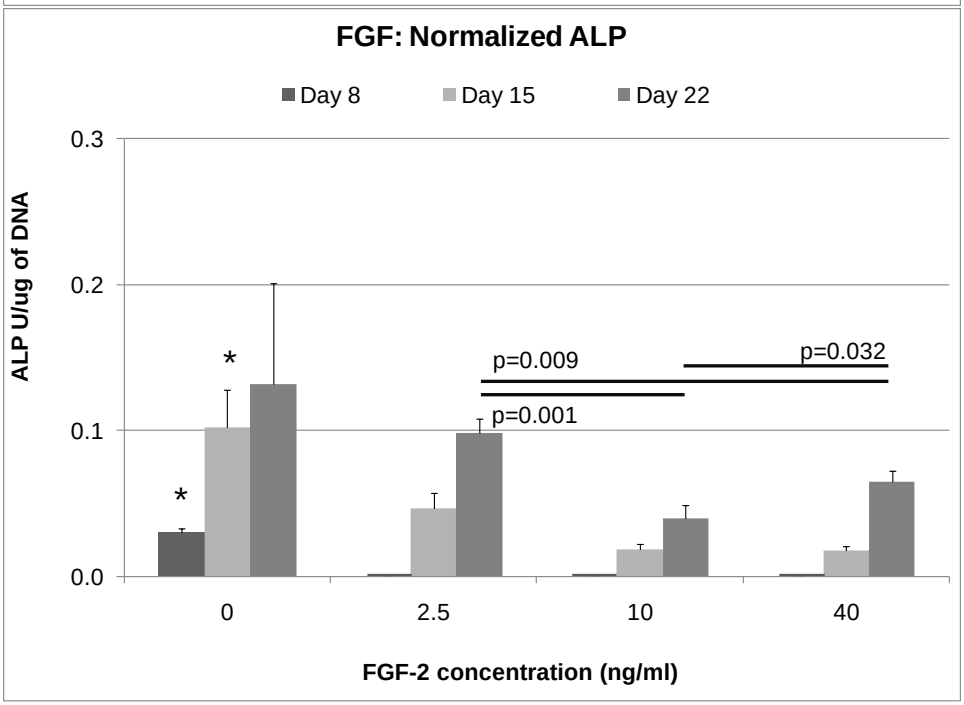

Figure 4.2: Normalized ALP with respect to total DNA. A) At Day 8, a BMP-2 concentration of 450 ng/ml led to higher ALP expression compared to the untreated controls. The BMP-2 concentration of 450 ng/ml was also significantly higher than the 50 ng/ml BMP-2 concentration. B) The normalized ALP of untreated controls was higher compared to all concentrations of FGF-2 for Day 8 and Day 15 (* indicates $p<0.05$) as determined by ANOVA at the respective timepoints. The normalized ALP on Day 22 was also higher for the 2.5 ng/ml concentration compared to both 10 ng/ml and 40 ng/ml (Bars indicates $p<0.05$).

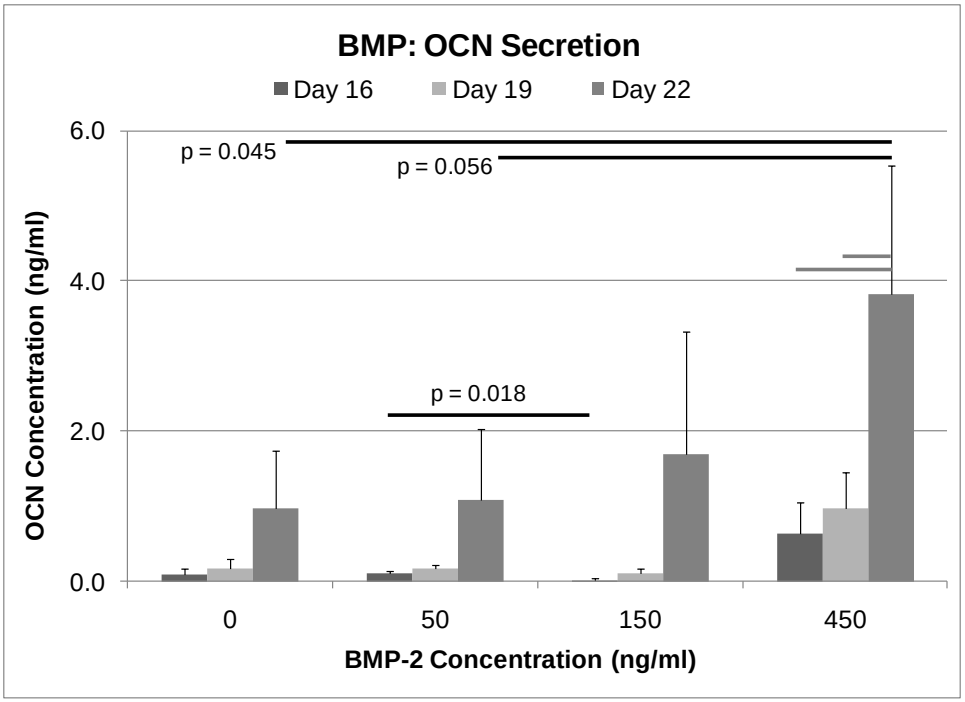

Figure 4.3: Osteocalcin secretion levels determined by ELISA. For Day 22, the cells treated with 450 ng/ml of BMP-2 demonstrated significantly higher OCN levels compared to the untreated controls as determined by ANOVA. OCN level for the 450 ng/ml was also marginally higher compared to the 50 ng/ml BMP-2 treatment group. (Gray bars indicate $p<0.05$).

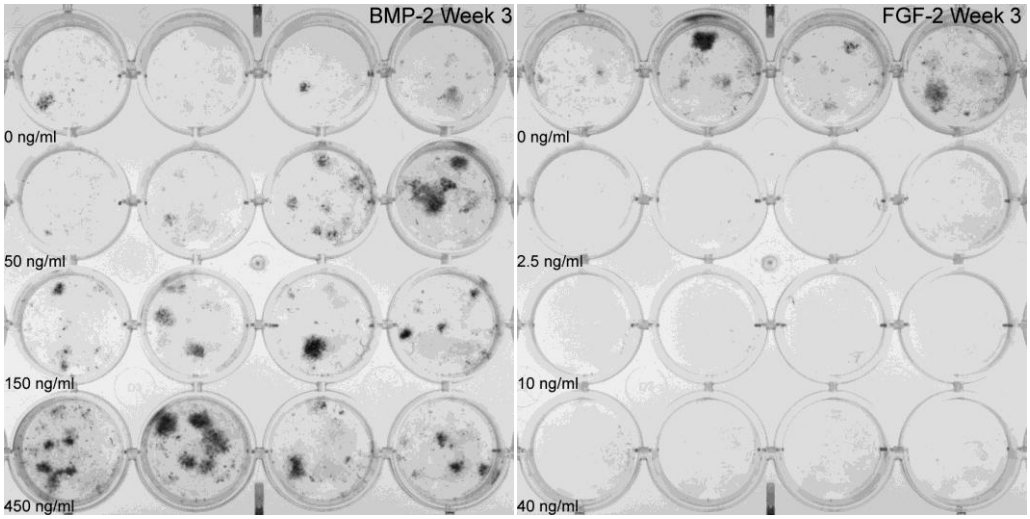

Figure 4.4: von Kossa staining of mineral deposition from BMSCs A) BMSCs treated with BMP-2 at 0, 50, 150, and 450 ng/ml. B) BMSCs treated with FGF-2 at 0, 2.5, 10, 40 ng/ml.

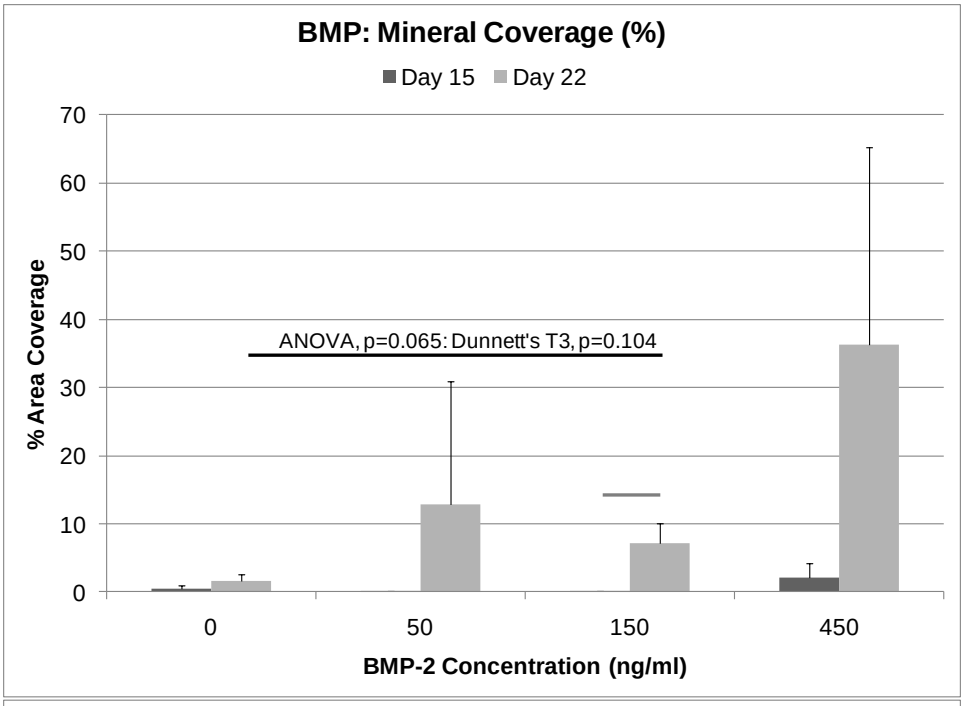

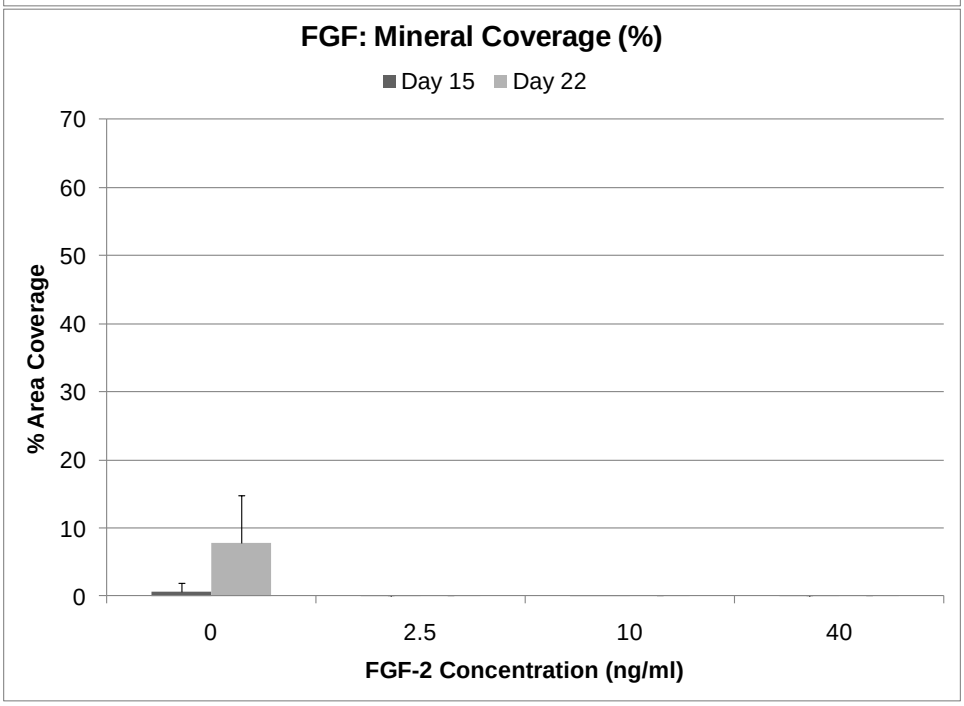

Figure 4.5: Mineral deposition (% of area covered) determined using von Kossa staining. A) For Day 22, the area covered with mineral for the group treated with 150 ng/ml of BMP-2 was marginally higher than the control group (Dunnett's T3, p=0.104). There is a general trend towards higher mineral coverage when BMSCs are treated with BMP-2 compared to untreated controls. B) In contrast, treatment with FGF-2 in any concentration inhibits the deposition of mineral. Although this was not statistically significant, the control cells demonstrated mineral deposition.

Growth Factor Administration	
Day 1	**Day 4**
None	None
FGF-2	FGF-2
BMP-2	BMP-2
FGF-2	BMP-2
BMP-2	FGF-2
BMP-2	BMP-2 & FGF-2
FGF-2	BMP-2 & FGF-2
BMP-2 & FGF-2	BMP-2 & FGF-2

Table 4.1: List of growth factor sequences. On Day 1, the growth factor(s) in media is added. On Day 4, the media is removed and new media containing the new growth factor(s) is/are added.

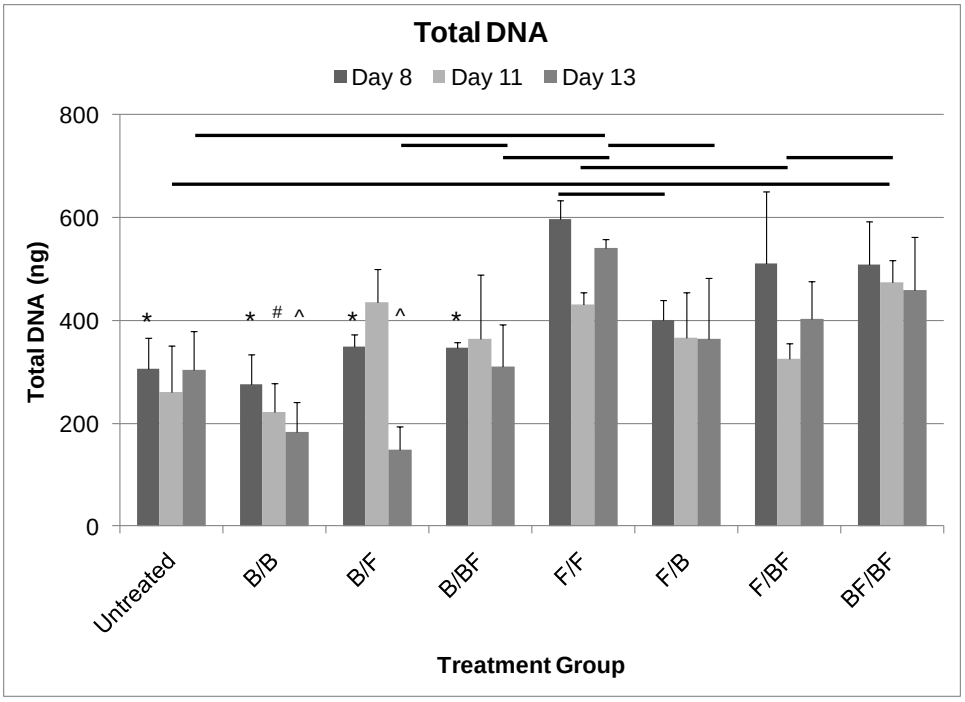

Figure 4.6: Total DNA quantified using Picogreen based on exposure to BMP-2 and FGF-2. At Day 8, F/F, F/BF, and BF/BF have significantly higher DNA levels compared to untreated controls and the groups that delivered BMP-2 first (Tukey, $p<0.05$). At Day 11, B/F, F/F, and BF/BF had significantly higher levels of DNA compared to the group that only delivered BMP-2 (Dunnett's T3, $p<0.05$). At Day 13, F/F, F/B, F/BF, and BF/BF had higher DNA content compared to B/B and B/F where BMP-2 is delivered first (Tukey, $p<0.05$). Bars represent $p<0.05$. (* denotes significance compared to F/F, F/BF, BF/BF; # denotes significance compared to B/F, F/F, BF/BF; and ^ denotes significance compared to F/F, F/B, F/BF, BF/BF)

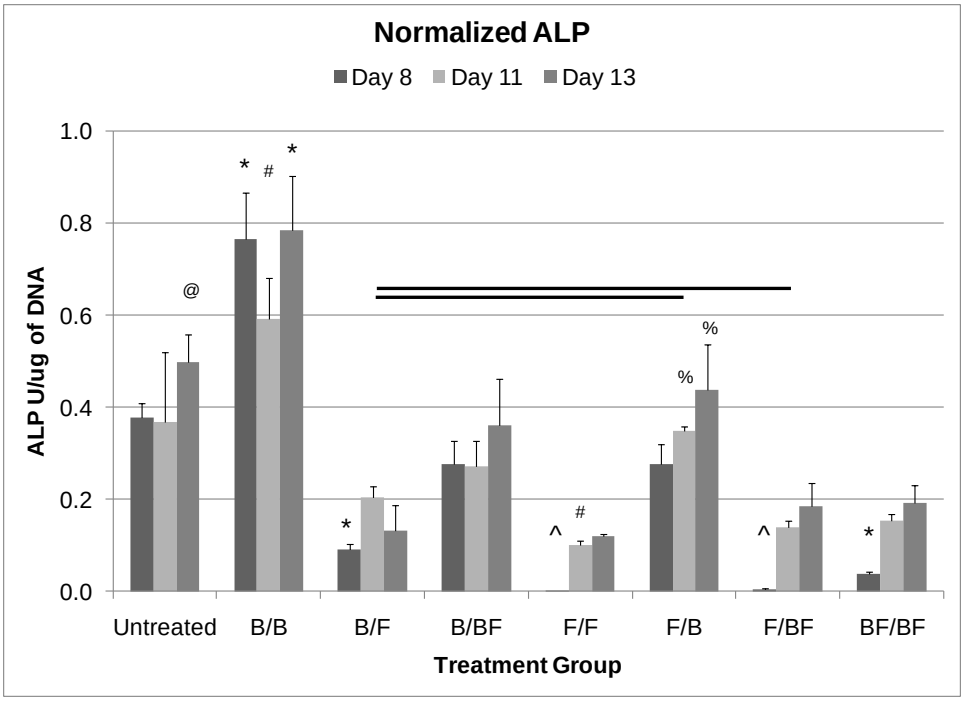

Figure 4.7: Normalized ALP with respect to total DNA. For Day 8, the ALP activity of B/B was significantly higher than all other groups (Dunnett's T3, $p<0.05$). The ALP levels for F/F and F/BF are significantly lower compared to all other groups. Sequential delivery of FGF-2 followed by BMP-2 led to significantly higher ALP levels compared to delivering both factors simultaneously. Delivering FGF-2 first, and then BMP-2 resulted in higher ALP levels compared to delivering BMP-2 first, followed by FGF-2. Additionally delivering BMP-2 the entire time period also resulted in higher ALP levels compared to delivering FGF-2 the entire time period. Inclusion of FGF-2 resulted in significantly lower levels in all groups except B/BF and F/B. For Day 11, F/B still demonstrated higher ALP compared to all groups except the untreated cells and B/BF. For Day 13, F/B continued to demonstrate high ALP levels compared to all groups except the controls and B/BF. Untreated cells, B/B, and F/B had significantly higher ALP levels compared to BF/BF. Bars also indicate $p<0.05$. (* denotes significance compared to all groups; ^ denotes significance compared to all other groups; # denotes significance compared to all groups except the untreated cells; % denotes significance compared to all groups except untreated cells and B/BF; and @ denotes significance compared to all groups except B/BF and F/B)

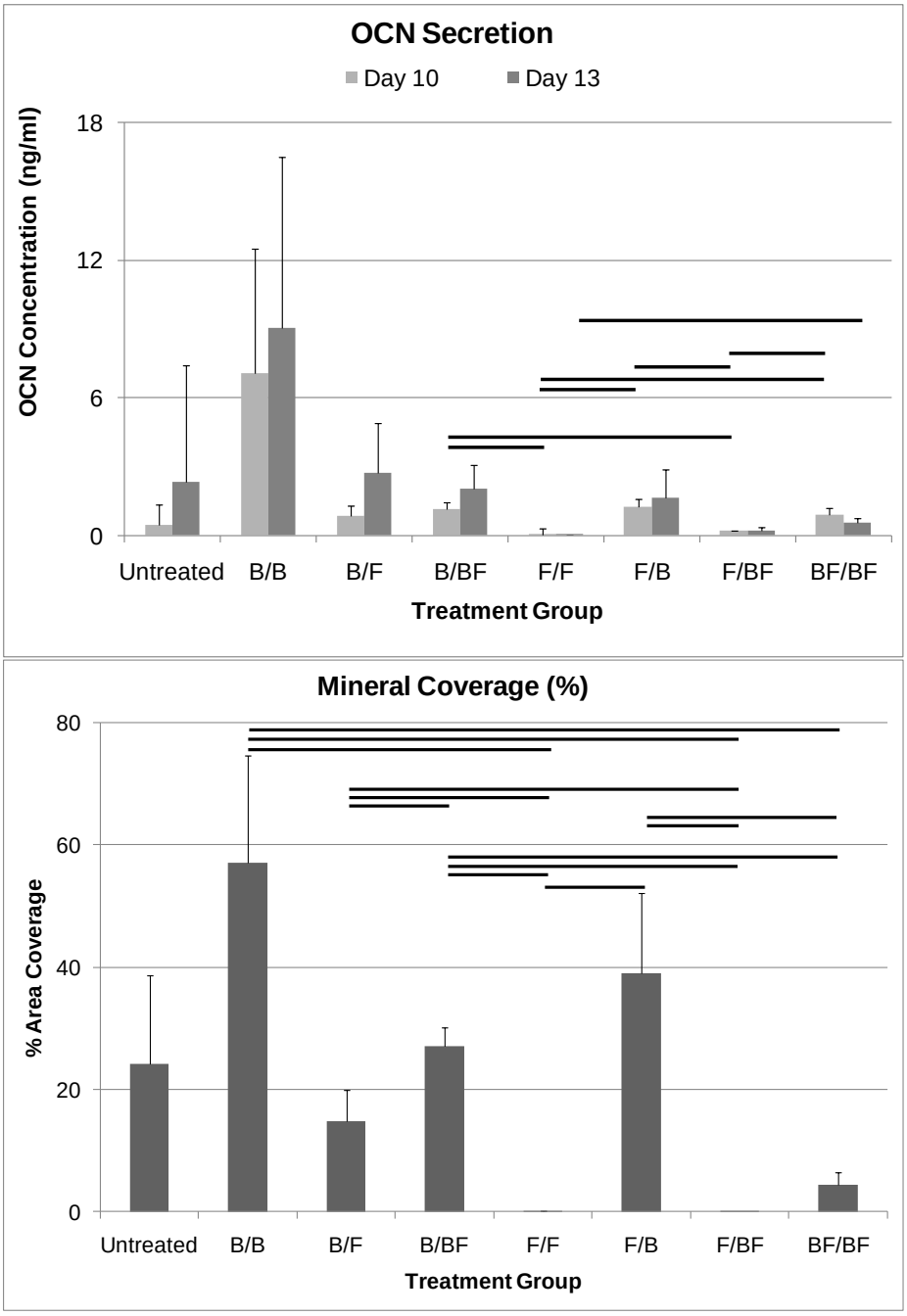

Figure 4.8: A) OCN secretion of BMSCs in response to BMP-2 and FGF-2 administration. F/B, B/BF, and BF/BF had higher levels of OCN compared to F/F and F/BF (Dunnett's T3, $p<0.05$). Delivering BMP-2 the entire time period when both growth factors are included led to higher OCN compared to delivering FGF-2 the entire time period. B) Mineral deposition (% of area covered) determined using von Kossa staining. Delivering FGF-2 first followed by BMP-2 had higher mineral coverage compared to delivery both factor simultaneously. Groups that delivered FGF-2 the entire time period tended to have lower mineral coverage including the delivery of both growth factors at the same time (Dunnett's T3, $p<0.05$).

References

1. Tabata Y. Tissue regeneration based on growth factor release. Tissue Eng 2003;9:S5-S15.

2. Hanada K, Dennis JE, Caplan AI. Stimulatory effects of basic fibroblast growth factor and bone morphogenetic protein-2 on osteogenic differentiation of rat bone marrow-derived mesenchymal stem cells. Journal of Bone and Mineral Research 1997;12:1606-1614.

3. Yeh LCC, Adamo ML, Olson MS, Lee JC. Osteogenic protein-1 and insulin-like growth factor I synergistically stimulate rat osteoblastic cell differentiation and proliferation. Endocrinology 1997;138:4181-4190.

4. Huang WB, Carlsen B, Wulur I, Rudkin G, Ishida K, Wu B, et al. BMP-2 exerts differential effects on differentiation of rabbit bone marrow stromal cells grown in two-dimensional and three-dimensional systems and is required for in vitro bone formation in a PLGA scaffold. Exp Cell Res 2004;299:325-334.

5. Peng H, Wright V, Usas A, Gearhart B, Shen HC, Cummins J, et al. Synergistic enhancement of bone formation and healing by stem cell-expressed VEGF and bone morphogenetic protein-4. J Clin Invest 2002;110:751-759.

6. Ripamonti U, Crooks J, Petit JC, Rueger DC. Periodontal tissue regeneration by combined applications of recombinant human osteogenic protein-1 and bone morphogenetic protein-2. A pilot study in Chacma baboons (Papio ursinus). Eur J Oral Sci 2001;109:241-248.

7. Raiche AT, Puleo DA. In vitro effects of combined and sequential delivery of two bone growth factors. Biomaterials 2004;25:677-685.

8. Yamaguchi A, Katagiri T, Ikeda T, Wozney JM, Rosen V, Wang EA, et al. Recombinant Human Bone Morphogenetic Protein-2 Stimulates Osteoblastic Maturation and Inhibits Myogenic Differentiation Invitro. J Cell Biol 1991;113:681-687.

9. Cho TJ, Gerstenfeld LC, Einhorn TA. Differential temporal expression of members of the transforming growth factor beta superfamily during murine fracture healing. Journal of Bone and Mineral Research 2002;17:513-520.

10. Hurley MM, Marie PJ, Florkiewicz RZ. Fibroblast Growth Factor (FGF) and FGF Receptor Families in Bone. In: Bilezikian JP, Raisz LG, Rodan GA, editors. Principles of bone biology. San Diego: Academic Press, 2002. p. 825-851.

11. Canalis E, Centrella M, Mccarthy T. Effects of Basic Fibroblast Growth-Factor on Bone-Formation Invitro. J Clin Invest 1988;81:1572-1577.

12. Hanada K, Dennis JE, Caplan AI. Stimulatory effects of basic fibroblast growth factor and bone morphogenetic protein-2 on osteogenic differentiation of rat bone marrow-derived mesenchymal stem cells. J Bone Miner Res 1997;12:1606-1614.

13. Dobson KR, Reading L, Haberey M, Marine X, Scutt A. Centrifugal isolation of bone marrow from bone: an improved method for the recovery and quantitation of bone marrow osteoprogenitor cells from rat tibiae and femurae. Calcif Tissue Int 1999;65:411-413.

14. Berrada S, Lefebvre F, Harmand M. The effect of recombinant human basic fibroblast growth factor rhFGF-2 on human osteoblast in growth and phenotype expression. In vitro cellular developmental biology.Animal 1995;31:698-702.

15. Zellin G, Linde A. Effects of recombinant human fibroblast growth factor-2 on osteogenic cell populations during orthopic osteogenesis in vivo. Bone 2000;26:161-168.

16. Debiais F, Hott M, Graulet AM, Marie PJ. The effects of fibroblast growth factor-2 on human neonatal calvaria osteoblastic cells are differentiation stage specific. J Bone Miner Res 1998;13:645-654.

17. Fujimura K, Bessho K, Okubo Y, Kusumoto K, Segami N, Iizuka T. The effect of fibroblast growth factor-2 on the osteoinductive activity of recombinant human bone morphogenetic protein-2 in rat muscle. Arch Oral Biol 2002;47:577-584.

18. Vonau RL, Bostrom MPG, Aspenberg P, Sams AE. Combination of growth factors inhibits bone ingrowth in the bone harvest chamber. Clin Orthop 2001;:243-251.

19. Hauschka PV, Wians FH. Osteocalcinâ? • hydroxyapatite interaction in the extracellular organic matrix of bone. Anat Rec 1989;224:180.

20. Fakhry A, Ratisoontorn C, Vedhachalam C, Salhab I, Koyama E, Leboy P, et al. Effects of FGF-2/-9 in calvarial bone cell cultures: differentiation stage-dependent mitogenic effect, inverse regulation of BMP-2 and noggin, and enhancement of osteogenic potential. Bone 2005;36:254-266.

21. Ono I, Tateshita T, Takita H, Kuboki Y. Promotion of the osteogenetic activity of recombinant human bone morphogenetic protein by basic fibroblast growth factor. J Craniofac Surg 1996;7:418-425.

22. Maegawa N, Kawamura K, Hirose M, Yajima H, Takakura Y, Ohgushi H. Enhancement of osteoblastic differentiation of mesenchymal stromal cells cultured by selective combination of bone morphogenetic protein-2 (BMP-2) and fibroblast growth factor-2 (FGF-2). J Tissue Eng Regen Med 2007;1:306-313.

23. Nakamura Y, Tensho K, Nakaya H, Nawata M, Okabe T, Wakitani S. Low dose fibroblast growth factor-2 (FGF-2) enhances bone morphogenetic protein-2 (BMP-2)-induced ectopic bone formation in mice. Bone 2005;36:399-407.

Chapter 5

Organic/Inorganic Hybrid Biomaterial Designed to Deliver Multiple Growth Factors to BMSCs

5.1 Introduction

The clinical basis for bone regeneration is the correction of bone defects caused from trauma, congenital malformations, and progressively deforming skeletal disorders. Bone tissue engineering provides an alternative to bone grafting and direct usage of growth factors to regenerate bone. Bone tissue engineering uses engineering design to strategically combine the following biological components essential in regeneration: cells, an extracellular matrix (ECM) analogue, and signaling molecules [1]. An ideal bone tissue engineering approach would incorporate osteoconductivity and osteoinductivity into the design of the supporting biomaterial, as well as biocompatibility, degradability, mechanical integrity, and the ability to support cell transplantation. Osteoconductive properties are derived from the implantation of synthetic or natural materials, which can serve as ECM analogs, allowing the recruitment of targeted host cells while simultaneously preventing unwanted cells from entering. Osteoinductive properties can be integrated into a tissue engineering system by a variety of methods such as immobilization of a biomolecule to a biomaterial surface, or encapsulation within a biomaterial.

Employing an inductive approach to bone regeneration in the form of growth factors can regulate cellular responses (proliferation, migration, differentiation), and have either synergistic or antagonistic effects on other growth factors. Although the activation of a single growth factor can have an impact on several signaling pathways, in the cellular environment, activation is not limited to single growth factor but a multitude of growth factors at different locations and times. In developing a delivery system to better simulate the microenvironment that cells are subjected to *in vivo*, exposure to multiple biological agents with a spatial and temporal gradient would be most advantageous. For example, vascular endothelial growth factor (VEGF) alone is not sufficient in healing of critical size bone defects, however by combining VEGF with BMP-4 healing is enhanced [2]. On the other hand, combined application of osteopontin-1 (OP-1) and BMP-2 did not enhance bone regeneration over single growth factor applications [3], implying that simultaneous administration of multiple factors is sometimes not sufficient to induce an osteogenic response. Therefore, the sequential delivery of multiple factors must be examined.

To deliver multiple biomolecules, a delivery system must be developed that expands on the advantages that a single factor delivery system exhibits. Polymeric dual delivery systems have been developed that are based the fusion of a polymer containing one biomolecule with microspheres containing a second biomolecule [4]. Another approach is to coat a scaffold using polymer hydrogel coatings containing biomolecules, where the biomolecules can diffuse through the different coatings instead of their release being degradation based [5]. However, protein aggregation within the polymer matrix can occur, resulting in incomplete release [5]. A third approach uses a peptide-modified

alginate hydrogel, where multiple factors are delivered in conjunction with cells to induce ectopic bone formation. However, the sequence of delivery was not controlled [6].

An alternative to polymeric systems is the coprecipitation of proteins with biomimetic apatite onto an implant or scaffold surface. In addition to providing spatial-temporal control of delivery like many polymer systems, bioceramic coatings provide a high degree of osteconductivity. The formation of a bone-like mineral layer leads to the interfacial bonding between implants and bone [7]. The bone-like mineral layer may enhance the conduction of host cells into scaffolds [8], in addition to inducing the osteogenic differentiation of cells transplanted [9]. Additionally, the apatite is a better source of mechanical integrity (e.g. substrate stiffness), a design parameter not provided by polymer systems capable of temporal delivery. An important advantage to coprecipitation is the ability to produce calcium phosphate coatings at a physiological temperature [10, 11], minimizing conditions that would alter the biological activity of the factors [12]. Biomolecules can be incorporated at different stages of the deposition of the calcium phosphate coatings [12], which spatially localizes the biomolecule through the apatite thickness [13], thus impacting biomolecule release.

In the design and development of our hybrid organic/inorganic delivery system, BMP-2 and FGF-2 were chosen as the growth factors. BMP-2 is a potent osteogenic factor that has an important role in bone regeneration, while FGF-2 plays an active mitogenic role for various cells types. Because both BMP-2 and FGF-2 regulate osteogenesis, they have been used in combination. FGF-2 stimulates cell growth and osteoblastic differentiation of dexamethasone treated MSCs, and upon exposing cells to both BMP-2 and FGF-2, bone formation was enhanced more than either growth factor

individually [14], confirming again the importance of temporal gradients. In Chapter 4, the effects of BMP-2 and FGF-2 on BMSCs cultured on tissue culture polystyrene were examined. Low concentrations of FGF-2 increased cell number while increasing concentrations of BMP-2 enhanced osteogenic activity (ALP, OCN, and mineral deposition. The delivery of FGF-2 followed by BMP-2 or even the delivery of BMP-2 followed by the delivery of both BMP-2 and FGF-2 resulted in enhanced osteogenic differentiation compared to the simultaneous delivery of both factors. Thus, the sequence in which multiple growth factors are delivered has a substantial effect on cellular response.

In this chapter, the hybrid delivery system was designed to allow for the sequential delivery of FGF-2 and BMP-2 with the aim of mimicking the concentration and sequence of growth factor administration discovered to optimally differentiate BMSCs on TCPS. First, the release of BMP-2 and FGF-2 from apatite was determined by varying their concentrations in mSBF during coprecipitation. Growth factor concentrations chosen for their release profile, were then used in coprecipitation schemes to mimic the sequential exposure of FGF-2 and BMP-2. By controlling the location of FGF-2 and BMP-2 within the biomimetic apatite, the sequence of delivery can be manipulated to provide a desired release. DNA content, alkaline phosphatase activity (ALP), and osteocalcin (OCN) content, were analyzed for BMSCs seeded on coprecipitated samples containing different sequences of the two growth factors.

5.2 Materials and Methods

5.2.1 Growth factors and additives

The growth factors rhBMP-2 and rhFGF-2 were obtained from Peprotech (Rocky Hill, NJ). FGF-2 was reconstituted in 5 mM Tris buffer containing BSA. BMP-2 was reconstituted in sterile water containing BSA. Heparin sodium salt derived from porcine intestinal mucosa was purchased from Sigma Aldrich (St. Louis, MO).

5.2.2 PLGA film preparation

The films were prepared using 5 wt. % PLGA, 85:15 PLA:PGA ratio (Alkermes), in chloroform solution. The films (approximately 200-300 µm thick) were cast onto 15 mm round glass coverslips, covered with aluminum foil and air dried for at least 24 hours under a fume hood. Prior to mineralization, the films were etched in 0.5 M NaOH for seven minutes. They were rinsed thoroughly with Millipore water before use.

5.2.3 Modified simulated body fluid

A modified simulated body fluid (mSBF, which contains 2X the concentration of Ca^{2+} and HPO_4^{2-} as standard SBF) was used to mineralize the films [13]. mSBF consists of the following reagents dissolved in Millipore water: 141 mM NaCl, 4.0 mM KCl, 0.5 mM $MgSO_4$, 1.0 mM $MgCl_2$, 4.2 mM $NaHCO_3$, 5.0 mM $CaCl_2 \cdot 2H_2O$, and 2.0 mM KH_2PO_4. mSBF was prepared at 25°C and titrated to pH 6.8 using NaOH to avoid homogeneous precipitation of calcium phosphate.

5.2.4 Mineralization and BMP-2 and FGF-2 coprecipitation for release kinetics

For mineralization, samples were incubated in mSBF at 37°C. mSBF was exchanged every 24 h. Samples were mineralized between 6-8 days before

coprecipitation. Before coprecipitation, mineralized films were sterilized under UV light for 30 min.

For coprecipitation, mineralized films were placed into a new petri dish. A mSBF solution containing either BMP-2 (0, 0.5, 5 μg/ml) or FGF-2 (0, 0.01, 0.05 μg/ml) and heparin (1:1 mass ratio with FGF-2) was prepared and placed into each dish containing the premineralized films. The films were incubated for 24 h at 37°C. Samples containing neither BMP-2 nor FGF-2 were mineralized for 24 h at 37°C in mSBF.

5.2.5 BMP-2 and FGF-2 release kinetics

Samples (n=7) were placed into 24 well plates. One ml of calcium free PBS (BMP-2) or 1 ml PBS with 0.1% BSA (FGF-2) was placed into each well and gently agitated at ca. 75 rpm. PBS was removed and replaced at each of the following time points: 6 h, 1 d, 3 d, 7 d, and 14 d. Samples were frozen for later analysis.

ELISA (Antigenix America, Huntington Station, NY) was used to analyze the release of BMP-2 and FGF-2. Kits were adapted for each growth factor and optimized for sample analysis. Briefly, tracer antibody was reconstituted in 0.1% BSA solution. BMP-2 and FGF-2 standard curves were prepared using diluent composed of 0.1% BSA and 0.05% Tween 20. Samples were diluted and added in duplicate. Color development was read at 450 nm with a plate correction at 650 nm after stop solution was added.

5.2.6 Murine bone marrow stromal cell extraction and cell culture

Six week old C57BL6 mice were utilized for BMSC extraction. Freshly extracted long bones (6 per mouse) were suspended in Hank's Balanced Salt Solution (HBSS). The metaphyses of each bone were cut (to allow for an opening to the marrow cavity), and 2 bones were placed into a 200 μl pipette tip and then placed in a microcentrifuge

tube. Tubes were spun for 8-12 sec up to a maximum speed of 2000 rpm [15]. An 18 gauge needle was used to gently agitate the cell pellets. Cell pellets were then pooled and split into T75 flasks. Media was exchanged and non-adhesive cells were removed after 5 days. Media was exchanged every 3 days until cells reached confluency, at which time cells were split 1:3 and replated. After reaching confluency, cells were counted and replated in 24 well plates.

Growth medium for primary cell culture and plating was composed of 10% FBS, 1% penicillin-streptomycin, and MEMα. After 48 h, osteogenic medium was utilized, which was growth medium supplemented with dexamethasone, 50 mg/L L-ascorbic acid-phosphate, and 10 mM β-glycerol phosphate hydrate disodium salt.

5.2.7 Mineralization and BMP-2 and FGF-2 coprecipitation for sequential release

For mineralization, samples (n=6 for ALP/DNA and n=5 for OCN) were incubated in mSBF at 37°C. mSBF was exchanged every 24 h. Samples were mineralized between 8-10 days before coprecipitation. Before coprecipitation, mineralized films were sterilized under UV light for 30 min.

For coprecipitation, mineralized films were placed into a new petri dish. The samples were then mineralized according to Figure 5.1. A mSBF solution containing either BMP-2 (5 μg/ml) or FGF-2 (0.05 μg/ml) was prepared and placed into each dish containing the premineralized films. The films were incubated for the specified time period and specified mSBF solution at 37°C.

5.2.8 Substrate mediated sequential delivery of BMP-2 and FGF-2 to BMSCs

Mineralized films containing growth factors were placed in 24 well-plates. An o-ring was placed into each well to prevent films from floating during media exchange.

Cells were plated into 24 well-plates (n=6 per group) at a density of 50,000 cells per well and allowed to attach for 48 h. Medium was then removed and replaced with osteogenic growth medium. Every 3 days thereafter, the osteogenic medium was replaced.

5.2.9 DNA content

To determine DNA content and ALP activity, cells were washed twice with HBSS and harvested utilizing a buffer containing 10 mM Tris-HCl, 0.2% Igepal, and 2 mM PMSF in ethanol. Samples were then placed at -80^{o}C for later analysis.

For DNA determination, samples were thawed, and homogenized on ice. Samples were then centrifuged at 12,500 rpm for 10 min at 4^{o}C and used for ALP activity. Samples were resuspended for DNA quantification. The DNeasy kit (Qiagen, Valencia, CA) was used to determine DNA content according to the protocol adapted from the manufacturer. Absorbance was determined using a microplate reader and DNA quantity was calculated. DNA content was determined at day 8, 15 and 22.

5.2.10 Alkaline phosphatase (ALP) activity

Thawed homogenized samples were then vortexed with assay buffer (glycine, $MgCl_2$), harvest buffer, and p-nitrophenyl-phosphate (PnPP) substrate solution (Sigma, St. Louis, MO) and incubated at 37^{o}C for 15 min. The reaction was then terminated by adding 0.1 N NaOH and samples were placed in a 96 well-plate. A standard curve using alkaline phosphatase from calf intestine (Roche, Indianapolis, IN) was used to compare the activity and absorbance was determined at 405 nm. Values were then normalized to DNA content. ALP activity was determined at day 8, 15 and 22.

5.2.11 Osteocalcin (OCN) content

Samples were rinsed with PBS and demineralized with 0.5 M EDTA and phenylmethanesulfonylfluoride (PMSF). Samples were gently shaken at ca. 80 rpm for 24 h at 4 °C. Demineralization solution was removed and spun at 10,000 rpm for 1 min. Supernatant was removed at Day 22 and frozen for analysis. OCN content was determined using a mouse OCN EIA kit (Biomedical Technologies, Stoughton, MA) according to manufacturer's protocol. Samples were thawed and placed into the 96 well-plate. A standard curve was also prepared ranging from 0 ng/ml to 50 ng/ml. After reaction termination, measure the absorbance at 450 nm immediately.

5.2.12 Statistical analysis

ANOVA with repeated measures was used to analyze the concentration of BMP-2 and FGF-2 released at each time. ANOVA was used to analyze DNA content, ALP activity, and OCN content, with regards to treatment. Tukey or Dunnett's T3 post hoc comparison test was used for pair-wise comparisons depending on whether or not the assumption of equal variance was met.

5.3 Results

5.3.1 BMP-2 and FGF-2 have differing release kinetics

Varying the concentration of BMP-2 used during coprecipitiation had significant effects on BMP-2 release (ANOVA repeated measures, $p<0.001$) (Figure 5.2). Adding 5 µg/ml of BMP-2 during coprecipitation resulted in significantly higher release compared to a concentration of 0.5 µg/ml, suggesting a higher BMP-2 incorporation into the apatite. The amount of BMP-2 released per time period was also significantly different ($p<0.001$)

(Figure 5.2b). Over time, the amount of BMP-2 released decreased. There was also a significant interaction ($p<0.001$) between the time period of release and concentration, which suggests that BMP-2 release profile was significantly dependent on the concentration of BMP-2 used during coprecipitation.

Varying the concentration of FGF-2 in mSBF also had significant effects on the concentration released (ANOVA repeated measures, $p<0.001$) (Figure 5.3). Adding 0.05 μg/ml of FGF-2 during coprecipitation resulted in significantly higher concentration released compared to a concentration of 0.01 μg/ml, suggesting a higher FGF-2 incorporation into the apatite. The amount of FGF-2 released per time period was also significantly different ($p<0.001$) (Figure 5.3b). For 0.05 μg/ml, the amount of FGF-2 released per time period does not change significantly with the exception of the last time period (7-14 d). There is also a significant interaction ($p<0.001$) between the time period of release and concentration, which suggests that the FGF-2 release profile was also significantly dependent on the concentration of FGF-2 used during coprecipitation.

5.3.2 Delivering FGF-2 and BMP-2 to BMSCs had moderate effects on DNA content

On Day 8, there were no significant differences in DNA content of BMSCs exposed to growth factors (Figure 5.4). On Day 15, simultaneous administration of FGF-2 and BMP-2 (Tukey, $p=0.022$) led to significantly higher DNA content compared to cells that were cultured on TCPS. Delivering FGF-2 first, followed by BMP-2 led to marginally higher DNA levels compared to cells seeded on TCPS (Tukey, $p=0.061$). There is a trend of increased DNA content for cells seeded on mineral compared to TCPS. At Day 15, there is also a trend of increased DNA level for groups in which FGF-

2 was delivered immediately compared to cells cultured on mineralized films containing no growth factors.

5.3.3 Delivering FGF-2 and BMP-2 at these concentrations had minimal effects on osteogenic differentiation of BMSCs

On Day 8, cells seeded on mineralized films demonstrated significantly higher normalized ALP activity compared to delivering BMP-2 first, followed by FGF-2 (Dunnett's T3, $p=0.009$) (Figure 5.5). On Day 15, normalized ALP activity was significantly higher for cells seeded on TCPS compared to all other treatment groups (Tukey, $p<0.001$). At all three times, there is a trend of increased ALP expression for cells cultured on TCPS compared to all groups that were cultured on mineralized substrates. At Day 22, there is a trend of increased ALP levels for the groups that delivered the growth factors in a sequence compared to cells that were only cultured on mineral (FGF-2 followed by BMP-2 and BMP-2 followed by FGF-2). OCN levels were not significantly different amongst the different experimental groups (Figure 5.6).

5.4 Discussion

The aim of these studies was to design a hybrid delivery system that would deliver multiple growth factors at concentrations and sequences determined to optimally differentiate BMSCs in the *in vitro* cell experiments from Chapter 4. Briefly, the sequence in which growth factors are delivered has a statistically significant effect on osteogenic differentiation (Figure 4.7 and Figure 4.8). An early marker (ALP) and a late marker (OCN) were used to measure osteogenic differentiation of BMSCs subjected to different sequences of FGF-2 and BMP-2. The delivery of FGF-2 followed by BMP-2

resulted in significantly increased expression of ALP and mineral deposition compared to the simultaneous delivery of both factors (Figure 4.7 and Figure 4.8). In order to design a delivery system based on controlling the delivery of growth factors from an apatite coating, the concentrations of both of the growth factors needed during coprecipitation were examined. Based on these findings (Figure 5.2 and Figure 5.3), FGF-2 and BMP-2 were spatially localized within biomimetic apatite using coprecipitation.

Osteoconductivity, in the form of biomimetic apatite, and osteoinductivity, in the form of growth factors, were integrated in the development of the hybrid delivery system. The aim was to utilize coprecipitation to control the spatial location of multiple growth factors, and thereby dictate the sequential release of the two factors shown to more optimally differentiate BMSCs compared to simultaneous administration. However, in this first iteration of the delivery system, minimal effects of growth factor sequence on DNA content (Figure 5.4) and osteogenic differentiation (Figure 5.5 and Figure 5.6) was shown. A trend of increased DNA content for cells seeded on mineral compared to TCPS suggests that the mineral had an osteoconductive effect on BMSCs. The trend of increased DNA content for treatment groups in which FGF-2 was delivered immediately compared to cells seeded on mineralized films containing no growth factors implies that FGF-2 has a mitogenic effect when delivered to BMSCs. Normalized ALP levels at day 15 were significantly higher for cells that were seeded on TCPS compared to all other groups (Figure 5.5), similar to the results in Chapter 4 when BMSCs were only seeded on TCPS (Figure 4.7). However, the presence of mineral resulted in a significant inhibition of ALP activity (Figure 5.5). At Day 22, the trend of higher ALP expression for the sequential delivery of the growth factors (FGF-2 followed by BMP-2 and BMP-2

followed by FGF-2) compared to cells that were only cultured on mineral implies that growth factor delivery compensates for the inhibitive effects of mineral. Additionally, the trend of higher ALP expression for sequential delivery compared to simultaneous delivery suggests that prolonged FGF-2 delivery inhibits osteogenic differentiation. The comparable ALP expression for both sequences of delivery (FGF-2 followed by BMP-2 and BMP-2 followed by FGF-2) demonstrates the potency of BMP-2 in initiating osteogenic differentiation in the early absence of FGF-2. Additionally, a late osteogenic differentiation marker, OCN, did not demonstrate significant differences among the different treatment groups (Figure 5.6).

There are many possible reasons for the minimal success of the hybrid delivery system in mimicking the cellular response that was expected from Chapter 4. The significant decrease in ALP expression by cells seeded on mineralized substrates compared to TCPS suggests that the mineral may have led to a decrease in osteogenic differentiation. Although bone-like apatite formed using a supersaturated ionic solution and calcium phosphate cements, such as 70% carbonated apatite and 90% hydroxyapatite have been demonstrated to increase osteogenic differentiation [9, 16], it has inhibited osteogenic differentiation of human mesenchymal stem cells while increasing cellular proliferation [17]. Rat bone marrow stromal cells cultured on plastic also express higher levels of ALP compared to cells attached to a calcium phosphate coating [18]. Differences in osteogenic differentiation of cells seeded on bone-like mineral may be attributed to differences in the ionic strength and pH of the solution used to form the bone-like mineral, where the level of supersaturation can drive the material characteristics of the apatite formed.

The composition of the mineral may play a significant role in controlling osteogenic differentiation. Varying the type of SBF utilized during mineralization has significant effects on osteogenic differentiation [19]. The hydroxyapatite that is typically formed from a supersaturated ionic solution is carbonated [20]. For instance, osteoblastic differentiation was increased on 70% carbonated apatite compared to amorphous calcium phosphate [16]. It is possible that the quantity of carbonated apatite in our experimental study may have led to a decreased osteogenic effect of the BMSCs.

Surface topography, crystallinity, and dissolution may also have inhibited or delayed the osteogenic differentiation of the BMSCs in this study. The amount of carbonate that is incorporated during mineralization influences crystallinity, and solubility [21]. Changing the composition of mSBF can change the topography and the crystallinity of the apatite formed [22]. Increasing the roughness of HA results in a delay in ALP expression of hMSCs [23]. In our study, the roughness of the apatite may have contributed to the inhibition in osteogenic activity [24]. HA coatings with lower crystallinity exhibit higher cellular attachment compared to highly crystalline HA [25]. However lower crystallinity also results in higher solubility, which would affect pH, and could lead to toxic effects [25]. The crystallinity of the bone-like mineral formed during this study may have affected the initial attachment of BMSCs to the apatite surface compared to TCPS, resulting in a lower number of cells exposed to the dual growth factor release. The influence of crystallinity suggests that the composition of the SBF, which dictates the material properties of the mineral formed, can be manipulated to minimize the inhibitive effects that the mineral may have on osteogenic differentiation.

Another possibility for the minimal effects of the sequential release of BMP-2 and FGF-2 on differentiation is related to the delivery of the growth factors. More BMP-2 was released in the earlier time periods, with decreases at subsequent times (Figure 5.2). However, while FGF-2 also demonstrated a "burst" release, it was more sustained over time (Figure 5.3). The differing release kinetics suggests the affinity of the factors for apatite influenced their release. This interpretation is supported by data showing that increasing adsorption affinities of antibacterial agents to apatite surfaces results in decreased release rates [26]. Based on the release kinetics, it is possible that BMP-2 may have a lower affinity to the bone-like mineral layer relative to FGF-2. BMP-2 has a pI of 8.2 while FGF-2 has a pI of 9.6 [27, 28], therefore, at the same pH, slightly different charges exist that may affect their binding to apatite.

From Chapter 4, a high concentration of BMP-2 was necessary for significant enhancement of osteogenic differentiation of BMSCs, while a low concentration of FGF-2 for short time periods was necessary to minimize inhibition/delay (Figure 4.2). Therefore, the coprecipitation time of FGF-2 was adjusted to lower the amount of FGF-2 incorporated into the coatings, thus lowering the amount of FGF-2 released. On Day 15, ALP activity was higher for cells on mineralized films compared to delivering FGF-2 first, followed by BMP-2 (Figure 5.5). Therefore, it is still possible that the FGF-2 concentration was high enough to have inhibitive effects. Another possibility is that the concentration of BMP-2 (5 μg/ml) may have still been too low to sufficiently initiate the cells into an osteogenic pathway due to its relatively higher release rate.

The interaction of BMP-2 and FGF-2 may have also contributed to the inability of the first iteration of the delivery system to mimic the cellular response of the same two

growth factors when they were added exogeneously to BMSCs seeded on TCPS (Chapter 4). In the study from Chapter 4, when FGF-2 was administered exogeneously for the entire 6 day time period, lower levels of osteogenic activity resulted compared to when FGF-2 was administered for half the time. FGF-2 derived osteogenic enhancement could be dependent on the stage of cellular differentiation [29]. *In vivo*, low nanogram levels of FGF-2 with BMP-2 can synergistically increase osteogenic differentiation, but on a microgram level serve to inhibit bone regeneration [30], which may extend towards *in vitro* experiments. For this study, the concentration of FGF-2 remaining within the mineral may have prolonged the exposure that the cells were subjected to in their immediate environment.

BMP-2 has been incorporated in similar calcium phosphate coatings where bioactivity was preserved [18, 31] and heparin has been used to increase FGF-2 stability by protecting it from acid or heat induced inactivation [32]. However, growth factor instability may still have contributed to minimal effects on osteogenic response even with the inclusion of heparin to stabilize FGF-2. Possible mechanisms of protein instability include protein unfolding, aggregation, and chemical inactivation [33]. Coprecipitation may have initiated conformational changes leading to reduced bioactivity due to possible interactions within the supersaturated solution or when the growth factors are precipitated onto the surface of the apatite. With adsorption to a hydrophilic surface, which is the case with the carbonated apatite, the factor may desorb without a conformational change or it may change to better bind to the substrate.

ALP levels were lower in cells were seeded on mineralized substrates (Figure 5.5), however, there was a non-significant increase in ALP levels within each treatment

group by Day 22 suggesting that if the differentiation was allowed to proceed, differences between the treatment groups may have become significant. The lack of significance in OCN levels between all groups suggests that osteogenic differentiation was also delayed. If differentiation was allowed to proceed longer, differences among the groups may have become significant since OCN is a late marker of osteogenic differentiation. Delayed differentiation may be due to the inhibitive properties of FGF-2, but it may also have been a result of the heterogeneous population of BMSCs. While stromal cells were selectively passaged, other cell types were also present. The effects of BMP-2 and FGF-2 on BMSCs can differ depending on the stage of differentiation. For example, dose dependency of BMP-2 may be different for osteoblast progenitor cells compared to more mature osteoblasts [34].

From this study, we have demonstrated that incorporating growth factors during coprecipitation can significantly dictate their release kinetics. Even though this first iteration of a hybrid substrate-based delivery system did not fully mimic the cellular response of BMSCs to BMP-2 and FGF-2, it still has potential to deliver multiple growth factors or other biological molecules including DNA and peptides. In Chapter 4, the importance of delivering BMP-2 and FGF-2 in a specific sequence compared to delivering them simultaneously was demonstrated. Incorporating biomolecules using coprecipitation potentiates the integration of the conductivity of apatite with the inductivity of biomolecules in a hybrid delivery system that can better control the sequential delivery of multiple biomolecules. Further iterations of the delivery system to could involve changing the: formulation of mSBF, growth factor concentration during coprecipitation, and time period for coprecipitation. In changing the composition of the

mSBF, mineral characteristics such as surface chemistry, and dissolution, would also change. Changing dissolution rates would also change the rate of release of the growth factors. Increasing or decreasing the growth factor concentrations during coprecipitation and changing the time period for coprecipitation would alter the amount and the duration that a growth factor is released. For example, decreasing the time period of coprecpitation or the concentration for FGF-2 would most likely decrease the inhibitive effects that FGF-2 has on osteogenic activity. This hybrid delivery system has the potential to be beneficial in many clinical applications including fractures or dental implants since delivery is not limited to only growth factors [26, 35].

5.5 Conclusion

For this model system, BMP-2 and FGF-2 were chosen for the design of a hybrid delivery system based on dual release. ALP and OCN expression were evaluated as a means of measuring the ability of the delivery system to mimic the osteogenic response demonstrated in Chapter 4. The release of BMP-2 and FGF-2 was significantly affected by the concentration used during coprecipitation. BMP-2 demonstrated a higher "burst" release compared to FGF-2. In the first iteration of the hybrid substrate delivery system, minimal effects on both DNA content and osteogenic differentiation were shown. DNA levels were not significantly different between the groups that delivered multiple growth factors. Normalized ALP activity was significantly higher for untreated cells that were seeded on TCPS compared to all other groups. The mineral inhibited or delayed osteogenic activity. However, the trend of increased ALP expression for sequential growth factor delivery indicated that the delivery of BMP-2 and FGF-2 in either order

compensated for the inhibitive effects of mineral. With further experimentation, this organic/inorganic delivery system based on coprecipitation has the potential to deliver multiple biological factors to better mimic spatial and temporal gradients that cells are exposed to *in vivo* by controlling the release of biomolecules from within apatite.

Acknowledgements

This research is supported by NIH DE 015411, DE 13380, and the Tissue Engineering and Regeneration Grant T32 DE 07057. I would like to thank Janani Ramaswamy and Erin McNerny for their support and advice during this work. I would also like to thank Erica Scheller for her helpful advice.

Growth Factor Coprecipitation Order			
First	**Hrs**	**Second**	**Hrs**
Cells Only	-	Cells Only	-
Cells + Min	-	Cells + Min	-
FGF	6	BMP	24
BMP	24	FGF	6
BMP + FGF	30	BMP + FGF	30

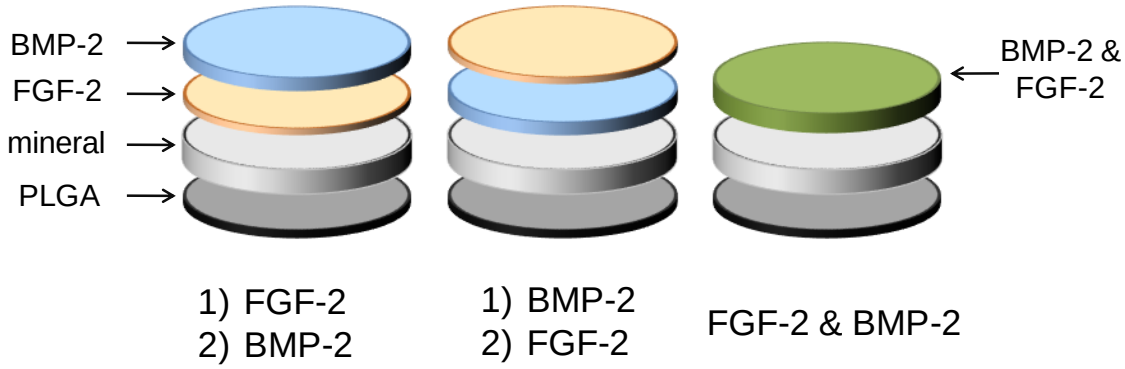

Figure 5.1: Experimental groups for substrate-mediated delivery of growth factors to BMSCs. The table lists the coprecipitation order of the experimental groups. The diagram is a pictorial representation of the spatial distribution of growth factors based on the coprecipitation order. The "thickness" of the layers with regards to time were: mineral (8-10 days), BMP-2 (24 or 30 hr), and FGF-2 (6 or 30 hr). For example, for the 3rd group, FGF-2 will be coprecipitated for 6 h, and then BMP-2 will be coprecipitated for 24 h. Therefore, BMP-2 is the topmost layer, followed by FGF-2 below it.

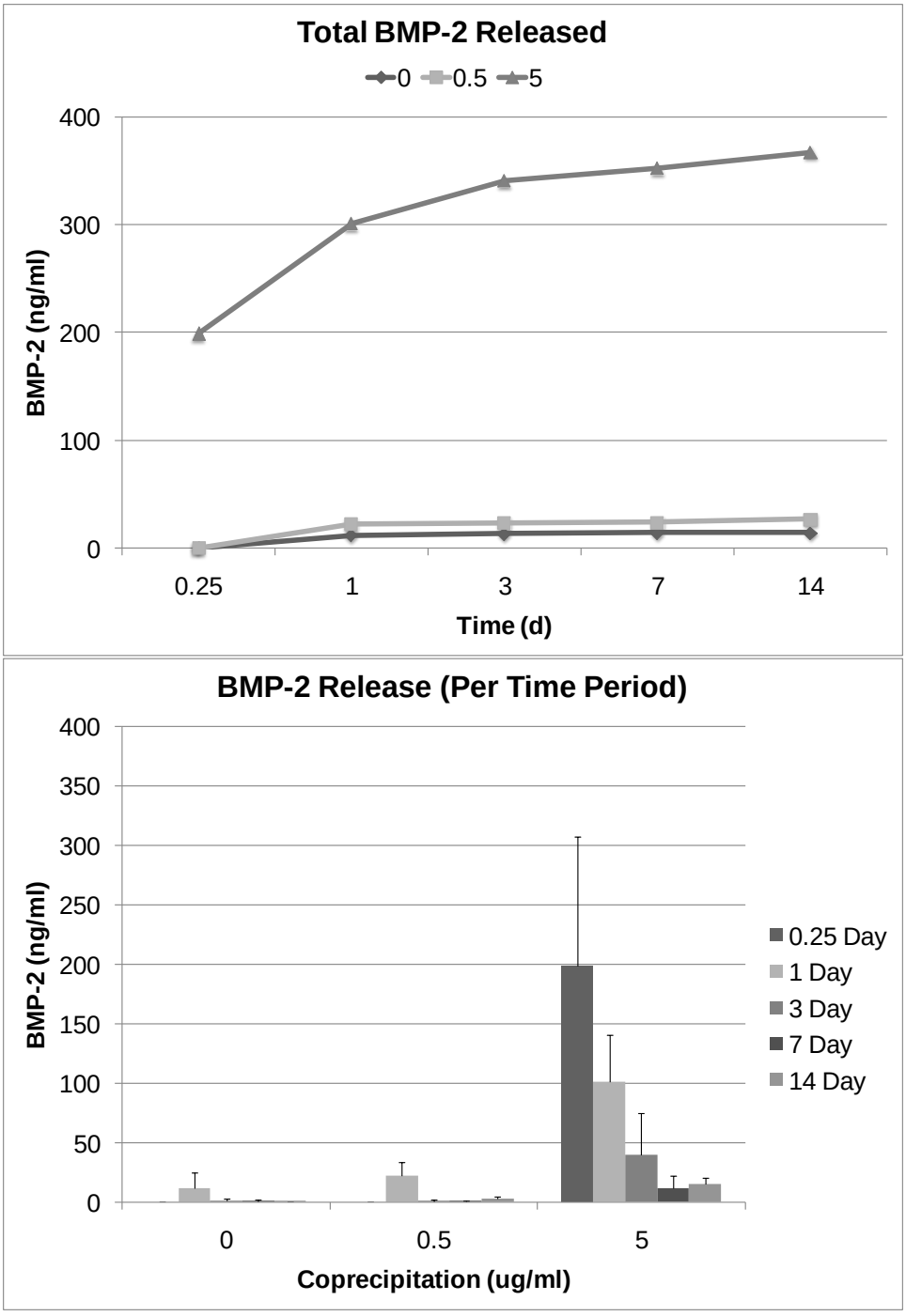

Figure 5.2: Release of BMP-2 is dependent on BMP-2 concentration in mSBF. A) Cumulative release of BMP-2 over the 14 day time period. B) Release of BMP-2 during each time period (6 h, 1, 3, 7, 14 d). Varying the BMP-2 concentration during coprecipitation had a significant effect on BMP-2 release (ANOVA repeated measures, $p<0.001$). There are also significant changes in the amount of BMP-2 released for each time period ($p<0.001$). Additionally, there is significant interaction ($p<0.001$) between time and concentration, further suggesting that BMP-2 release is significantly dependent on the concentration of BMP-2.

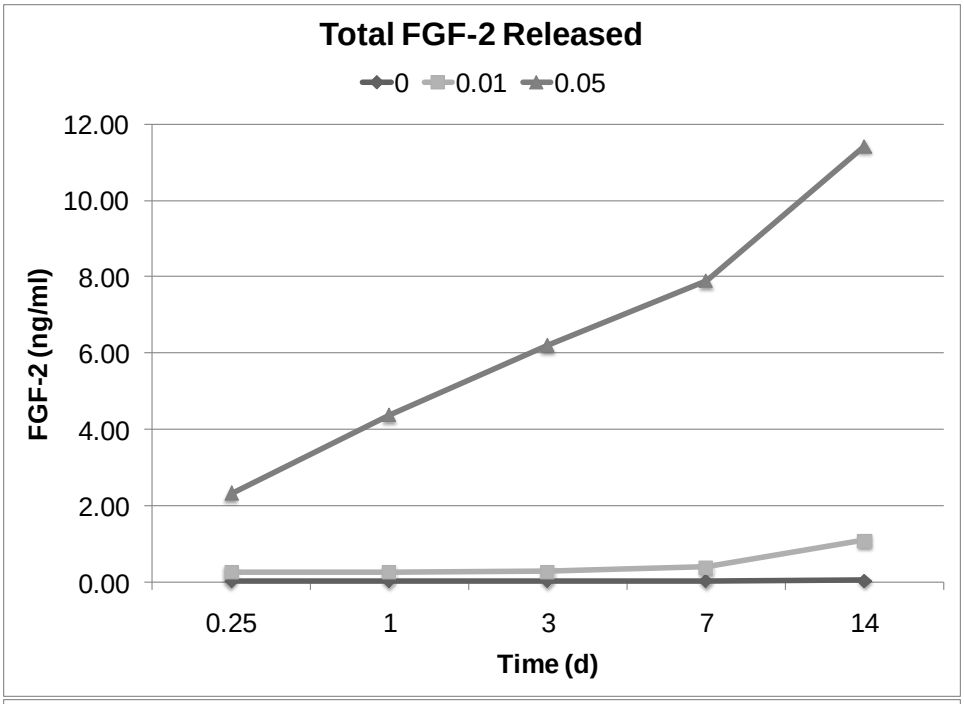

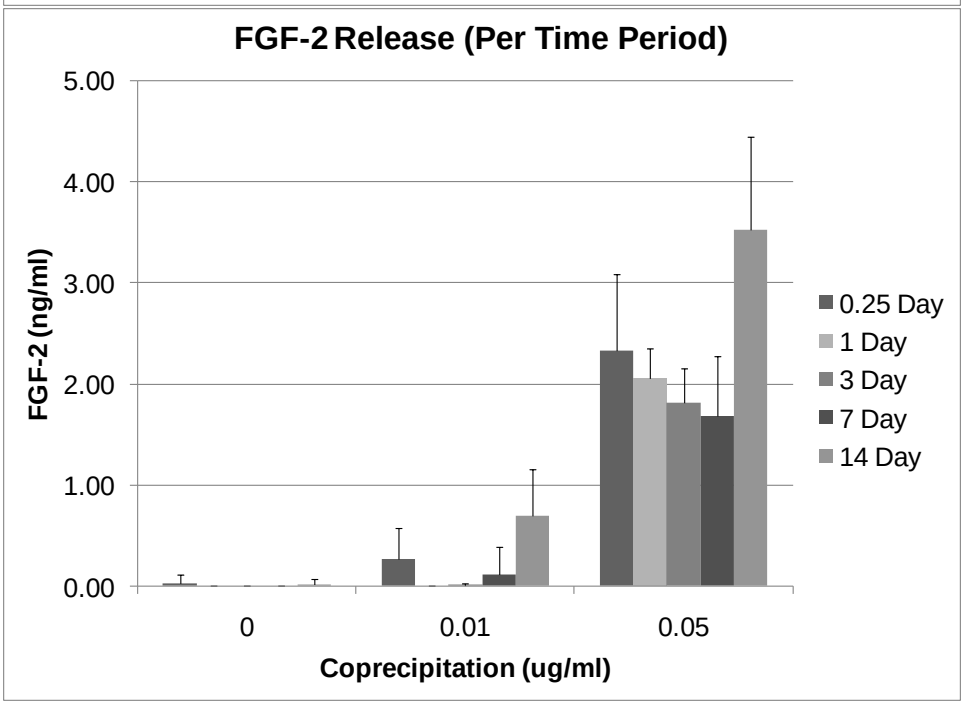

Figure 5.3: Release of FGF-2 is dependent on FGF-2 concentration in mSBF. A) Cumulative release of FGF-2 over the 14 day time period. B) Release of FGF-2 during each time period (6 h, 1, 3, 7, 14 d). Varying the FGF-2 concentration during coprecipitation had a significant effect on FGF-2 release (ANOVA repeated measures, $p<0.001$). There are also significant changes in the amount of FGF-2 released for each time period ($p<0.001$). Additionally, there is significant interaction ($p<0.001$) between time and concentration, suggesting that FGF-2 release kinetics is significantly dependent on the concentration of FGF-2.

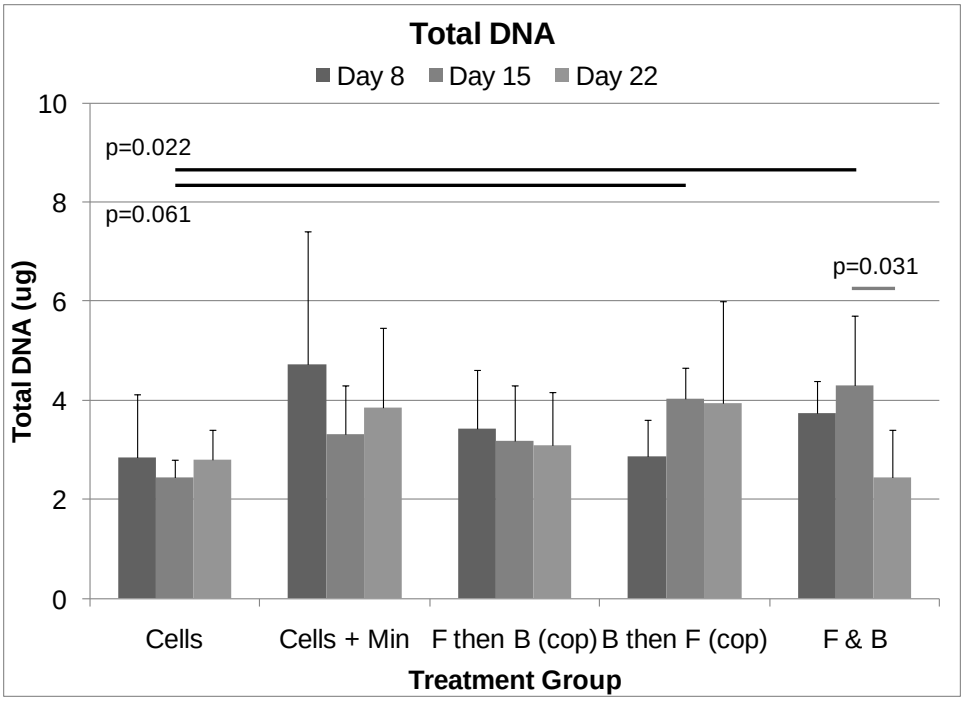

Figure 5.4: Total DNA quantified using DNeasy. On Day 15, the DNA content was significantly higher for the simultaneous administration of FGF-2 and BMP-2 (Tukey, p=0.022) and marginally higher when FGF-2 was delivered first, followed by BMP-2 second (Tukey, p=0.061) compared to cells seeded on TCPS. Simultaneous delivery of BMP-2 and FGF-2 was significantly higher at Day 15 compared to Day 22 (Tukey, p=0.031). For the coprecipitation groups, the order of coprecipitation is the reverse order of release.

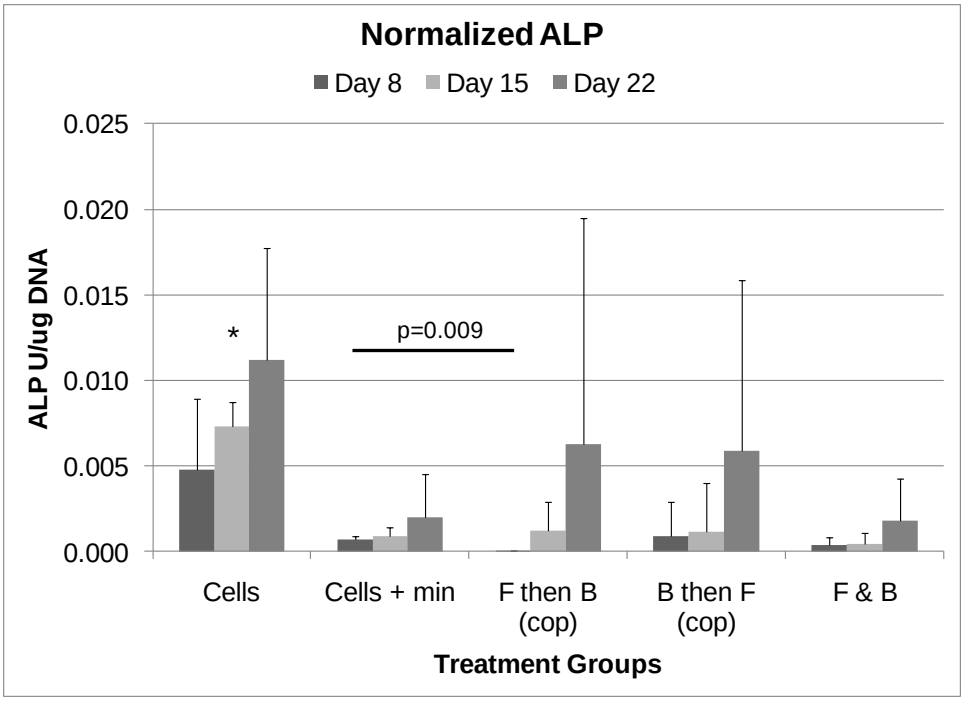

Figure 5.5: ALP normalized with respect to total DNA. A) On Day 8, ALP expression was significantly higher for cells on mineralized films compared to treating cells with BMP-2 first, followed by FGF-2 (Dunnett's T3, p=0.009). On Day 15, normalized ALP activity was significantly higher for cells seeded on TCPS compared to all other treatment groups (Tukey, $p<0.001$).

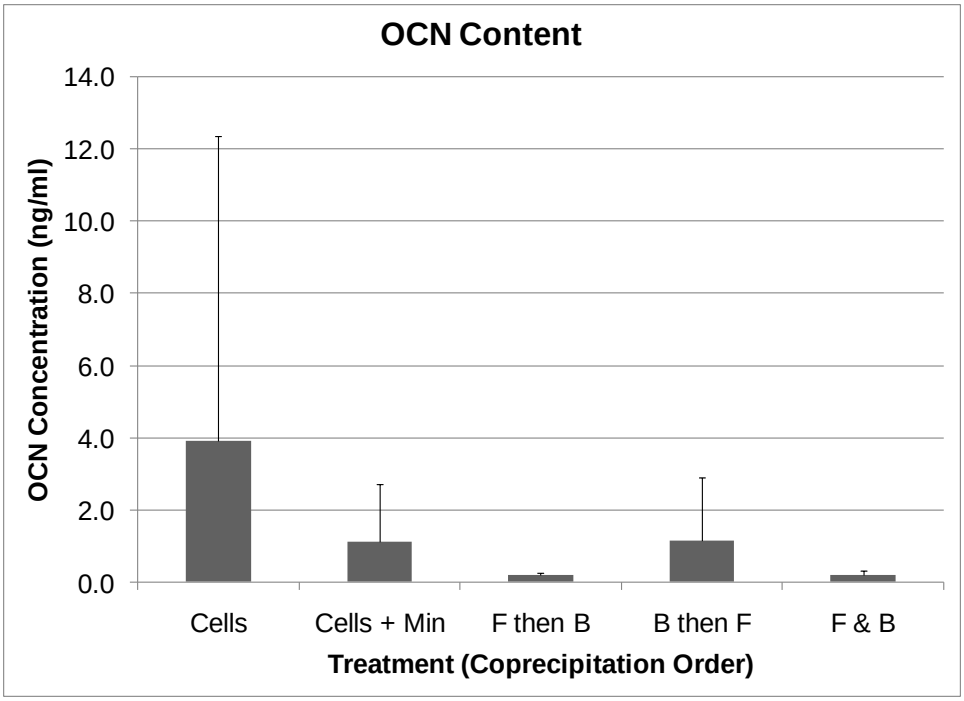

Figure 5.6: Osteocalcin secretion levels determined by ELISA. There was no significant difference in OCN levels on Day 22.

References

1. Tabata Y. Tissue regeneration based on growth factor release. Tissue Eng 2003;9:S5-S15.

2. Peng H, Wright V, Usas A, Gearhart B, Shen HC, Cummins J, et al. Synergistic enhancement of bone formation and healing by stem cell-expressed VEGF and bone morphogenetic protein-4. J Clin Invest 2002;110:751-759.

3. Ripamonti U, Crooks J, Petit JC, Rueger DC. Periodontal tissue regeneration by combined applications of recombinant human osteogenic protein-1 and bone morphogenetic protein-2. A pilot study in Chacma baboons (Papio ursinus). Eur J Oral Sci 2001;109:241-248.

4. Richardson TP, Peters MC, Ennett AB, Mooney DJ. Polymeric system for dual growth factor delivery. Nat Biotechnol 2001;19:1029-1034.

5. Sohier J, Vlugt TJH, Cabrol N, Van Blitterswijk C, de Groot K, Bezemer JM. Dual release of proteins from porous polymeric scaffolds. J Controlled Release 2006;111:95-106.

6. Simmons CA, Alsberg E, Hsiong S, Kim WJ, Mooney DJ. Dual growth factor delivery and controlled scaffold degradation enhance in vivo bone formation by transplanted bone marrow stromal cells. Bone 2004;35:562-569.

7. Hench LL. Bioceramics - from Concept to Clinic. J Am Ceram Soc 1991;74:1487-1510.

8. Murphy WL, Kohn DH, Mooney DJ. Growth of continuous bonelike mineral within porous poly(lactide-co-glycolide) scaffolds in vitro. J Biomed Mater Res 2000;50:50-58.

9. Kohn DH, Shin K, Hong SI, Jayasuriya AC, Leonova EV, Rossello RA, et al. Self-Assembled Mineral Scaffolds as Model Systems for Biomineralization and Tissue Engineering. In: Proceedings of the Eighth International Conference on the Chemistry and Biology of Mineralized Tissues; W. J. Landis and J. Sodek, editors. Toronto, Canada: University of Toronto Press; 2005.

10. Wen HB, de Wijn JR, van Blitterswijk CA, de Groot K. Incorporation of bovine serum albumin in calcium phosphate coating on titanium. J Biomed Mater Res 1999;46:245-252.

11. Wen HB, Wolke JG, de Wijn JR, Liu Q, Cui FZ, de Groot K. Fast precipitation of calcium phosphate layers on titanium induced by simple chemical treatments. Biomaterials 1997;18:1471-1478.

12. Azevedo HS, Leonor IB, Alves CM, Reis RL. Incorporation of proteins and enzymes at different stages of the preparation of calcium phosphate coatings on a degradable substrate by a biomimetic methodology. Materials Science & Engineering C-Biomimetic and Supramolecular Systems 2005;25:169-179.

13. Luong LN, Hong SI, Patel RJ, Outslay ME, Kohn DH. Spatial control of protein within biomimetically nucleated mineral . Biomaterials 2006;27:1175-1186.

14. Hanada K, Dennis JE, Caplan AI. Stimulatory effects of basic fibroblast growth factor and bone morphogenetic protein-2 on osteogenic differentiation of rat bone marrow-derived mesenchymal stem cells. J Bone Miner Res 1997;12:1606-1614.

15. Dobson KR, Reading L, Haberey M, Marine X, Scutt A. Centrifugal isolation of bone marrow from bone: an improved method for the recovery and quantitation of bone marrow osteoprogenitor cells from rat tibiae and femurae. Calcif Tissue Int 1999;65:411-413.

16. Oreffo ROC, Driessens FCM, Planell JA, Triffitt JT. Growth and differentiation of human bone marrow osteoprogenitors on novel calcium phosphate cements. Biomaterials 1998;19:1845-1854.

17. Murphy WL, Hsiong S, Richardson TP, Simmons CA, Mooney DJ. Effects of a bone-like mineral film on phenotype of adult human mesenchymal stem cells in vitro. Biomaterials 2005;26:303-310.

18. Liu YL, Hunziker EB, Layrolle P, De Bruijn JD, De Groot K. Bone morphogenetic protein 2 incorporated into biomimetic coatings retains its biological activity. Tissue Eng 2004;10:101-108.

19. Chou YF, Huang W, Dunn JC, Miller TA, Wu BM. The effect of biomimetic apatite structure on osteoblast viability, proliferation, and gene expression. Biomaterials 2005;26:285-295.

20. Murphy WL, Mooney DJ. Bioinspired growth of crystalline carbonate apatite on biodegradable polymer substrata. J Am Chem Soc 2002;124:1910-1917.

21. Tang RK, Henneman ZJ, Nancollas GH. Constant composition kinetics study of carbonated apatite dissolution. J Cryst Growth 2003;249:614-624.

22. Shin K, Jayasuriya AC, Kohn DH. Effect of ionic activity products on the structure and composition of mineral self assembled on three-dimensional poly(lactide-co-glycolide) scaffolds. Journal of Biomedical Materials Research Part A 2007;83A:1076-1086.

23. Deligianni DD, Katsala ND, Koutsoukos PG, Missirlis YF. Effect of surface roughness of hydroxyapatite on human bone marrow cell adhesion, proliferation, differentiation and detachment strength. Biomaterials 2001;22:87-96.

24. Segvich S. Design of Peptides with Targeted Apatite and Human Bone Marrow Stromal Cell Adhesion for Bone Tissue Engineering [dissertation]. Ann Arbor: University of Michigan; 2008.

25. Chou L, Marek B, Wagner WR. Effects of hydroxylapatite coating crystallinity on biosolubility, cell attachment efficiency and proliferation in vitro. Biomaterials 1999;20:977-985.

26. Oyane A, Yokoyama Y, Uchida M, Ito A. The formation of an antibacterial agent-apatite composite coating on a polymer surface using a metastable calcium phosphate solution. Biomaterials 2006;27:3295-3303.

27. Nugent MA, Iozzo RV. Fibroblast growth factor-2. Int J Biochem Cell Biol 2000;32:115-120.

28. Kirsch T, Nickel J, Sebald W. Isolation of recombinant BMP receptor IA ectodomain and its 2:1 complex with BMP-2. FEBS Lett 2000;468:215-219.

29. Debiais F, Hott M, Graulet AM, Marie PJ. The effects of fibroblast growth factor-2 on human neonatal calvaria osteoblastic cells are differentiation stage specific. J Bone Miner Res 1998;13:645-654.

30. Fujimura K, Bessho K, Okubo Y, Kusumoto K, Segami N, Iizuka T. The effect of fibroblast growth factor-2 on the osteoinductive activity of recombinant human bone morphogenetic protein-2 in rat muscle. Arch Oral Biol 2002;47:577-584.

31. Liu Y, de Groot K, Hunziker EB. BMP-2 liberated from biomimetic implant coatings induces and sustains direct ossification in an ectopic rat model. Bone 2005;36:745-757.

32. Gospodarowicz D, Cheng J. Heparin Protects Basic and Acidic Fgf from Inactivation. J Cell Physiol 1986;128:475-484.

33. Schwendeman SP, Cardamone M, Klibanov A, Langer R. Stability of Proteins and their delivery from biodegradable polymer microspheres. In: Cohen S, Bernstein H, editors. Microparticulate systems for the delivery of proteins and vaccines. New York: Marcel Dekker, 1996. p. 1-49.

34. Yamaguchi A, Katagiri T, Ikeda T, Wozney JM, Rosen V, Wang EA, et al. Recombinant Human Bone Morphogenetic Protein-2 Stimulates Osteoblastic Maturation and Inhibits Myogenic Differentiation Invitro. J Cell Biol 1991;113:681-687.

35. Luong LN, McFalls KM, Kohn DH. Gene delivery via DNA incorporation within a biomimetic apatite coating. Biomaterials 2009;30:6996-7004.

Chapter 6

Conclusions and Future Work

6.1 Conclusions

Bone defects resulting from trauma, congenital malformation, and skeletal diseases present major challenges not only for the medical community but also for the scientific community. While current medical therapies are successful, there is still a continuing need for the development of a more ideal treatment for bone healing. Emerging strategies in bone regeneration have focused on the use of natural or synthetic materials to support cell transplantation or to guide bone growth. Necessary characteristics of the ideal biomaterial used for implantation are: biocompatibility, osteoconductivity, osteoinductivity, mechanical support, and biodegradability, with the measure of success based on its ability to induce cells to infiltrate, grow, and replace the implant. The work throughout this thesis is aimed at the development of an organic/inorganic delivery system utilizing coprecipitation, a biomimetic approach that precipitates apatite onto a biomaterial, to enhance cell response in a spatially and temporally controlled manner. Employing coprecipitation imparts osteoconductivity, derived from apatite (inorganic), and osteoinductivity, derived from DNA and growth factors (inorganic), into the design of a biomaterial.

In the development of biomaterials for bone tissue engineering, the inclusion of inductive factors has been researched as a means of enhancing bone regeneration.

Methods of immobilizing biomolecules include adsorption, covalent binding and physical entrapment, with varying levels of loading efficiency and retention. Coprecipitation is a biomimetic approach designed to incorporate a bioactive factor within a conductive layer of apatite, which is formed using a supersaturated ionic solution that heterogeneously precipitates in a defined range of pH, temperatures, and ionic concentrations. The ease at which coprecipitation can be manipulated demonstrates that this process is beneficial in creating biomaterials with conductive surfaces that can control the release of any bioactive factor including DNA, growth factors, peptides, or proteins to better mimic the cellular microenvironment where cellular response is highly dependent on spatial and temporal gradients.

In Chapter 2, our experiments elucidated the ability of coprecipitation to spatially localize a protein within mineral, which is necessary for designing a desired release profile and an effective delivery system for bone regeneration. Using BSA as a model protein, we have demonstrated that higher quantities of protein can be incorporated and retained within the apatite via coprecipitation compared to adsorption (Figure 2.2 and Table 2.1). Furthermore, employing coprecipitation as a means to distribute the protein allowed for more control over the spatial localization of the protein (Figure 2.6 and Figure 2.7). The spatial location and quantity of the protein can be controlled by manipulating the start, extent, and end of the coprecipitation process resulting in numerous release profiles that can be tailored to enhance a specific cellular response. Additionally, the mineralization process can also be controlled to change the type of apatite produced. Changing apatite chemistry and structure affects the dissolution rate of apatite, thereby changing the release of the biomolecules incorporated.

Next, we employed coprecipitation in the development of an organic/inorganic hybrid that delivers genes (Chapter 3). Coprecipitation of DNA-Lipoplexes into biomimetically nucleated apatite has the potential to be used in bone regeneration as additional means of controlling cellular behavior *in vivo*. By combining the methods of calcium phosphate based precipitation and cationic lipid assisted transfection, plasmid DNA complexed with a cationic lipid (Lipofectamine 2000®) was incorporated into biomimetic apatite. Through coprecipitation, the stability of the plasmid-DNA Lipoplexes was retained (Figure 3.4 and Figure 3.5) and colocalization of the complexes on the mineralized polymer substrates was confirmed (Figure 3.3). DNA-Lipoplex coprecipitation demonstrated higher transfection efficiency in comparison to other forms of delivery, including adsorption (Figure 3.7). Integrating calcium phosphate based transfection with cationic lipid transfection increases substrate stiffness and conductivity via the presence of the apatite, in addition to serving as a carrier for DNA. Complexation of the lipid to DNA condenses the DNA enabling easier cellular internalization, while the deposition of apatite with the DNA-Lipoplexes facilitated high, homogeneously distributed concentrations of DNA on the apatite surface that are available for uptake. By incorporating DNA-Lipoplexes during coprecipitation, aggregation of the complexes was minimized (Figure 3.6). Since nuclear uptake is dependent on size, by distributing the complexes on the apatite surface, cells have a higher probability of uptake and therefore transfection efficacy.

The ability to spatially localize a biomolecule within the apatite can be extended to genes. Upon successful entry of the complex into the cell and further into the nucleus for transcription and translation, secretion of the desired bioactive protein occurs,

instigating a more delayed release compared to an immediate delivery of the protein. This enables the development of a more clinically relevant delivery system in which a gene for an osteogenic factor can be incorporated. The promising use of cationic lipid transfection suggests that by manipulating the complexation agent via reducing cellular toxicity and increasing cellular internalization, the transfection efficiency can be improved. Additionally, since this system is adaptable for the incorporation of DNA based complexes, the emergence of siRNA technology offers another possibility for exerting control at the gene level. The successful transfection of the cell line via gene incorporation in biomimetic apatite serves as a foundation the development of a gene based scaffold system that can deliver multiple genes at specified times or for specified durations further enhancing the bone healing process.

Directing the spatial localization of a protein within apatite (Chapter 2) was next extended to the development of an organic/inorganic substrate based delivery system that could deliver multiple growth factors to regulate osteogenic differentiation (Chapter 4 and Chapter 5). The two growth factors, BMP-2 and FGF-2, have important roles in osteogenic differentiation and were used in conjunction to elucidate their combined effects on osteogenic response. BMP-2 is a widely known osteogenic factor with the ability to regulate growth and osteoblastic differentiation of cells. FGF-2, a well known angiogenic factor, also stimulates the proliferation and the differentiation of osteoprogenitor cells. Delivering FGF-2 can result in an angiogenic response, however, its efficacy can vary with dose in a nonlinear relationship [1]. For angiogenesis, FGF-2 concentrations can range from 1 μg to 100 μg, with the dose dependent on the type of delivery system used [2]. To best design a delivery system for BMP-2 and FGF-2, we

first needed design criteria for the two growth factors to determine if the sequence of delivery is critical in controlling osteogenic differentiation (Chapter 4). Evaluating the growth factors separately, low concentrations of FGF-2 increased DNA content (Figure 4.1), while BMP-2 concentrations greater than 150 ng/ml enhanced osteogenic activity (Figure 4.2 – Figure 4.5).

Employing the optimal concentrations determined from the studies on individual growth factors, the sequence of delivery of BMP-2 and FGF-2 was ascertained to have a significant impact on the extent of osteogenic differentiation of BMSCs. Delivery of FGF-2 followed by BMP-2 or even the delivery of BMP-2 followed by the delivery of both BMP-2 and FGF-2 enhanced osteogenic differentiation compared to the simultaneous delivery of both factors (Figure 4.7 and Figure 4.8). The delivery of FGF-2 followed by BMP-2 enhanced osteogenic differentiation better compared to the reverse administration, suggesting that FGF-2 may selectively increase the population of cells that are more receptive to BMP-2. However, the overall extent of osteogenic differentiation was still highest for the delivery of BMP-2 alone, suggesting that the inclusion of FGF-2 had a strong influence in delaying or inhibiting osteogenic response, even at nanogram levels. Clinically, these findings have great significance in bone regeneration. If a population of osteoprogenitor cells seeded on a three-dimensional matrix can be increased by FGF-2, a greater number of cells will then be osteogenically induced by BMP-2 to enhance bone formation *in vivo*. Additionally, if host cells are the target population, FGF-2 can serve to increase the proportion of cells that can be osteogenically induced by BMP-2.

The design criteria provided by the osteogenic response of BMSCs to BMP-2 and FGF-2 (Chapter 4) were then applied in the development of a coprecipitation based delivery system (Chapter 5) in which the concentration and the timing of the release of multiple growth factors can be controlled to mimic the osteogenic response of BMSCs to the sequential exposure of the growth factors in Chapter 4. First, the release profile of each growth factor was determined as a function of concentration of each growth factor during coprecipitation. The release of BMP-2 and FGF-2 was significantly impacted by the concentration used (Figure 5.2 and Figure 5.3), with BMP-2 exhibiting a higher release in the earlier time periods compared to FGF-2.

Applying the design criteria from Chapter 4 with the release characteristics of the individual growth factors into a first iteration of the organic/inorganic delivery system resulted in minimal effects on both DNA content and osteogenic differentiation (Figure 5.4 and Figure 5.5). Among the treatment groups delivering FGF-2 and BMP-2, DNA levels were not significantly affected. There was a trend of increased DNA content on cells that were seeded on mineralized substrates compared to cells on TCPS. There was also a trend of increased DNA levels for treatment groups that delivered FGF-2 first. Normalized ALP activity was significantly higher for untreated cells seeded on TCPS compared to cells that were seeded on mineralized substrates, which suggests that the inhibited activity may be due to the presence of the apatite. Specifically, the material properties of the apatite formed via mineralization, such as surface topography, and crystallinity, may have played a role in determining the osteogenic response of the cells. The trend of higher ALP expression for the sequential delivery of the growth factors (FGF-2 followed by BMP-2 and BMP-2 followed by FGF-2) compared to cells that were

only cultured on mineral implies that growth factor delivery compensated for the inhibitive effects of mineral.

With further iterations of the design, the organic/inorganic delivery system has the potential to deliver multiple biological factors to better mimic spatiotemporal gradients that cells are exposed to *in vivo* by controlling the release of biomolecules from within the apatite. Translating the delivery system from *in vitro* to *in vivo* requires consideration of blood flow, other extracellular proteins and cells endogenous to the defect site, immune response, the varying pH, and the interactions of other signaling molecules. Dissolution would have a significant role in the *in vivo* environment, and thereby, have a significant effect on the release of the growth factors in a defect site. Cell response in a 2D environment can differ from cells in a three-dimensional environment. While biomimetic mineral may have delayed or inhibited osteogenic response in cell culture on a 2D surface, the bone-like apatite may induce an improved osteogenic response in a three-dimensional environment.

In regards to clinical relevance, this system is not limited to the use of BMP-2 and FGF-2; it can be applied to other osteogenic growth factors or other bioactive factors including genes. This biomimetic approach can also be applied to metal substrates, which would be preferred for load bearing applications. The development of a three-dimensional system applying the same design approach utilizing coprecipitation would enable the study of the sequential delivery of multiple inductive factors *in vivo*. Bone-like apatite has already demonstrated its advantage at improving the bone-implant interface by enhancing interfacial bonding. With the inclusion of multiple inductive factors that can be released in a controllable manner on a surface that enhances

mechanical integrity, this delivery system can advance the development of biomaterials in the area of bone regeneration.

6.2 Future work

Based on the work detailed in this thesis, there are a number of directions that future research could take. In Chapter 2, the ability of coprecipitation to spatially localize a protein through the thickness of biomimetically nucleated apatite was examined using a simulated body fluid. One of the advantages of using such a biomimetic approach is that the apatite can be altered via modification to the ionic concentrations of the salts used to precipitate the mineral heterogeneously onto the substrate. By altering the concentrations, material properties that influence cellular response can be controlled including surface morphology, crystallinity, dissolution, and surface chemistry. These material characteristics can affect cellular attachment, migration, proliferation, and differentiation. Cellular response can be further directed when bioactive factors are incorporated within the apatite. In Chapter 5, the mineral may have inhibited or delayed osteogenic differentiation. The ability to manipulate the material properties of apatite would not only be beneficial in furthering biomaterial development but also in illuminating the complexities that exist between bone-like apatite and the surrounding cells.

In Chapter 3, a gene delivery system comprised of DNA-Lipoplexes and apatite successfully transfected cells. One avenue of research that naturally follows would be the incorporation of a gene to induce osteogenic differentiation, such as BMP-2. Another direction is to improve the transfection efficacy of this non-viral gene delivery method.

A commercially available cationic lipid was complexed to the gene of interest. Developing different lipid complexes has the potential to reduce cellular toxicity, and increase transfection efficacy. Research into altering the complexes to target a specific cell type or the inclusion of a nuclear localization signal to increase the chance of uptake and transfection by cells would also enhance the clinical relevance of this technique. The advancement of gene therapy has led to many new arenas of research including siRNA technology. Therefore, cellular pathways can be influenced by silencing a factor of interest that possibly inhibits or enhances a cellular response.

The work discussed in Chapter 4 and Chapter 5 serves as a foundation for the development of a multiple factor delivery method where the release is controlled by the incorporation of the factors spatially within the mineral matrix. In the process of designing the delivery system, and assessing the DNA levels, ALP activity, and OCN content, we encountered a few limitations with previously established protocols. Further adaptation or the development of new protocols to better assess a system based on apatite would advance the development of improved biomaterials utilized in bone regeneration.

As demonstrated in Chapter 5, the presence of the mineral may have negated the osteogenic effects of BMP-2 and FGF-2. The next iteration of the delivery design could entail changing the type of SBF used, increasing the concentrations of the individual growth factors, changing the time period of coprecipitation for each of the growth factors, and increasing the time period for study. By manipulating the ionic concentrations, the type of apatite can be changed, which would affect cellular response. Changing the growth factor concentrations, and the time period of coprecipitation could also change the osteogenic response of the cells. To address the clinical significance of this research

requires the translation of the *in vitro* delivery of the factors to *in vivo* application via an apatite coating on a 3D implant or scaffold. For example, the release of the growth factors can be controlled via changing the concentration of the SBF used during the coprecipitation process, which influences the dissolution rate of the apatite entrapping the growth factors. The pH in the cellular environment also affects the dissolution rate of apatite, thereby, also affecting the release of the growth factors to cells. The concentrations of BMP-2 and FGF-2 in SBF during coprecipitation could be increased for *in vivo* application. While the concentration of BMP-2 and FGF-2 incorporated is important, the ratio of the growth factors in relation to each other may also have a significant impact on osteogenic response, especially in a three-dimensional environment. While BMP-2 and FGF-2 were used in Chapter 4 to provide the design criteria for the system developed in Chapter 5, other biological factors such as peptides, proteins, growth factors, and genes, can also be dually delivered in a sequentially controlled manner to enhance a preferred cellular response (attachment, migration, proliferation, and differentiation).

Clinically, rhBMP-2 has been used in conjunction with absorbable collagen sponges (ACS) in human clinical trials for open tibial fractures at doses of 6 or 12 mg [3]. Gelatin hydrogels containing rhFGF-2 have also been applied to tibial shaft fractures at doses of 0.8 or 2.4 mg [4]. Since a high quantity of BMP-2 or FGF-2 is required for advanced healing of these fractures, treatment can be costly. With the usage of ACS/BMP-2, the retention of the growth factor is improved over buffer delivery [5], however different defect sites have varying requirements in regards to treatment period as well as treatment profile. For example, in environments where fluid clearance is high, a

slow release is more beneficial. With coprecipitation, the strong affinity of apatite for osteogenic factors can be utilized to better retain and to better control the release of the factor to the local cell environment by manipulating the concentration of the SBF, the growth factor concentration in SBF during coprecipitation, and/or the coprecipitation time period. With a higher retention capability, the need for a high dose of BMP-2 or FGF-2 can be mitigated and therefore lower the costs of treatment. With the use of ACS and gelatin hydrogels, the inherent properties of collagen and gelatin must also be considered including the interaction with the growth factors at varying pH, the effects that processing and sterilizing may have on structure and cross-linking, and mechanical properties. With the deposition of apatite, the mechanical integrity and increased interfacial bonding ability can be taken advantage of in conjunction with the incorporation of the growth factors.

For both gene and growth factor delivery, in order to increase biological as well as clinical relevance, a three-dimensional scaffold delivery system would need to be developed. To extend a two-dimensional design to a clinically relevant three-dimensional matrix necessitates the re-evaluation of the process of coprecipitation in incorporating biological factors homogeneously through the scaffold. The overall release kinetics of a biological factor would change since the release of a factor from the inner pores of a scaffold can differ greatly from the release of a factor that is on the surface of the scaffold with the presence of diffusion. Other controllable characteristics of a matrix design would be porosity, pore size, and interconnectivity. Additionally, the homogeneous precipitation of the biomimetic apatite layer on all surfaces of the scaffold is critical for developing a delivery system. Developing a scaffold enables the design of

in vivo studies where cellular response can differ greatly from the response that occurs in *in vitro* environments.

The approach detailed in this dissertation could be used to incorporate a combination of osteoinductive factors with apatite onto a biodegradable implant. This implant could accelerate bone healing, while requiring minimal intervention and eliciting minimal immune response, due to ability of the implant to degrade, leaving behind a natural matrix that has characteristics of natural bone. However, the approach is not limited to biodegradable scaffolds; it can be applied to different base materials depending on the defect location. For instance, for more load-bearing applications, increased mechanical support from metal implants would be required. Application of a bone-like apatite layer containing bioactive factors as a coating on a metal implant would increase interfacial bonding between the bone and implant. However, a secondary surgery is necessary if the implant fails. The culmination of this research would be the development of a scaffold system that can enhance the generation of multiple tissue types such as bone and cartilage via the localization of several genes or growth factors within the mineral deposited.

Integrating the research from this dissertation, and future studies that better simulate the biological environment that cells reside in would be advantageous in the field of bone tissue engineering, especially with interfaces involving apatite.

References

1. Norrby K. Basic fibroblast growth factor and de novo mammalian angiogenesis. Microvasc Res 1994;48:96-113.

2. Zisch AH, Lutolf MP, Hubbell JA. Biopolymeric delivery matrices for angiogenic growth factors. Cardiovascular Pathology 2003;12:295-310.

3. Geiger M, Li RH, Friess W. Collagen sponges for bone regeneration with rhBMP-2. Adv Drug Deliv Rev 2003;55:1613-1629.

4. Kawaguchi H, Oka H, Jingushi S, Izumi T, Fukunaga M, Sato K, et al. A Local Application of Recombinant Human Fibroblast Growth Factor 2 for Tibial Shaft Fractures: A Randomized, Placebo-Controlled Trial. J Bone Miner Res 2010;25:2459-2467.

5. Li RH, Wozney JM. Delivering on the promise of bone morphogenetic proteins. Trends Biotechnol 2001;19:255-265.

Appendix A

Thin Film Coprecipitation Protocol

Materials Needed:

Petri Dishes

NaOH

1XM SBF

Corning 0.22 µm CA 150 ml bottle top filter

Pre-cut PLGA (85:15) films (2 X 2 cm^2)

3-6 50 ml or 100 ml beakers

Millipore H_2O

Tweezers

70% Ethanol

Media bottle (33mm) for SBF changes (autoclaved)

½ gallon waste bottle for SBF/BSA (autoclaved)

Time in the Tissue Culture hood

BSA

Etching samples

1. Prepare 0.5M NaOH for etching. Prepare approximately 50 ml per 6 films etched.
2. Each Petri dish can etch 6-7 films. Lay out as many dishes as needed.
3. Pour 0.5 M NaOH in each Petri dish, about ½ full.
4. Submerge 6-7 films per dish. After submerging your first dish, start the timer. Each film is etched 7 minutes per side. Takes approximately 30 s to 1 min to submerge one dish. Ensure that the films in each of the dishes have been etched for 7 minutes (but not longer).

5. Flip the films when 7 minutes have passed, again time accordingly for the rest of the samples.
6. Pour H_2O into beakers for rinsing.
7. After etching place each film in a beaker full of H_2O. You can place more than one film per beaker.
8. Layout dishes and pour H_2O near the top of the Petri dish.
9. Place the films in the beaker into a Petri dish (approximately 6-7 films per dish).
10. Approximately 5-10 minutes later, flip each film and submerge.
11. Replace the H_2O in the beakers with fresh H_2O. Resubmerge films into the beakers.
12. Replace H_2O in the dishes with fresh H_2O. Resubmerge films into the dishes.
13. Repeat steps 10-11 one or two more times.

Preparing samples

1. Label as many dishes as needed
2. Cut parafilm for closing dishes.
3. Bring paper towels, tweezers, and a dumping container for old SBF.
4. About ½ hour before going up to the TC hood, warm up SBF in warm water.
5. Make sure all containers that contact SBF have been washed the previous day with soap, hot water, and then DI water from the faucet. (ie grad cylinders, graduated flasks, beakers)
6. Take Petri dishes and other equipment upstairs.
7. Turn off UV.
8. Turn on blower to hood.
9. Spray down inside of hood with ethanol. Wipe with paper towels.
10. Whenever you put your hands back inside the hood, spray them with ethanol first.
11. Spray tweezers with ethanol, and wipe thoroughly. Place in fume hood on a paper towel.

Mineralization only (Petri dishes should be switched every 3 days)

1. For the first day of mineralization: Filter SBF

2. Pipette 40 ml of SBF in each of the Petri dishes.
3. Using clean tweezers, submerge one film per Petri dish. Make sure that the film is completely submerged.
4. Carefully parafilm the cover of the Petri dish to the bottom.
5. Repeat steps 1-3 for all samples.
6. Carefully transport all samples back to the incubator. The incubator should be set to 37 °C.
7. For each consecutive day of mineralization (up to 3 for samples, up to 6 for controls): carefully unwrap the parafilm.
8. Using clean tweezers, carefully pick up the film, pour the old SBF into a dump container. Place the film back into the now empty Petri dish. If the film had been floating, make sure to flip the film before placing back in the dish.
9. Filter SBF.
10. Pipette 40 ml of SBF into the Petri dish. Take care to submerge each sample completely in SBF. If the film had been floating, put the side that was in contact with solution contact side up. Mineralization need only take place on one side.
11. Parafilm each Petri dish.
12. Transport back to incubator.
13. Repeat steps 6-10 for each day of mineralization.

Coprecipitation only (Petri dishes should be switched every day)

1. Pour out the total amount of SBF needed to make a specific concentration of SBF/BSA.
2. Place magnetic stirbar into the ½ gallon autoclaved bottle.
3. Measure BSA. Pour BSA into the ½ gallon autoclaved bottle.
4. Filter SBF. Pour into bottle.
5. Mix contents of bottle on the mixer for approximately 10-15 minutes. Bring back to the TC hood.
6. Filter SBF for controls.
7. Again pour out contents of dishes while carefully holding the films.
8. Pour in SBF in controls, pour SBF/BSA into the coprecipitation samples

9. Parafilm and incubate.
10. Repeat per day of coprecipitation.

Appendix B

Protocol for Hoescht and Vybrant for Cells

Materials

Bisbenzimide H 33258

Vybrant 22886

PBS

70% EtOH

Pipetters

Pipette tips

Microcentrifuge tubes

Methods

To make stock solution using 25 mg of B2883 (10 mg/ml):

1) Prepare a 10 mg/ml Hoechst 33258 solution in DD H_2O.
2) Add 2.5 ml of DD H_2O to 25 mg. Aliquot into microcentrifuge tubes (100 µl) and store covered in foil.
3) Store at -20°C.

To make dilute staining solution:

4) Use a 15 ml Falcon tube to prepare **1:500 dilution (0.02 mg/ml)** solution of dye.
5) Add 4.65 ml of 1 X PBS. Add 10 µl of Hoechst to the PBS.
6) Prepare a **1:200 dilution** of Vybrant to the PBS solution. Add 5 µl for every 1 ml of solution. Add 25 µl of Vybrant to the PBS solution.
7) Mix well. Store in the dark covered in foil.
8) Take out samples needed and place into 12 well plate.

9) Wet samples with 200 µl of water, and then remove.
10) Add 150 µl of the staining solution per well. Cover entire plate in the dark.
11) Place dish in the incubator for 15-30 min.
12) Remove solution, and wash 4 to 5 times with ddH_2O, let sit for 1-2 minutes per rinse.
13) Remove samples from 24 well plate and place them on microscope slides. Place GelMount onto the sample and coverslip. Must image same day or early next day.
14) Image on fluorescence microscope.

Appendix C

Determining Alkaline Phosphatase activity for a 24 well plate

Materials:

HBSS

70% EtOH

10mM Tris-HCl, pH=7.4

0.2% Igepal (CA-630)

PMSF

EtOH

Glycine

$MgCl_2$

p-nitrophenylphosphate

NaOH

ALP standard

Consummables:

Gloves

50 ml Falcon tubes

Sterile aspirating pipets

Pipette tips

Plastic vials

1.5 ml tubes

Tissue culture flasks T75

Kim-wipes

Stericup Filter 1 L

Equipment:

Laminar flow hood

Tweezers

Pipettor

Test tube rack

Microscope

Centrifuge

Markers

Sonicator

Vortexer

Methods:

1. Make harvest buffer for the cells.
    a. Ingredients to the harvest buffer are
    - 10 mM Tris-HCl, pH=7.4
    - 0.2% Igepal
    - 2 mM PMSF in EtOH (make 200 mM PMSF: 0.3484 g/10ml EtOH→ aliquot to 1 ml each)
    b. Example: 10 ml of harvest buffer for one entire 24 well plate (Make aliquots)
    - 9.78 ml of acid free DNase RNase free H_2O
    - 100 µl 1 M Tris-HCl, pH=7.4
    - 20 µl of Igepal
    - 100 µl of 200 mM PMSF in EtOH (added fresh the day of making the harvest buffer)
    - *NOTE: If used within a month or two, make and place in fridge without the PMSF added.
2. Make assay buffer for the cells.
    - 100 mM glycine (3.785g/500ml)
    - 1 mM $MgCl_2$, (47.61mg/500ml)
    - pH=10.5 (Titrate up or down with NaOH or HCl)

- *NOTE: Aliquot the buffer and freeze them at -20°.

3. PNPP: 50 mM of p-nitrophenylphosphate
    a. Use it straight from the bottle, thaw before you setup for the sonication.
    b. Aliquot and cover with foil (light sensitive) if you know that you need to do more than one assay. Thaw completely, aliquot 4 ml.
4. Make stop solution: 0.1N NaOH. Add 2 ml of NaOH to 18 ml of DNase/RNase free water. Make aliquots.
5. Thaw samples from the freezer.
6. Homogenize at low power (7-8 level, 2 times x 10sec) (sonicator in Dr. Franceschi's lab)
7. Keep the tube on ice before and after the homogenization
8. Keep the tube on a beaker (ice + 70% ethanol) during the homogenization so that the sample is not overheated by the sonicator tip
9. Centrifuge the homogenized sample at 12,500 rpm for 10 min (Set the centrifuge at 4^{o}C in advance)
10. Standard curve preparation for the ALP standard.
    a. Make 50 mM Tris buffer. Add 500 µl of 1M Tris to 9.5 ml of DNase/RNase free water. Make aliquots of this.
    b. Make a 1 mg/ml solution of BSA. Add 10 mg to 10 ml of Tris buffer.
    c. Add 4 µl of ALP (81.3 U) to 3.996 ml of Tris/BSA solution. This makes a stock solution of 20.33 U/ml

ul of assay	ul of harvest*	ul of PnPP	ul of ALP	ul of BSA/Tris	[ ] U/ml	[ ] ug/ml
250	120	100	5	25	0.203	0.100
250	120	100	4	26	0.163	0.080
250	120	100	2	28	0.081	0.040
250	120	100	5	25	0.014	0.0067
250	120	100	5	25	0.002	0.0011
250	120	100	0	30	0.000	0.0000

*ul of ALP is from the previous standard

ul of ALP	ul of BSA/Tris
10	50
8	52
4	56
10	50
10	50
0	60

11. Vortex the following components in a new eppendorf tube placed in 37^{o}C water bath
    - 250ul assay buffer
    - 120ul harvest buffer *This gets adjusted if the sample needs to be concentrated
    - 100ul PnPP

    *Mix these components thoroughly using the vortexer, place them into a rack and place them into the 37^{o}C water bath with the caps open
    - 30ul sample (set the timer from this moment to measure exactly 15 min); for example, put the sample into the tube every 30 seconds. Therefore at most, 30 samples can be done per assay or if 3 samples can be done per minute, then 45 samples can be done.
12. At the end of 15 minutes, put 500ul 0.1N NaOH (stop solution); for example, put this stop solution every 30 seconds so that every tube are on reaction for exact 15 min, or every 20 secs if you plan to do 3 samples per minute.
13. Cap the tubes, and vortex to mix thoroughly. Immediately, pipette 200 µl per well in a 96 well plate.
14. Read them at A405nm in the spectrophotometer.

Appendix D

EDTA Demineralization Protocol for Mineralized Substrates

Materials:

PBS

EDTA

PMSF

70% EtOH

Consummables:

Gloves

Sterile aspirating pipets

Pipette tips

Plastic vials

1.5 ml tubes

Kim-wipes

Equipment:

Laminar flow hood

Tweezers

Pipettor

Test tube rack

Centrifuge

Markers

Vortexer

Method:

1. Rinse samples with Ca Free PBS 2X.
2. Make a 9.997 ml 0.5 M EDTA (pH 8.0) + 3 ul 200 mM PMSF.
3. Add 300 ul to each well. Tape with a cell plate sticker. Place in a plastic bag.
4. Shake at ~80 rpm for 24 h at 4°C.
5. Pipette up and down a few times, remove solution and place in a 1.5 ml centrifuge tube. Spin samples down in the minicentrifuge at 10,000 rpm for 1 min.
6. Remove 250 ul of the supernatant into a new tube. Assay this tube for OCN.

Appendix E

Publications and Presentations

Publications

Luong LN; McFalls, KM; Kohn DH. Gene Delivery via DNA incorporation within a biomimetic apatite coating. Biomaterials 30: 6996-7004. 2009.

Luong LN; Sun Ig Hong; Patel RJ; Outslay M; Kohn DH. Spatial Control of Protein within Biomimetically Nucleated Mineral. Biomaterials 27: 1175-1186. 2006.

Segvich SJ; Luong LN; Kohn DH. Biomimetic Approaches to Synthesize Mineral and Mineral/Organic Biomaterials. Editors: Ahmed W; Ali N; Öchsner A In: Biomaterials and Biomedical Engineering. TTP, Switzerland. 2008.

Segvich S; Smith HC; Luong LN; Kohn DH, "Uniform Three-Dimensional Biomineralization of Protein Incorporated Mineral Layer on Porous Polymer Scaffolds," submitted to Journal of Biomedical Materials Research: Part B, 2006.

Presentations

Luong LN. Dr. Dominic D. Dziewiatkowski Award Seminar. Spatially Controlled Organic/Inorganic Hybrids Designed to Enhance Cellular Response. University of Michigan; May 2010; Ann Arbor, MI.

Luong LN, McFalls K, Kohn DH. Gene Delivery via DNA Incorporation Within a Biomimetically Coprecipitated Apatite Coating. In: BMES; Oct 2008; St. Louis, MO.

Luong LN, Kohn DH. Effects of FGF-2 and BMP-2 Sequence on Osteogenic Differentiation of Bone Marrow Stromal Cells. In: BMES; Oct 2008; St. Louis, MO.

Mandair GS, Luong LN, Kohn DH, Morris MD. Raman Spectroscopy of Biomimetic Polymers for Bone Tissue Engineering. In: FACSS; Oct 2007; Memphis, TN.

Segvich S, Smith HC, Luong LN, Kohn DH. Uniform Three-Dimensional Biomineralization of Protein Incorporated Mineral Layer on Porous Polymer Scaffolds, Proceedings of the 2006 Annual Meeting of the Society of Biomaterials, Presentation 514, Pittsburgh, PA.

Luong LN; Patel RJ; Kohn DH. Spatial Control of Protein within Biomimetically Nucleated Mineral. In: Society for Biomaterials, Biomaterials in Regenerative Medicine: The Advent of Combination Products; 2004 Oct; Philadelphia, PA.